Addis Ababa University

Addis Ababa Institute of Technology

School of Civil and Environmental Engineering

Hydraulic Engineering Stream

Dam Breach Analysis Using HEC-RAS 2D Flow Method for Yanda Dam

A Thesis Submitted to the School of Graduate Studies of Addis Ababa University in

Partial Fulfillment of the Degree of Master of Science in Civil Engineering

(Major in Hydraulic Engineering)

By

AMIR KEMAL

ADVISOR: DANEAL F/SELASSIE (PHD)

MARCH, 2025

Addis Ababa, Ethiopia

A Thesis

Submitted in Partial Fulfillment of the Requirements for the Degree of Master of Science

The undersigned have examined the thesis entitled '**Dam Breach Analysis Using HEC-RAS 2D Flow Method for Yanda Dam**' presented by **Amir Kemal**, a candidate for the degree of **Master of Science** and hereby certify that it is worthy of acceptance.

Daniel Fikadu Advisor	Signature	17/03/2025 Date
Yilma Seleshi Internal Examiner	Signature	17/03/2025 Date
Belete Berhanu External Examiner	Signature	17/03/2025 Date
Tensay Gebremedhin Chair person	Signature	17/03/25 Date

UNDERTAKING

I affirm that the thesis titled "Dam Breach Analysis Using HEC-RAS 2D flow Method for ynada Dam" is my original work. This research has not been submitted elsewhere for assessment. Any material sourced from other authors has been appropriately credited

NAME AMIR KEMAL HASSEN

SIGNITURE

DATE 14/03/2025

ABSTRACT

The construction of dams offers numerous advantages to society, but the failure of dams has led to some of the most devastating flood disasters. Given that many dams are being built in Ethiopia so it is important to assess the potential for dam failure to prevent harm to downstream areas. Yanda Dam is also one them which currently under construction for irrigation purposes. This study analysis uses HEC-RAS 2D model to simulate breach events at Dam and examine the resulting consequences downstream.

After analyzing the hydrology of the study area HEC-HMS was used to produce PMF hydrographs based on PMP values and hourly hyetographs, which were critical for simulating dam breach scenarios within HEC-RAS. The generated hydrographs allowed for the representation of extreme hydrologic conditions and simulation of the breach dynamics and the subsequent downstream flooding. This is also critical for simulating the worst-case flood scenario associated with a dam breach.

The breach parameter (the Breach Width, Breach Side Slopes, and Breach Formation Time) is determined based on Dam and Reservoir Characteristics. Then the model is run using 2D unsteady flow method to route the inflow hydrograph, the result output shows failure of the dam causes significant amount of human life loss and economic loss. HEC-RAS 2D model predict at the dam failure the breach outflow Q = 14441.92m3/s, V = 7.9m/s and depth of flood 35.19m.

The study produces an Inundation Map that shows potential flooding areas to enhance decision-making processes and early warning systems with a comprehensive emergency action plan to enhance preparedness, improve response coordination, and ultimately save lives while minimizing economic losses during flood events.

ACKNOWLEDGMENTS

I want to sincerely thank Dr. Dr. Daneal F/Selassie my advisor, for all of his help and support during this research endeavor. His knowledge and perceptions have tremendously improved my work.

I am grateful to Ethiopian Construction Design and Supervision Works Corporation Hydropower & Head Work Staffs, Ministry of Water and Ethiopian Meteorological Agency for providing me valuable data.

I am extremely grateful for my parents for their prayer and tireless support, I also wish to thank my friends and my class mate for their support for information sharing and positive ideas.

Contents

List of Tables

List of Figures

ABBREVATIONS

ECDSWC	Ethiopian Construction Design and Supervision Works
WMO	World Meteorological Organization
HEC-RAS	Hydrologic Engineering Center - River Analysis System
HEC-HMS	Hydrologic Engineering Center-Hydrologic Modeling System
DEM	Digital Elevation Model
PMP	Probable Maximum Precipitation
PMF	Probable Maximum Flood
2D	Two Dimensional
HD	Head Water
SCS	Soil Conservation Service
UH	Unit Hydraulic
HS	Hydraulic Structure
LULC	Land Use Land Cover
GIS	Geographical Information System
SA/2D	Storage A rea 2-Dimensional Connection
MLR	Multiple Linear Regression
CN	Curve Number

1 INTRODUCTION

1.1 Background

A vital component of human civilization throughout history has been the Construction of dams. One of the most primitive engineering feats of humankind was probably building reservoirs for water supply. Antiquated historical narratives provide ample evidence of the importance of dams across time. In particular, for civilizations that mostly depend on irrigation, dam development and collapse have been closely linked (R.B. Jansen 1983).Dam failure has resulted in catastrophic flooding and dire implications for human life, despite the fact that dams are essential for meeting peoples' needs.(FEMA,2013)

Hydrologic, geological, seismic, and structural problems are some of the causes of dam failure. Dams can improve downstream development safety when it is properly designed, built, and operated. However, the possibility of a dam failing might make the impoundment of water by a dam a more dangerous situation for developments downstream than it would be in the absence of the dam. (FEMA 2004).

In the past few decades, there have been continuous efforts to improve our understanding of the theoretical foundations and practical aspects of dam failures because real-time field observations pose a challenge. Much research has been conducted on several hydrological and non-hydrological events, for extreme flood events using Probable Maximum Flood (PMF) Breach Condition and for Non-Hydrological events using Normal flow (Sunny Day) Breach Condition. (ICOLD 2009)

Modeling a dam breach requires predicting the dam breach hydrograph and then routing it downstream. There are several modeling tools for dam breach modeling, ranging from basic to advance. With the progress in GIS-based modeling, many models can connect with digital terrain data to generate automated dam breach inundation zone delineations. (FEMA 2013)

The analysis of dam collapses is intricate, and there is incomplete understanding of many historical dam failures. The main uncertainties in calculating the outflow from a dam failure relate to the manner and extent of the failure. (FEMA, 2013)

Ethiopia is heavily involved in the development and management of water resources, with a substantial number of dams serving various purposes such as hydroelectric power generation,

irrigation support, and flood control. Several dams are currently under construction, including the Yanda Dam.

The dam's ability to withstand a flood safely is being assessed through dam breach analysis using the HEC-RAS 2D Model at Yanda Dam.

According to Mesfin Kere's "Geotechnical Evaluation and Remediation Strategy for Seepage, Piping, and Liquefaction Hazard at Yanda Dam," the proposed project is located on deep alluvial deposits with shallow groundwater conditions. Seepage, liquefaction, and piping problems might arise from these conditions and affect the dam. A cutoff wall and a clay core trench to prevent seepage and piping are two of the corrective actions recommended by the study, which analyzes the foundation conditions using both empirical and numerical approaches. In order to further inhibit piping by creating a low-permeability barrier, it is also advised to utilize a soil-bentonite slurry.

Alluvial soil, or loose sediment, is composed of materials such as clay, silt, sand, gravel, cobbles, and boulders that have been eroded by streams. Based on the research findings, the dam foundation has been identified as vulnerable to liquefaction and piping, prompting the recommendation of corrective actions to mitigate these hazards.

1.2 Statement of the Problem

Hydraulic and hydrological aspects of dam breaks have become more important in water resource planning, environmental protection, and ecology management due to the possibility of extreme weather events caused by climate change and the devastating impact of past dam collapses.

There will be socioeconomic development downstream, as the construction of a dam provides economic benefits through increased agricultural output, balancing water availability with demand, providing flood protection, and facilitating fishing. To ensure this stability downstream and to prevent the damage that occurs after a dam failure, it is necessary to assess the dam failure scenario.

The Yanda Dam is situated upstream of heavily populated villages, and a dam failure could endanger the lives of a significant number of people. The dam is categorized as high risk, and the potential failure of the Yanda Dam is projected to pose moderate to high economic risk (EDCSWC). Due to the lack of documented data on dam breaches in the country, it is necessary

to conduct a pre-event analysis of the dam breach simulation for the Yanda Dam. The dam area experiences flash floods with extremely short-lived high energy, so the dam's capacity to safely withstand these floods needs to be assessed

1.3 Research Question

- ✓ How can we estimate dam breach parameters using validated empirical formulas for earthen dams?
- ✓ What methods can we use to determine the discharge from the dam based on various inflow hydrographs, including design flood and probable maximum flood scenarios?
- ✓ Which hydrodynamic modeling techniques are appropriate for modeling and routing these discharges downstream?
- ✓ How do we simulate water movement through the river or channel network and compare the results with historical flow data when applicable?
- ✓ What approaches can we take to analyze changes in downstream impacts, particularly regarding economic, social, and environmental factors?
- ✓ How can we create inundation maps to visualize potential flooding scenarios and assist in risk assessment and emergency response planning?

1.4 Objective of the Study

1.4.1 General Objective

To evaluate dam failure scenario on Yanda Dam and its failure impact on downstream areas by using 2D HEC-RAS unsteady flow modeling.

1.4.2 Specific Objective

- ✓ Estimate dam breach parameters using validated empirical formulas relevant to earthen dams.
- ✓ Determine the discharge from the dam based on inflow hydrographs of probable maximum flood scenarios.
- ✓ Model and route these discharges downstream using appropriate hydrodynamic modeling

techniques.

- ✓ Simulate water movement through the river or channel network, comparing results against historical flow data where applicable.
- ✓ Analyze changes in downstream impacts, focusing on economic, social, and environmental factors.
- ✓ Prepare inundation maps to visualize potential flooding scenarios and inform risk assessment and emergency response planning.

1.5 Significance of the Study

This study investigates the effects of dam breaches on the downstream area, focusing on potential loss of life and the economic repercussions of dam failures. The inundation maps illustrate the results of downstream routing, showing breach-wave travel times, maximum flow depths, and peak velocities at key downstream locations. These maps highlight habitable structures in the affected area.

The model assesses the economic, social, and environmental impacts of dam failure, including disruptions to social patterns, loss of services from local institutions, and reduced recreational opportunities. Environmental consequences encompass water and soil pollution, habitat loss, and stream bank erosion.

Emergency action plans (EAPs) for dam breaches are vital to minimizing risks to lives and property. Key components include identifying population density and infrastructure, establishing clear evacuation routes for affected communities, and collaborating with emergency management agencies, law enforcement, and fire services. Public awareness campaigns are also essential

1.6 Scope of the Study

Probable Maximum Precipitation (PMP) is estimated using statistical methods based on a 30-year rainfall dataset. Once the PMP is determined, hydrologic modeling is employed to generate the Probable Maximum Flood (PMF) hydrograph. This is typically done using the HEC-HMS (Hydrologic Engineering Center's Hydrologic Modeling System), which simulates

rainfall-runoff processes to predict the flood response of a watershed under extreme precipitation conditions. Two-dimensional (2D) hydrodynamic routing is conducted within the context of unsteady flow analysis.

The study also analyzes the impacts of dam breaches on communities, economies, and ecosystems. In the context of HEC-RAS (Hydraulic Engineering Center's River Analysis System), breach parameters typically include defining the breach width, side slopes, and formation time. Selecting appropriate breach parameters requires considering several factors, such as the type of dam, its dimensions, and the materials used in its construction. These parameters are essential for understanding and predicting the potential consequences of a dam failure.

To simulate downstream flooding after a breach occurs, RAS Mapper generates floodplain boundaries in conjunction with a Digital Elevation Model (DEM). The DEM provides detailed elevation data, which helps determine the floodplain's elevation and predicts how floodwaters will spread across the landscape

2 LITRATURE REVIEW

Dam is a structure Construct over a river or stream to restrict and manage the water's flow. Dams can be constructed with a variety of materials, such as rock, concrete, and soil, and they have a variety of uses. The primary uses and varieties of dams are as follows: build reservoirs upstream that are used for drinking, irrigation, and industrial processes, among other things. These reservoirs help control river flow, particularly during times of high precipitation. In dry areas, agricultural irrigation using stored water can increase crop yields. Important infrastructure, dams are essential for managing water supplies, preventing floods, producing energy, and facilitating leisure activities. However, to minimize any potential negative effects on the environment and society, care must be taken throughout building and operation.

Embankment dams filled with earth may have a water-tight core constructed from asphalt concrete. These dams are known as concrete-asphalt core embankment dams. The majority of concrete-asphalt dams utilize rock and/or gravel as the primary fill material. Areas prone to earthquakes find these dams particularly suitable because of the asphalt core's flexibility. (FEMA 2013)

Rock-fill dams consist of compacted earth fill and larger particles. The fill has good drainage properties, eliminating the need for a separate drainage layer. In order to prevent seepage, an impervious zone is incorporated into the upstream side of the dam or within the embankment. The impervious zone can be constructed using various materials such as masonry, concrete, plastic, steel pile sheets, timber, or clay. When clay is used, it is typically separated from the fill by a filter to prevent erosion of the clay into the fill material.

2.1 Common Dam Failure Mechanism

Floods of varying sizes can occur naturally as a result of intense precipitation or snowmelt, which causes hydrologic dam failures. The primary reasons behind hydrologic dam collapse include wave action and high velocity flow, overtopping, and structural overstressing.

2.1.1 Overtopping Failure

When a reservoir's water surface elevation rises above the dam's height, overtopping happens. Water may then flow over the dam's top crest, an abutment, or a low spot in the reservoir's rim. When a dam or spillway system is not built with the capacity to handle the subsequent flooding event, overtopping typically occurs. Another possible cause of a breakdown is improper operation of a reservoir's outlet system, which raises the dam's water level. (FEMA, 2013)

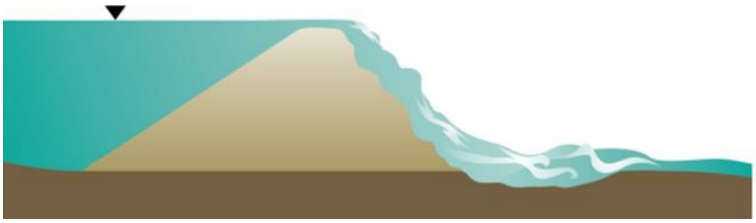

The breach is regarded as starting when erosion spreads across the dam crest. Once the breach begins at the top, it expands until it reaches its maximum size. (FEMA, 2013)

When the reservoir is empty and there is no longer any water to erode the dam, or when the dam has entirely eroded to the reservoir bottom or has hit bedrock, the breach may cease to spread (Gee, 2009). Either a linear or a sine wave progression can be used to model the breach evolution: (FEMA, 2013)

• Sine wave progression: breach expands very slowly at the beginning and conclusion of development and fast in between;

• Linear progression: rate of erosion remains constant throughout erosion development

When comparing linear and sine wave progression models across a case study in HEC-Hydrologic Modeling System (HMS) and HEC-RAS, the State of Colorado Department of Natural Resources found no discernible differences (2010). (FEMA, 2013)

2.1.2 Piping Failure

Concentrated seepage inside an embankment dam leads to piping. Large holes in the earth are left behind when the seepage gradually erodes the base or embankment of the dam. Erosion has the potential to grow and result in catastrophic dam failure once it reaches the reservoir. A direct pipe connection between the reservoir water and the dam face might be made if sufficient

material erodes. It is nearly hard to stop the dam from failing after such a pipe link has established. Piping failures start in the dam face at a specific location and progress to a circular opening. The circular aperture continues to grow until it reaches the top of the dam, taking the form of a trapezoid. (FEMA, 2013)

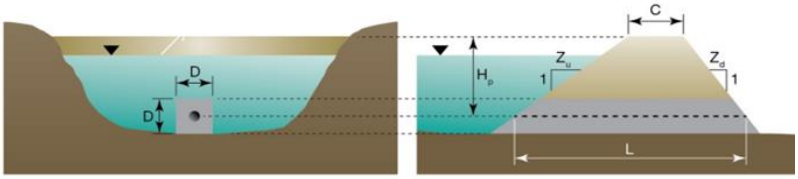

2.1.3 Structural Failure

The breakdown of a vital dam component may result in structural failures. The causes of structural failures can range from poor initial design to poor construction, poor materials used in construction, inadequate maintenance and repair, or weakening and gradual degradation over time.

2.1.4 Seismic Failure Modes

Dam breach analyses usually take into account two failure scenarios for embankment dams: seismic-induced pipework and liquefaction. A dam may be subjected to high stress during an earthquake, and soil liquefaction the transition of solid to liquefied soil may happen when soil is loaded. (FEMA.2013)

2.2 Dam Hazard Classification

Low Hazard Dam
Significant Hazard Dam

High Hazard Dam

2.2.1 Significance of Hazard

- **Low Hazard Dam**: - The failure of the dam can result in damage to unoccupied structures and

undeveloped areas, because of the remote location and lack of permanent structures for human habitation: minimal incremental damage, private agricultural lands, equipment, and isolated buildings; no disruption of services; and cosmetic or quickly reparable damage. (FEMA,2013)

- **Significant Hazard Dam**: -dam failure could put a few lives in danger or damage solitary homes, Uncertainty (rural area with few homes and only temporary or industrial development) Disruption of access to major public and private amenities.
- **High Hazard Dam**: - dam failure could potentially result in numerous fatalities or significant property damage to homes, commercial or industrial buildings, a public utility serving large-scale public and private infrastructure High expense of mitigation or impractical to mitigate (FEMA, 2013)

2.3 USACE HEC-RAS Program

The USACE HEC-RAS, launched in 1995, models steady and unsteady one-dimensional flows and performs four key tasks: water quality analysis, sediment transport analysis, steady-flow routing, and unsteady-flow routing. Its steady-flow component utilizes a standard step method for analyzing water surface profiles, accommodating subcritical, supercritical, and mixed flow regimes. Key computations are based on the one-dimensional energy equation, factoring in friction and channel changes. An upstream boundary condition, representing the maximum discharge from a breach, is necessary for steady-state analysis. (FEMA, 2013)

The unsteady component accounts for various flow regimes using the momentum and continuity equations derived from the St. Venant equations. It typically receives an inflow hydrograph from an upstream watershed for simulations. (FEMA, 2013)

HEC-RAS includes modeling for overtopping and piping failures, which can be adjusted for other failure modes. However, it does not estimate breach factors like width or development time, which are essential for accurate outflow and inundation predictions. (FEMA, 2013)

Inundation mapping is facilitated through RAS Mapper or HEC-GeoRAS, which generates data on floodplain boundaries and inundation depths using HEC-RAS results. (FEMA, 2013)

2.3.1 Two-Dimensional Models

Two-dimensional models are ideal for flat floodplain environments, effectively solving both channel and overland flow using shallow water equations (FEMA, 2013). Key two-dimensional models for dam breach analysis include DHI MIKE© and FLO-2D©. The DSS-WISE model, a simplified version of CCHE2D-FLOOD, can quickly generate inundation zones based on minimal input from dam owners, using existing data sources (FEMA, 2013).

FLO-2D simulates dam breach conditions, incorporating factors like overtopping and sediment movement, using dynamic wave momentum and conservation equations (FEMA, 2013). MIKE FLOOD combines various models (MOUSE, MIKE 11, MIKE 21) for flexible flood simulation in diverse environments, while XP-SWMM addresses complex flow patterns in urban settings and drainage networks (FEMA, 2013).

Inundation from dam breaches can be modeled using various approaches, including direct input of breach hydrographs and using dynamic simulations to visualize flow release and changes in topography (FEMA, 2013).

2.3.2 Parametric Regression Equations

Various empirical regression equations have been developed to estimate breach shapes and time-to-failure for different types of dams, based on case study data. These equations, grounded in hydraulic principles, facilitate the simulation of breach growth as a time-dependent linear process. The research uses data from rockfill dams, earthen dams, and those with impervious cores. Notable contributions to breach parameter estimation include equations from Froehlich (1995a, 2008), MacDonald and Langridge-Monopolis (1984), Von Thun and Gillette (1990), and Xu and Zhang (2009). The Xu and Zhang equations are particularly recognized for their comprehensive historical data. These regression formulas have been proven effective across various dam safety studies, providing a reliable range of values for earthen structures. (MEFA, 2013)

Froehlich(1995a): -Froehlich developed a set of equations to estimate average breach width, side slopes, and failure time using 63 earthen, zoned earthen, earthen with a core wall (i.e., clay), and rockfill data sets. The following ranges were present in the data that Froehlich used in his regression analysis (TD-39, 2014)

Height of the dams: 3.66 – 92.96 meters (12 – 305 feet)
(with 90% < 30 meters, and 76% < 15 meters)

Volume of water at breach time: 0.0130 – 660.0 m^3 x 10^6 (11 - 535,000 acre-feet)
(with 87% < 25.0 m^3 x 10^6, and 76% < 15.0 m^3 x 10^6)

Where:

B_{ave} = average breach width (meters)

K_o = constant (1.4 for overtopping failures, 1.0 for piping) V_w = reservoir volume at time of failure (cubic meters)

h_b = height of the final breach (meters) t_f= breach formation time (hours)

Froehlich states that the average side slopes should be:

1.4H:1V overtopping failures
0.9H:1V otherwise (i.e., piping/seepage)

Froehlich2008: - Dr. Froehlich revised his breach equations in 2008 in light of newly available information. Dr. Froehlich developed a series of equations to estimate average breach width, side slopes, and failure time using data sets from 74 earthen, zoned earthen, earthen with a core wall (i.e., clay), and rockfill. The following ranges were present in the data that Froehlich used in his regression analysis:

- **Height of the dams:** 3.05 – 92.96 meters (10 – 305 feet)
(with 93% < 30 meters, and 81% < 15 meters)
- **Volume of water at breach time:** 0.0139 – 660.0 m^3 x 10^6 (11.3 - 535,000 acre-feet)
(with 86% < 25.0 m^3 x 10^6, and 82% < 15.0 m^3 x 10^6)

Froehlich's regression equations for average breach width and failure time are:

$$B_{ave} = 0.27\ K_o\ V_w^{0.32}\ h_b^{0.04}$$

$$t_f = 63.2\sqrt{\frac{V_w}{g h_b^2}}$$

Where

B_{ave} = average breach width (meters)

K_o = constant (1.3 for overtopping failures, 1.0 for piping) V_w = reservoir volume at time of failure (cubic meters)

h_b = height of the final breach (meters)

g = gravitational acceleration (9.80665 meters per second squared) t_f = breach formation time (seconds)

Froehlich's 2008 paper states that the average side slopes should be:

1.0 H:1V overtopping failures
0.7 H:1V otherwise (i.e., piping/seepage)

MacDonald and Langridge-Monopolis(1984):- MacDonald and Langridge-Monopolis analyzed 42 data sets (primarily from rockfill and earthfill dams, including clay-core variants) to establish a "Breach Formation Factor." This factor is calculated by multiplying the water volume exiting the dam by the height of water above it. They correlated the volume of eroded material from the dam's embankment to this Breach Formation Factor. The regression study utilized specific data ranges for analysis. :(TD-39, 2014)

Wahl (1998) provided the MacDonald and Langridge-Monopolis equation for the volume of material degraded and the breach formation time.

For earthfill dams:

$$V_{eroded} = 0.0261\ (V_{out} * h_w)^{0.769}$$

$$t_f = 0.0179\ (V_{eroded})^{0.364}$$

For earthfill with clay core or rockfill dams:

$$V_{eroded} = 0.00348\ (V_{out} * h_w)^{0.852}$$

Height of the dams: 4.27 – 92.96 meters (14 – 305 feet)
(with 76% < 30 meters, and 57% < 15 meters)

Breach Outflow Volume: 0.0037 – 660.0 m^3 x 10^6 (3 - 535,000 acre-feet)
(with 79% < 25.0 m^3 x 10^6, and 69% < 15.0 m^3 x $10^{6)}$

The volume of material eroded from a dam embankment is called "eroded," measured in cubic meters. The water flowing through the breach, denoted as Vout, is calculated by adding the reservoir's volume at the time of the breach to the inflow, then subtracting the flow through gates and spillways. The depth of water above the breach is represented by hw, and tf denotes the time for breach formation.

Initially, Vout is an estimate based on the water in the reservoir when the breach occurs. After a breach analysis, a more accurate Vout can be determined, requiring recalculation of parameters iteratively. The breach dimensions are based on the volume eroded.

MacDonald and Langridge-Monopolis suggest a trapezoidal breach with a side slope of 0.5H:1V, assuming horizontal erosion until reaching the dam's abutments or vertical erosion to its bottom. The base width of the breach is calculated using the dam's shape as a reference.. :-(TD-39, 2014)

$$W_b = \frac{V_{eroded} - h_b^2 \ (CZ_b + h_b Z_b Z_3 / 3)}{h_b (C + h_b Z_3 / 2)}$$

Where

W_b = bottom width of the breach (meters)

h_b = height from the top of the dam to bottom of breach (meters) C = crest width of the top of dam (meters)

$Z_3 = Z_1 + Z_2$

Z_1 = average slope (Z_1:1) of the upstream face of dam

Z_2 = average slope (Z_2:1) of the downstream face of dam

Z_b = side slopes of the breach (Z_b:1), 0.5 for the MacDonald method

Von Thun &Gillette (1990): -To construct their methods, Von Thun and Gillette employed 57 dams from two different papers: the MacDonald and Langridge-Monopolis (1984) paper and the Froehlich (1987) paper. Except for dams with cohesive soils, where side slopes should be on the range of 0.5H:1V to 0.33H:1V, the approach suggests using breach side slopes of 1.0H:1.0V. The ranges of the data Von Thun and Gillette used in their regression analysis were as follows:

Height of the dams: 3.66 – 92.96 meters (12 – 305 feet)
(with 89% < 30 meters, and 75% < 15 meters)

Volume of water at breach time: 0.027 – 660.0 m^3 x 10^6 (22 - 535,000 acre-ft)
(with 89% < 25.0 m^3 x 10^6, and 84% < 15.0 m^3 x 10^6)

The Von Thun and Gillette equation for average breach width is:

$$B_{ave} = 2.5\, h_w + C_b$$

Were

B_{ave} = average breach width (meters)

h_w = depth of water above the bottom of the breach (meters)

C_b = coefficient, which is a function of reservoir size, see the following table.

For the breach development time, von Thun and Gillette created two distinct sets of equations. The breach development time as a function of water depth above the breach bottom is displayed in the first set of equations. (TD-39,2014)

Table 1coefficient a function of reservoir size

Reservoir Size (cubic meters)	C_h (meters)	Reservoir Size (acre-feet)	C_h (feet)
$< 1.23 \cdot 10^6$	6.1	< 1,000	20
$1.23 \cdot 10^6 - 6.17 \cdot 10^6$	18.3	1,000 - 5,000	60
$6.17 \cdot 10^6 - 1.23 \cdot 10^7$	42.7	5,000 - 10,000	140
$> 1.23 \cdot 10^7$	54.9	> 10,000	180

$$t_f = 0.02\, h_w + 0.25 \qquad \text{(erosion resistant)}$$

$$t_f = 0.015\, h_w \qquad \text{(easily erodible)}$$

Where:

t_f = breach formation time (hours)

h_w = depth of water above the bottom of the breach (meters)

The second set of equations represents the average breach width and water depth above the bottom of the breach as functions of breach development time. (TD-39, 2014)

$$t_f = \frac{B_{ave}}{4 h_w} \qquad \text{(erosion resistant)}$$

$$t_f = \frac{B_{ave}}{4 h_w + 61.0} \qquad \text{(easily erodible)}$$

Where

B_{ave} = average breach width (meters)

Xu and Zhang (2009): - Drs. Xu and Zhang published a study in the 2009 Journal of Geotechnical and Geo-Environmental Engineering, analyzing 182 earth and rockfill dams from China and the U.S., half of which were over 15 meters tall. Due to insufficient data, their analysis ultimately focused on 75 dams of various types, such as concrete fronted and zoned-filled. In their calculations, only 28 dam failures were used for determining collapse duration and 45 for average breach width. .(TD-39,2014)

Height of the dams: 3.2 – 92.96 meters (10 – 305 feet)
(with 78% < 30 meters, and 58% < 15 meters)

Volume of water at breach time: 0.105 – 660.0 m^3 x 10^6 (11.3 - 535,000 acre-feet)
(with 80% < 25.0 m^3 x 10^6, and 67% < 15.0 m^3 x 10^6)

Xu and Zhang's regression equation for average breach width is:

$$\frac{B_{ave}}{h_b} = 0.787 \left(\frac{h_d}{h_r}\right)^{0.133} \left(\frac{V_w^{1/3}}{h_w}\right)^{0.652} e^{B_3}$$

Where:

B_{ave} = average breach width (meters)

V_w = reservoir volume at time of failure (cubic meters) h_b = height of the final breach (meters)

h_d = height of the Dam (meters)

h_r = fifteen meters, is considered to be a reference height for distinguishing large dams from small dams

h_w = height of the water above the breach bottom elevation at time of breach (meters)

B_3 = b3+b4+b5 coefficient that is a function of dam properties

b_3 = -0.041, 0.026, and -0.226 for dams with corewalls, concrete faced dams, and homogeneous/zoned-fill dams, respectively

b_4 = 0.149 and -0.389 for overtopping and seepage/piping, respectively.

b_5 = 0.291, -0.14, and -0.391 for high, medium, and low dam erodibility, respectively

2.3.2.1 **Breach Parameter Definitions**

The following definitions are widely recognized for evaluating and selecting dam breach parameters:

- ✓ **Breach Formation Time (or Time-to-Failure)**: This is the time interval from the initial breach of the dam's upstream face (breach initiation) to when the breach reaches its maximum dimensions. (FEMA,2013)
- ✓ **Breach Depth (or Breach Height)**: This refers to the vertical measurement of the breach, taken from a designated elevation down to the bottom of the breach.
- ✓ **Breach Width**: This is the average width of the breach at its final stage, typically measured at the vertical midpoint of the breach. (FEMA,2013)
- ✓ **Breach Side Slope Factor**: This describes the angle of the breach sides, expressed as X horizontal to 1 vertical (XH: 1V). (FEMA,2013)

A dam breach typically occurs in two main phases: breach initiation and breach formation.

- ➢ **Breach Initiation**: In this phase, the flow through the dam is minimal, and the structure is not considered to have failed. If flow is managed properly, it may be possible to prevent a breach during this stage. (FEMA,2013)

- **Breach Formation**: This phase begins when the flow through the dam increases and moves uncontrollably from the upstream to the downstream face, ultimately leading to the dam's failure. (FEMA.2013)

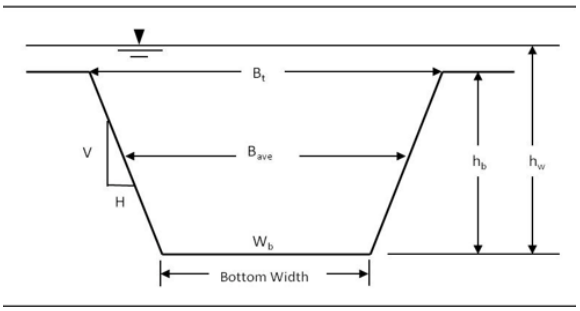

Figure 1Breach Shape

2.3.3 Flood Routing Method

Routing the incoming flood through a reservoir, determining the features of a dam break, and problems with downstream routing.

HEC-RAS can be used to route an inflowing flood hydrograph through a reservoir with any of the following three methods:

A reservoir will be routed using HEC-RAS using one of three techniques for an inflowing flood hydrograph.

- ✓ One-dimensional unsteady flow routing (full Saint Venant equations);
- ✓ Two-dimensional unsteady flow routing (Full Saint Venant equations or Diffusion wave equations); or
- ✓ Level pool routing (TD-39,2014)

2.3.3.1 1D Dynamic Routing

1D flow is calculated through a series of cross-sections along a river or path. 1D modeling requires knowledge of the flow path before laying out the model cross sections. The formulas are based on the supposition that the forces acting on a body of water are concentrated in one direction, x, along the centerline of the river channel. Discretized of the St. Venant Equation are used to solve Stage and Flow at each Cross-Section Simultaneously for each time step.

For both with and without breach scenarios, full unstable flow routing (one- or two-

dimensional) will be more precise. In addition to capturing the change in water surface slope that happens after a dam breach, the unstable flow routing approach can also record the water surface slope through the pool when the inflowing hydrograph arrives. (TD-39, 2014)

2.3.3.1 **2D Dynamic Routing**

2D simulations run through a mesh, solving flow one cell at a time, designing in 2D means using polygons, which are more flexible and can more accurately represent the real world. When the water's flow path is not entirely known for every occurrence, 2D modeling will be more precise and user-friendly. 2D models can manage events where the flow path changes. The equations are based on the supposition that the forces operating on a body of water are primarily directed in two directions: x (along the centerline of the river channel) and y (laterally across the channel or floodplain). Discretized of the St. Venant Equation are used to solve Stage and Flow at each cell mesh in a 2D Mesh. (TD-39, 2014)

2.3.3.1 **Level Pool Routing**

The pool area is modeled with a storage area Level Pool Routing requires an elevation-volume curve that describes the reservoir. The breach discharge will be calculated using the same equations as the whole dynamic wave approach when a dam break is modeled. The storage area will provide the dam with water, and when water flows out of the breach, the elevation of the storage area will decrease to form a level pool. That is the sole difference. (TD-39, 2014)

2.3.3.2 **Hydraulic Equation for 2D Unsteady Flow Analysis**

The downstream routing involves solving equations that describe the flow of water under various conditions. These equations can vary depending on the type of flow, the geometry of the channel, and the topography of the area. The primary equations used in downstream routing during a dam breach analysis

- A **continuity equation** (mass conservation)
- Two **momentum equations** (momentum conservation) in the x- and y-directions.

Mass Conservation (Continuity equation)

Assuming the flow is incompressible, the unsteady differential representation of the mass conservation (continuity) equation is

$$\frac{\partial H}{\partial t}+\frac{\partial(hu)}{\partial x}+\frac{\partial(hv)}{\partial y}+q=0$$

where

t is time, u and v are the velocity components in the x- and y- direction respectively and q is a source/sink flux term.

V=(u,v) is the velocity vector(CPD-69,2016)

This equation explains that any variation in water depth over time is matched by the movement of water either entering or leaving a specific area, as well as by any additional sources or losses of water. (B.R. Hogse, 2019)

Momentum Equation (Conservation of Momentum)

Volume conservation suggests that the vertical velocity is low when the horizontal and vertical length scales are significantly larger. The pressure is almost hydrostatic, and this can be supported by the Navier-Stokes vertical momentum equation. A vertically-averaged version of the momentum equation suffices when there is no non-hydrostatic pressure, severe wind forcing, or baroclinic pressure gradients (varying density). It is safe to ignore the vertical velocity and vertical derivative elements (in the equations for mass and momentum).

$$\frac{\partial u}{\partial t}+u\frac{\partial u}{\partial x}+v\frac{\partial u}{\partial y}=-g\frac{\partial H}{\partial x}+v_t\left(\frac{\partial^2 u}{\partial x^2}+\frac{\partial^2 u}{\partial y^2}\right)-c_f u+fv$$

Where g is the gravitational acceleration, vt is the horizontal eddy viscosity coefficient, cf is the bottom friction coefficient, R is the hydraulic radius, and f is the Coriolis parameter.

The velocities in the Cartesian directions are represented by u and v. the acceleration terms are on the left side of the equation. The forces acting on the fluid from the inside or outside are represented by the right side. The momentum equations are ultimately derived from Newton's second law, which dictates how the left- and right-hand side terms are normally arranged. (CPD-69, 2016)

One alternative representation of the momentum equations is a single differential vector form. The equation becomes more understandable and concise in this format, which is an advantage. The momentum equation has the following vector form:

$$\frac{\partial V}{\partial t} + V \bullet \nabla V = -g\nabla H + \nu_t \nabla^2 V - c_f V + fk \times V$$

where the differential operator ∇ represents the vector of partial derivative operators defined as $\nabla = \left(\frac{\partial}{\partial x}, \frac{\partial}{\partial y}\right)$, and k is the unit vector pointing in the vertical direction. (CPD-69,2016)

The equation features a conservative representation of nonlinear advection, with all variables contained within the gradient. (Ben.R.Hodges .2019)

Manning's n

Choosing the right Manning's n value significantly affects the accuracy of computed water surface elevations. Several factors influence this value, including surface roughness, vegetation, channel irregularities, alignment, and other conditions. Whenever measured data or high-water marks are available for water surface height, Manning's n values should be adjusted accordingly. It is advisable to base these adjustments on n values from similar streams or experimental data when gauged data is unavailable. (CPD-69, 2016)

$$n = \frac{R^{1/6}}{18 \log_{10}\left[12.2\frac{R}{k}\right]}$$

Where

n=Manning's roughness coefficient

R = Hydraulic radius (m)

k = equivalent roughness (m)

Review Paper 1

In Fasika Worku's study titled "Dam Breach Modeling and Flood Mapping: A Case Study of Ribb," the author discusses the Ribb Dam and Irrigation Development Project, situated on the eastern side of the Lake Tana Sub Basin within the administrative boundary of the South Gondar Zone in the Amhara National Regional State.

The study employs HEC-RAS 5.0.7 for dam breach modeling, specifically examining overtopping and piping as potential modes of failure. This modeling approach incorporates geometric data from the dam, including its type (Earth-Rockfill Dam), construction materials

(compacted clay core with central rockfill), and various physical specifications such as crest elevation (1945.50 m above sea level), height (72.50 m), and reservoir capacities (235.00 Mm^3 at normal water level and 270.00 Mm^3 at maximum water level).

Breach parameters were calculated using established equations from previous studies, including those by Froehlich, MacDonald and Langridge-Monopolis, Von Thun and Gillette, and Xu and Zhang. The hydrologic data includes flood event hydrographs and reservoir capacity from WWDSE (2007). The author generates 1.45PMF, 1.5PMF, and 1.55PMF inflow hydrographs. The modeling assessed the dam's capacity to manage the PMF inflow without breaching and considered various methodologies to evaluate worst-case scenarios.

The findings revealed that the dam could safely discharge the PMF inflow during the PMF scenario via the spillway without resulting in a breach. However, the author used the 1.5 PMF inflow value, asserting that the dam would fail due to overtopping at this level. The overtopping failure mode, including peak values and times to peak, was meticulously documented. The worst-case scenario for piping failure utilized the Von Thun and Gillette method, revealing potential impacts on twenty-five kebeles across two woredas, with additional effects noted in the Farta and Ebenat woredas.

According to the analysis presented in the study, the Von Thun and Gillette method was chosen. Although the MacDonald and Langridge-Monopolis method and the Xu and Zhang method yielded better results with lower percentage differences in peak discharge values (20.31% and 21.42%, respectively), the overall findings indicated inconsistencies in these methods. The author explicitly stated, "No method is consistent," leading to the decision to adopt the Von Thun and Gillette method based on its conservative approach to risk assessment. This approach often prioritizes caution in hydrological modeling and flood mapping scenarios..

Review paper 2

In Abdulawel Umer's study on Dam Breach Modeling and Inundation Mapping for Dabus Dam, the author stated that the Dabus Dam, located in the Abbay River Basin, Benishangul-Gumz National Regional State, features a rock-fill design with a central clay core. To simulate potential dam breach scenarios, HEC-RAS v5.0.1 software was utilized, employing a 1D flow Hydrological data were obtained from the Water Works Design and Supervision Enterprise, which included inflow hydrographs, probable maximum flood (PMF), and reservoir capacity metrics. The analysis focused on two failure scenarios: piping and overtopping, which took

into account various hydrologic and non-hydrologic events. Breach parameters were derived from geometric data of the dam using four established regression equations: MacDonald et al., Xu & Zhang, Von Thun and Gillette, and Froehlich (2008). Key geometric figures included a crest elevation of 1,011 m.a.s.l. and a reservoir capacity of 121.48 Mm^3.

The overtopping failure was assessed using a simulation corresponding to a 10,000-year return period, with the reservoir at full capacity; however, the model showed that it evacuates safely. The author stated that the model checked for PMF, but the PMF inflow surpassed the dam's capacity, resulting in potential overtopping.

The breaching simulations indicated a significant risk, with an estimated affected population of 47,076 in Menge Wereda and 1,666 in Oda Bildigilu Wereda. The breach parameters calculated using the different methods yielded varying peak outflows and times to peak. Using MacDonald et al. parameters, the maximum breach outflow was 9,702 m^3/s, with a time to peak of 2.86 hours. In contrast, the Von Thun and Gillette method suggested a peak outflow of 14,220 m^3/s and a time to peak of 0.91 hours. Other methods reported maximum outflows of 8,838.36 m^3/s and 1,316.61 m^3/s, with respective times to peak of 2.54 hours and 5.41 hours.

For the piping failure simulation at normal pool levels, peak outflows ranged between 12,514.57 m^3/s and 12,891.53 m^3/s, with corresponding times to peak varying significantly among the methods used. The Froehlich (2008) methodology was specifically noted for its illustration of the inundated area due to the breach.

Overall, the analysis reveals significant potential risks associated with the Dabus Dam, underlining the critical need for ongoing monitoring and risk management strategies to protect surrounding communities.

Review paper 3

In Kibire Tesssema study “Dam Breach Analysis and Flood Inundation Mapping For Lower Awash Multipurpose Dam”. According to the author the Middle Awash Multipurpose Dam project, located in the Middle Awash Valley, focuses primarily on flood control and irrigation management. A comprehensive breach analysis was conducted using HEC-RAS 5 Beta Version to evaluate potential dam failures due to overtopping and piping. The inflow design flood, generated from PMF, was used for dam breach analysis. PMF is estimated using Probable Maximum Precipitation (PMP) through the HEC HMS model. The PMF inflow hydrograph for the Middle Awash catchment, from the WWDSE (2015) hydrological study,

estimates a peak of 4483.6 m³/s for the 10,000-year return period flood.

For the breach analysis, key dam parameters were defined: the dam height was 120 m with a crest elevation of 943 m and a spillway crest elevation of 926 m, a total capacity of 501 million cubic meters, and it was characterized as an earth dam with a clay core rock-fill structure. Three breach methods (MacDonald, Froehlich 1995, and Froehlich 2008) were employed to estimate peak breach outflows.

The results indicated varying peak outflows depending on the failure mode and computational method:For MacDonald breach parameters, peak outflows were 62,888.9 m³/s (overtopping) and 72,688 m³/s (piping).For Froehlich (1995), peak outflows reached 111,663 m³/s (overtopping) and 118,039 m³/s (piping).For Froehlich (2008), estimated peak outflows were 104,814 m³/s (overtopping) and 100,045 m³/s (piping).These peak outflows corresponded to substantial releases of water, ranging from approximately 4.63 to 4.76 billion cubic meters, highlighting the potential catastrophic impact of a dam failure on surrounding communities and infrastructure. The findings underscore the importance of rigorous breach analysis in dam engineering and flood risk management.

Review paper 4

In Yonatan Sisay's study “Dam Breach Analysis & Inundation Map for Melka Wakena Dam,” the author indicates that the study area is centered on the Melka Wakena Dam, which is a rock-fill structure located on the Wabe Shebelle River in the Bale Zone highlands. The study employed HEC-RAS version 4.1 to simulate one-dimensional unsteady flow, utilizing inflow hydrograph data from flood events provided by the dam owner. The methodology specifically examined potential failure modes, including overtopping and piping, under probable maximum flood (PMF) and fair-weather conditions.

Key physical characteristics of the dam, such as a crest length of 2,000 m, a crest width of 10 m, and a maximum height of 42 m, were used to calculate breach parameters. Hydrographs generated from three days of half PMF were used for both spillway design and breach analysis. The study calculated regression equations to estimate breach parameters using the following three methods: Froehlich (1995a), Froehlich (2008), and MacDonald and Langridge-Monopolis (1984).

The modeling yielded peak flow estimates for the various scenarios as follows: Froehlich (1995a) produced peak flows of 35,494.02 m³/s (overtopping) and 25,255.13 m³/s (piping).

Froehlich (2008) showed values of 28,067.77 m^3/s (overtopping) and 25,087.70 m^3/s (piping). MacDonald and Langridge-Monopolis provided the highest values at 36,527.15 m^3/s (overtopping) and 32,627.70 m^3/s (piping).

In conclusion, the study selected the peak flow values generated by the MacDonald and Langridge-Monopolis method for downstream routing, inundation mapping, and emergency action planning, highlighting the importance of reliable model results in dam safety assessments.

Review Paper 5

In Addisalem Eyob's study "Dam Breach Analysis and Flood Inundation Mapping for Lower Awash," the focus is on a zoned earth-rock fill dam in the Afar Region's Awash Basin, built on the Logia River. Due to low rainfall reliability in January, February, October, and December, agriculture relies entirely on irrigation. The dam has a crest length of 335 meters, width of 10 meters, height of 48 meters, and is designed for a 10,000-year return period flood.

Data was collected from the Ethiopian Dam Control and Safety Work Environment (EDCSWE) and the Ministry of Water, addressing missing rainfall data through methods like double mass curve analysis. The Harshfield method was used to estimate Probable Maximum Precipitation (PMP), and inflow hydrographs were generated using SCS unit hydrographs.

Breach analysis utilized HEC-RAS version 5.0.3 with a focus on the piping failure mode, applying Froehlich (2008) and Von Thun & Gillette methods. Simulated outflows were 65,822 m^3/s for Froehlich and 60,072 m^3/s for Von Thun & Gillette, with the latter deemed more appropriate based on historical data. Findings indicated potential flooding risks downstream, threatening property and lives.

3 General Description of the Study Area

3.1 Location of the study area

The Yanda earth Dam and irrigation development project located in the rift valley lakes Basin, which is found in the southern part of the country; Konso Zone Konso wereda. The dam site is located at Easting 340704 and Northing 593322 UTM. The dam is proposed to be Construct on the Yanda River, one of the tributaries of the Segen River, which originates from the Delebana Mountains. The Yanda River flows in a southwest direction, leading to the location of the proposed dam.

Figure 2 Site Location by Google Earth

The watershed is found in the Segen River basin, and the catchment area extends to 670 sq. km. The river catchment is predominantly characterized by ephemeral streams typical of hilly areas upstream of the dam, as well as a flat valley where the dam site is located (ECDSWE).

The dam site is situated in a wide U-shaped valley, where the main channel features a wide meandering belt and relatively steeply sloping abutments on both sides. Near the dam site, the river has a meandering belt that spans 500 to 800 meters. The riverbed is at an elevation of 940.0 m.a.s.l. The dam site is nearly 3.2 km away from the widest command area, and there is a sufficient head difference between the command area and the dam outlet level. Exposed rock can be observed at the abutments, along with fine soil deposits mixed with coarse gravel in the curves of the stream channel. The center of the Yanda River contains thick alluvium deposits

that extend up to 50 m deep. The dominant coarse gravel alluvium deposit layer is intermingled

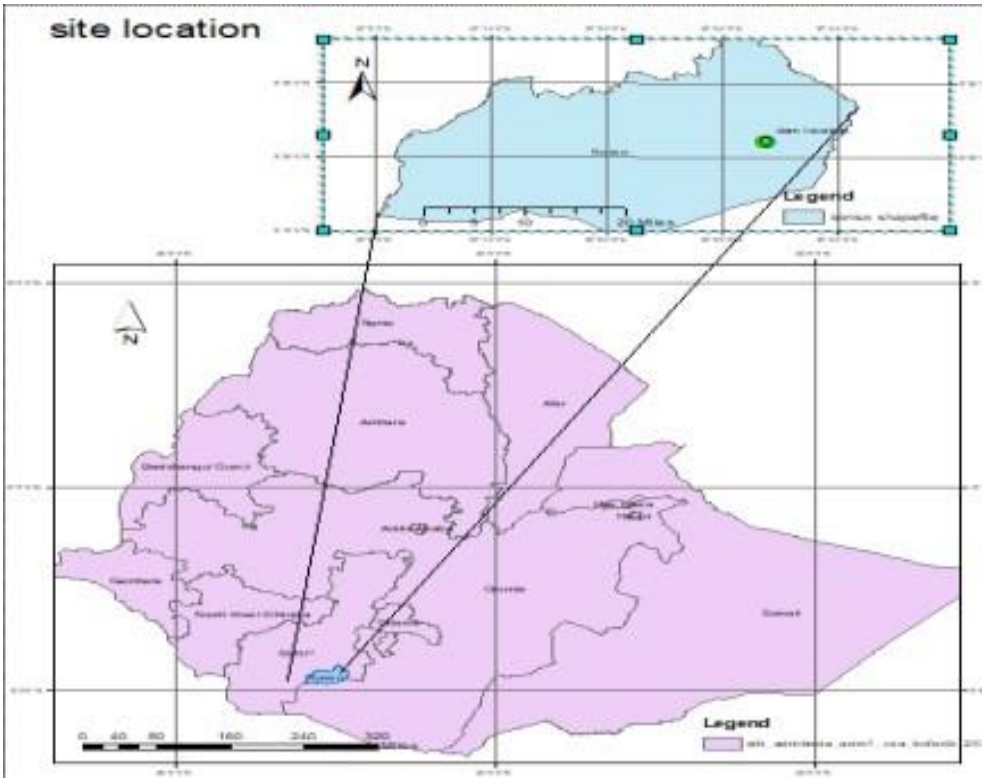

Figure 3 Site Location by regional on GIS

with silty sand, silty clay, clayey silt, silty sand, and silty gravel layers. Constant and falling-head permeability tests were carried out on the alluvium deposits, and according to the test results, the alluvium is classified as "low to semi-pervious" (k = 1.94 × 10^-7 cm/sec and 2.1 × 10^-4 cm/sec). (ECDSWE)

The dam is proposed to harness the surface water resource to supply water to the irrigable downstream of the dam

3.2 Climate of the area

According to the climate classification (D.Gemechu, 1977) Yanda watershed area is situated in the range of Cold humid zone to semi-arid zone. Specific to the dam site and command area the climate fails in semi-arid zone. (ECDSWC)

3.3 Hydrology of the Area

The dominant hydrology of the site is (yanda) appears to be flash flood with extreme short

lived high energy. Mean monthly rainfall pattern of the project area is bio-modal with major peak experiencing between February and May and second peak from September to October. The highest peak rainfall recorded in April and October, while the lowest rainfall recorded in July and January. (ECDSWC)

4 METHODOLOGY

4.1 Conceptual Framework

4.2 Data Collection

The process of data collection used for model simulation involves information gathered from different sources: rainfall data was collected from the Ethiopian Meteorological Agency, dam geometry data from the Ethiopian Construction Design and Supervision Work Enterprise, land use and land cover data from the Ministry of Water, and DEM data from the USBR portal (online database).

4.2.1 Rainfall data

The following data illustrates the rainfall patterns in my study area, as collected from the Ethiopian Meteorological Agency. This study focused on the nearest rainfall stations, which include Gato, Arfiade, and Konso. Each of these stations provided 30 years of recorded data, allowing for a comprehensive analysis of the rainfall trends over time. This information is crucial for understanding the local climate and its impact on the surrounding environment.

4.2.2 Stream flow Data

Stream flow data was collected from the Ministry of Water since my study area does not have recorded stream flow data. Consequently, the nearest stream flow data from the Weito River (Above bridge) station was used, which has similar topographic characteristics to my study area. This data is essential for transforming ungauged stream flow information and analyzing the trends in my river's stream flow. Additionally, it is useful for calibrating the HEC-HMS rainfall-runoff model results.

4.2.3 DEM Data

Digital Elevation Model (DEM) data is downloaded from the U.S. Geological Survey (USGS) Earth Explorer website. This dataset provides significantly higher resolution than other available resources, specifically a resolution of 12.5 meters. This high-quality data is used to conduct a comprehensive study of the Earth's topographic surface and terrain, enabling greater accuracy and detail in my analyses.

4.2.4 Dam Geometry

The geometric data of the dam, along with the reservoir capacity, is collected from the Ethiopian Construction Design and Supervision Works Corporation (ECDSWC), which indicates that the Full Reservoir Level of Yanda Dam is set at 975 meters (m.a.s.l.). It is designed to accommodate an estimated dead storage capacity of 8.87 million cubic meters and a live storage capacity of 26.52 million cubic meters. The dam type is a Zoned Earth (Shell)-fill dam with a clay core.

Top of dam to be provided 981.30 Full Reservoir Level 975

River Bed Level 940.0

Full Supply Level 975.0

Maximum Water Level 980.1

Dam Crest Level Including Freeboard 981.3

Dam height 42.3m (982.3 m.a.s.l dam crest level)

Reservior Capacity 46MCM

Dam Height up to MWL and Freeboard 41.3

Maximum dam height (above river bed) 42.3

Dam crest width 11.0m

Spillway Crest Level is 975.00m.a.s.l

Crest length 766.7m

Maximum Water Level corresponding to half PMF years is 980.10 m.a.s.l.

The optimized slope for downstream slope is 1:2.4(V:H)

The optimized slope for upstream slope is 1:2.2(V:H).

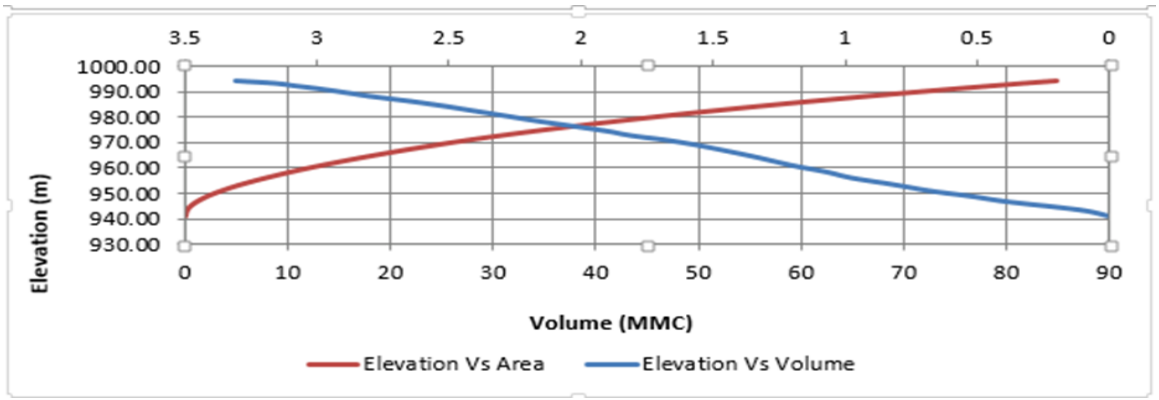

Figure 4Volume capacity curve

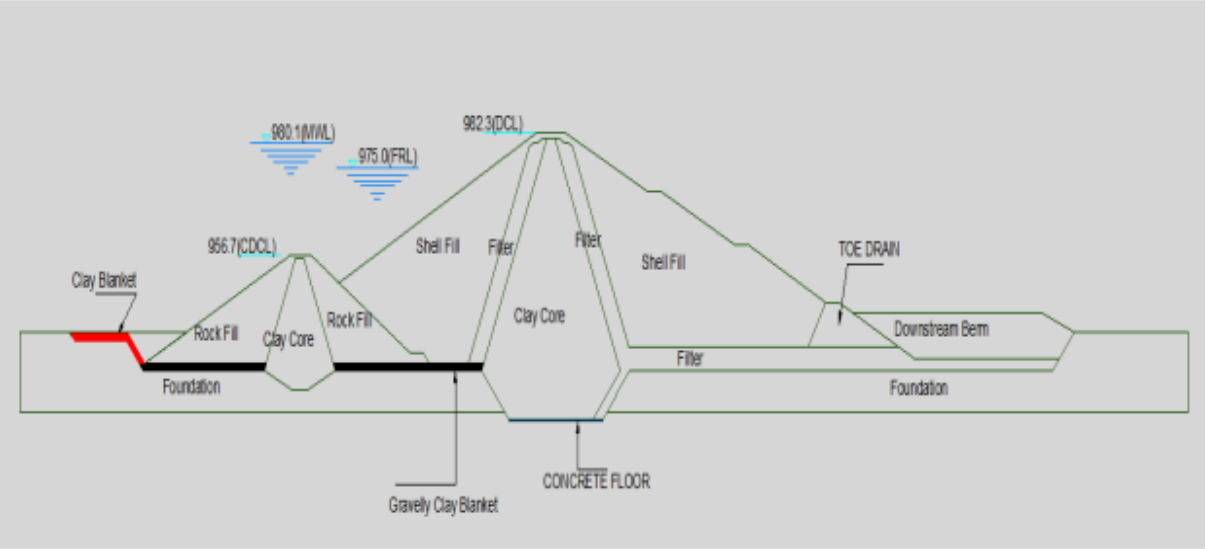

Figure 5Typical dam zoning section for Yanda dam

4.2.5 Material used

HEC-RAS 6.3.1 Version is used for my study to model dam breach simulation analysis. HEC-RAS (Hydrologic Engineering Center's River Analysis System) is a widely used computer program developed by the U.S. Army Corps of Engineers for modeling the hydraulics and hydrology of water bodies. HEC-RAS supports both steady and unsteady flow water surface profile calculations,1D, 2D and combined 1D and 2D hydrodynamics, sediment transport and mobile bed computations, water temperature analysis, and water quality analyses (including nutrient transport and fate). It also enables spatial mapping of many computed parameters, such as depth, water surface elevation, velocity, and more. (CPD, 69, 2016). It is particularly useful for dam breach analysis, assessing the potential impact of a dam failure on downstream areas. The software allows users to simulate various breach scenarios, including different breach shapes, sizes, and failure mechanisms (e.g., overtopping and piping). This flexibility enables analysts to understand the potential consequences of different types of breaches. Additionally, the program can produce flood inundation maps based on simulated breach events.

Furthermore, GIS version 10.4 is utilized for effective visualization of inundation areas by overlaying inundation maps on satellite imagery. This enhances the understanding of flood impacts and helps in identifying high-risk areas. GIS is also employed to quantify the area of

different Land Use/Land Cover (LULC) classes and soil types. Thematic maps can be created to visually represent the spatial distribution of LULC classes and soil types. These maps use color coding and symbols to depict various classes, making it easy to identify and interpret spatial relationships.

Additionally, HEC-HMS version 4.10 is used to assess rainfall-runoff patterns in the study area based on given rainfall inputs, modeling runoff effectively.

4.3 Data Analysis

Rainfall (precipitation) is one of the key inputs for this thesis. Three meteorological stations are selected (Konso, Gato, and Arfiade); the stations have a missing value.

Recording processes may be affected by human error or device malfunctions, which can lead to inaccurate recorded reading. The absence of data in rainfall time series can also significantly impact statistical analysis, affecting the likelihood of the process being in a wet or dry state and influencing the characterization of its extremes.

4.3.1 Preparation of Meteorological Data

4.3.1.1 **Filling Missing Rainfall Data**

Before using the rainfall records of a station. It is necessary to first check the data for Continuity and consistency.

Using Multiple Linear Regression method rainfall missing data was filled. When the errors are independent and regularly distributed, the approach works well. Its capacity to withstand outliers and to prevent overemphasizing large-tailed distributions is its primary advantage. (J.K.Eischeid, 1995)

It is a statistical technique for determining the relationship between a dependent variable and two or more independent, or predictor, variables.

Multiple linear regressions (MLR). Predict the dependent, or criterion, variable, finds the best-weighted combination of independent variables.

The methods yield the best result with the least error (M. Abdullah et al., 2022).

Most suitable methods for more than one neighboring station and have relatively high correlation coefficients (HH.P.G.M. Caldera et al. 2016).

$$Y = b_0 + \sum_{i=1}^{n}(b_i \times X_i)$$

Where

b_i i = 1, 2, 3, 4, …. n are the regression coefficients, and X_i is the daily rainfall at the nearest stations.

Rainfall data are estimated considering a linear correlation between the target station and some of the other (multiple) neighboring stations. Where Y = dependent variable, also called response variable (produced by the regression model).X = independent variable or explanatory variable, also called input, regression, or predictor variable.

In the multiple regression procedure used by Hydro-Quebec for extending data series,

The relation between the dependent variable Y and the explanatory variables Xl, X2, .. ,

Xp is linear (K.W.Hipel et.al ,1994)

$$b = (rxy)\left(\frac{sy}{sx}\right)$$

$$biased\ \ X_T = \sqrt{\frac{\sum(Xt_n - mean)^2}{N}}$$

$$Unbiased\ X_T = \left(\frac{\sum x^2 - \frac{(\sum x)^2}{n}}{n-1}\right)^{1/2}$$

$$Y_T = \sqrt{\frac{\sum(Yt_n - mean)^2}{N}}$$

$$Unbiased\ Y_T = \left(\frac{\sum y^2 - \frac{(\sum y)^2}{n}}{n-1}\right)^{1/2}$$

Cross-correlation coefficient b/n x & y

$$rxy = \frac{\sum xy - \frac{(\sum x)(\sum y)}{n}}{\sqrt{(\sum x^2 - \frac{(\sum x)^2}{n})(\sum y^2 - \frac{(\sum y)^2}{n})}}$$

4.3.1.2 **Outlier Checking**

Outliers are data points that depart significantly from the trend of the remaining data.

To check if there is a surprise data (outlier) in the given gauge station, record or if there is a non-normally distributed or outlier in the time series trend.

Normality and homogeneity of variance throughout the series may be adversely affected by outliers and missing data in parametric tests.

It is a change in the level of data series, usually over time but sometimes in space. It is a general increase or decrease in the observed values of random variables over time.

Testing the existence of a linear (monotonic) trend (serial correlation) within the whole time series was done by XLSTAT by the method of the Dixon test which interprets results based on Z-scores.

This test is applicable for data sets with sample sizes ranging from 3 to 30 and can assess whether the minimum value, the maximum value, or either of these values is considered an outlier. (NLST)

Z score is a statistical measure that describes how far a particular data point far is far from the mean of a dataset, measured in standard deviations.

Z score = (x -mean) / std. deviation

Data points that have a z score more than three are considered to be significantly distinct from the others. This type of data point may be an anomaly.

Positive and negative Z-scores are both possible. A data point is more likely to be an outlier if it is farther from 0. Generally, a Z-score of more than three is regarded as excessive.

Example of Detected

Outlier detected outlier data for January 1994 at Gato Station is 549.6 mm. This value exceeds all other recorded January rainfall amounts, and the daily rainfall data also does not

appear normal; it seems to contain adjusted values with some random values repeating themselves. Therefore, this data is considered missing and should be filled in again using the provided method.

JAN	G	Critical valu	p-value	Step
549.600	0.776	0.298	< 0.0001	1

Value	Z-score
11.500	-0.272
35.500	-0.034
7.900	-0.308
107.500	0.679
549.600	**5.062**
10.200	-0.285
32.700	-0.062
5.800	-0.329
122.900	0.832
7.600	-0.311
0.000	-0.386
33.200	-0.057
43.000	0.040
3.800	-0.349
33.400	-0.055
25.000	-0.139
3.100	-0.356
13.400	-0.254
3.700	-0.350
44.400	0.054
44.000	0.050
0.000	-0.386
0.000	-0.386
18.400	-0.204
1.900	-0.368
0.000	-0.386
10.800	-0.279
0.000	-0.386
0.000	-0.386
0.000	-0.386

Gato January

1	15.5
2	15
3	16
4	16.5
5	16
6	18
7	19
8	17.5
9	19
10	18.5
11	18.5
12	16.5
13	16.5
14	16.5
15	19
16	18
17	18.5
18	18
19	16.5
20	15.5
21	19
22	15.5
23	17.5
24	18.5
25	19.5
26	19.5
27	20
28	18.6
29	20
30	18
31	19
total	549.6

Konso rainfall station monthly data (for January)

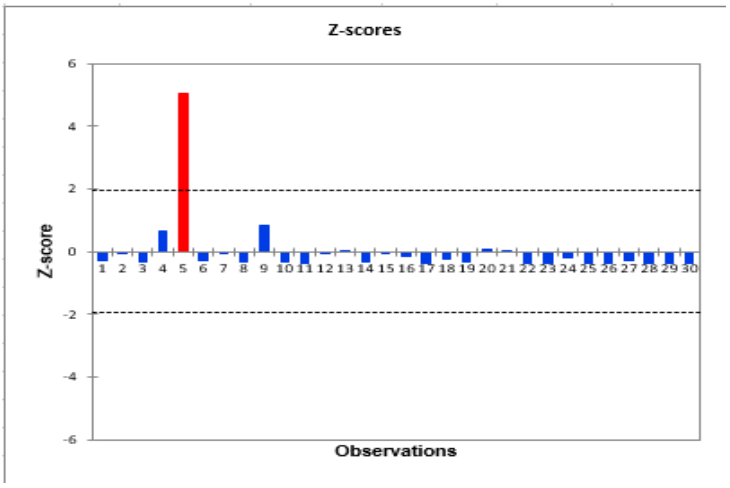

Figure 6 Outlier graph by EXSTAT

4.3.1.3 **Consistency Test**

It is a plot of the cumulative values of one variable against the accumulation of another quantity during the same time period. The double mass curve is used to check the consistency of many kinds of hydrologic data by comparing data for a single station with that of a pattern composed of the data from several other stations in the area. The double- mass curve can be used to adjust inconsistent precipitation data.

Hydrognomon 4.1 software was used to check the consistency of cumulative rainfall from one station to another station. Hydrognomon is a software tool for the management and analysis of hydrological data. The main part of hydrological data analysis consists of time series processing applications, such as time step aggregation and regularization, interpolation, regression analysis and filling in of missing values, consistency tests, data filtering, graphical and tabular visualization of time series, etc.

One practical method for verifying the consistency of a record is to utilize a double mass curve. Plotting the cumulative numbers of one variable against the cumulative figures of another variable over a consistent length of time on an arithmetic cross-section paper is known as a double mass curve. (J.K.Searcy, 1996)

According to the double mass curve, the relationship between values X and Y can be represented by a line with an equation of the form Y=bX, where b is the double mass curve's slope Y is estimated value and X is measured value. For many relationship-only precipitation scenarios this assumption is largely accurate. (J.K.Searcy, 1996)

$$Y = bX$$

$$b = \frac{b_a}{b_o}$$

$$Y = \frac{b_a}{b_o} X$$

Where

Y= Adjusted precipitation

X= Observed precipitation

ba = slope of grph to which record are adjusted

bo = slope of graph at time X was observed

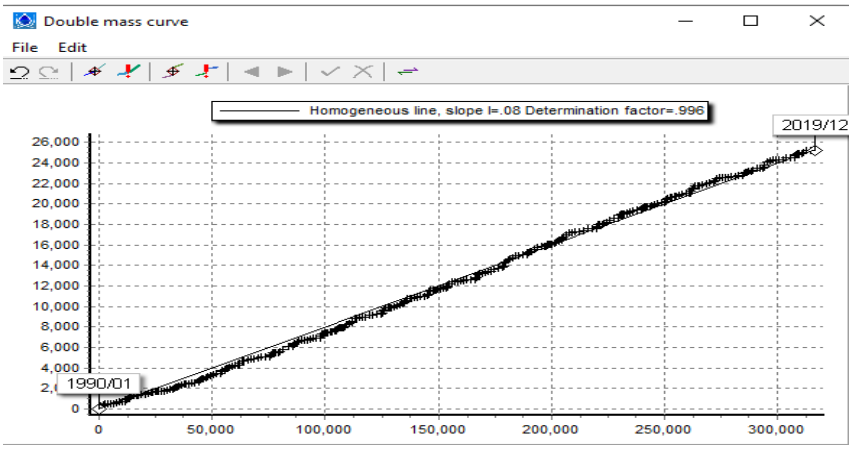

Figure 7 Double mass curve result for Arfiade

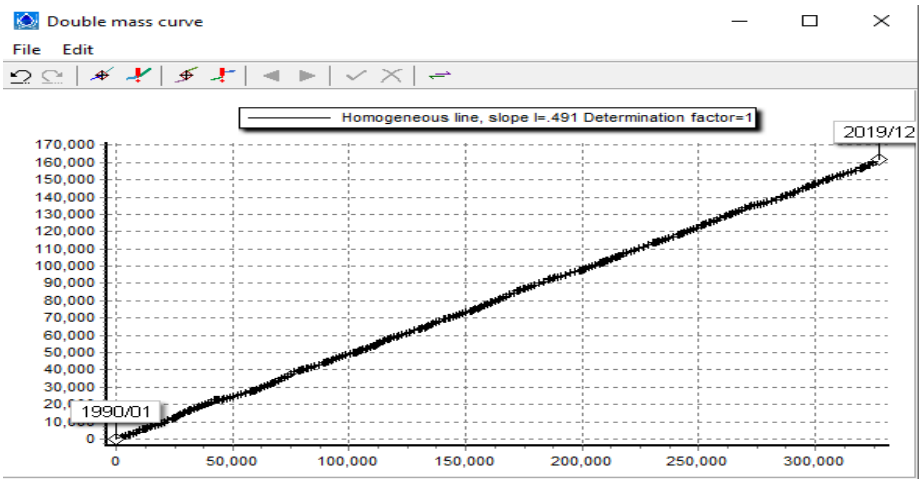

Figure 8Double mass curve result for Gato Rainfall station

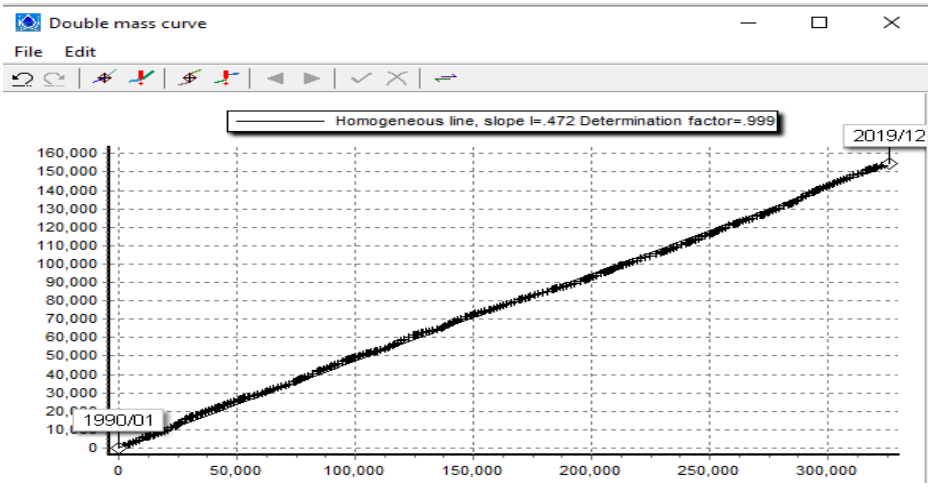

Figure 9 Double mass curve result for Konso Rainfall station

4.3.1.4 **Average Rainfall of the Stations**

The average monthly rainfall patterns of three stations (Afraide, Gato and Konso), after performing consistency checks and rainfall data analysis

The following graph depicts the mean monthly rainfall patterns for the project area, showing a bio-modal distribution after performing a consistency check and rainfall data analysis. The rainfall pattern is characterized by two prominent peaks: the first peak occurs between February and May, with April recording the highest rainfall of the year, and the second peak is observed from September to October, with October also showing a significant rainfall spike. Conversely, the lowest rainfall is recorded in the months of July and January, where dry conditions prevail. This variation in monthly rainfall highlights the seasonal shifts in the project area, with wetter periods concentrated in spring and fall, and drier conditions during the mid-year months.

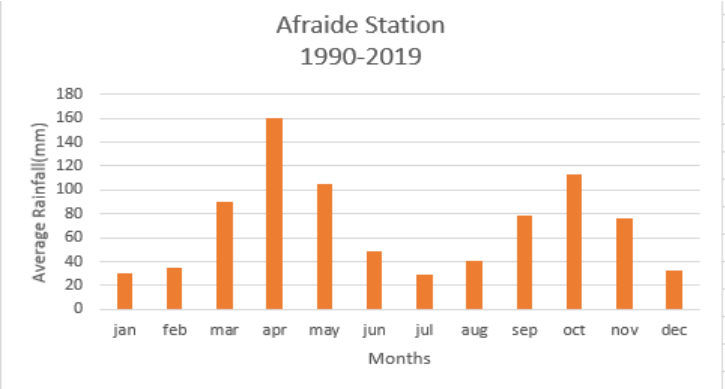

Figure 10 Mean Monthly Rainfall Distribution of Afraide Station

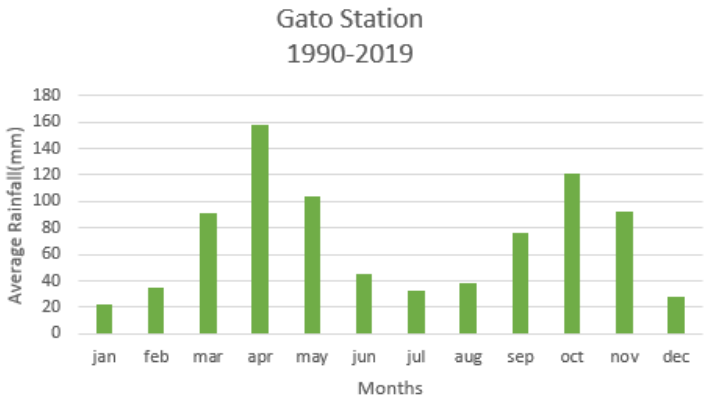

Figure 11Mean Monthly Rainfall Distribution of Gato Statio

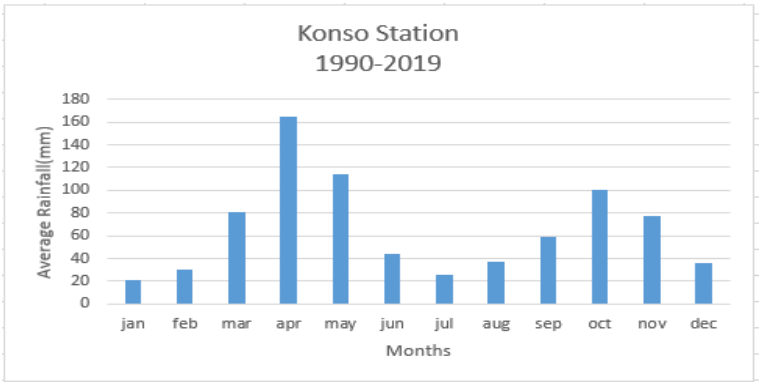

Figure 12Mean Monthly Rainfall Distribution of Konso Statio

4.4 PMP/PMF Estimation

The terms PMP and PMF relate to the physical upper limits of storms and the corresponding floods.

The upper bounds of storms and the corresponding floods are currently only approximate Due to data limitations and the physical complexity of the processes in the meteorological and hydrological sciences.

4.4.1 Probable Maximum Precipitation (PMP)

The term "probable maximum precipitation" (PMP) refers to the highest depth of precipitation that is meteorologically likely to occur at a given place during a given duration. To ensure that the likelihood of exceedance is extremely minimal, this information is crucial for any water infrastructure, such as drainage networks, culverts, and dams. (Sarkar Subharthi et al., 2020)

The Hershfield method is utilized in this work to estimate PMP using several approaches. Since the Hershfield approach is a reliable and effective statistical technique for PMP estimation. Accurate PMP estimation requires the measurement of frequency factor K. An extremely high value of K will lead to an overestimation of PMP and an uneconomical design. Conversely, a lower value of K will lead to an underestimate of PMP, hence raising the danger of any Construction of hydraulics structure is constructed based on that estimate. As a result, factor K must be properly established in order for the design that is based on it to have an appropriate balance between acceptable risk and economy. **(** S. Sarkar et al., 2020)

$$X_t = \overline{X_n} + K_m S_n$$

Where,

X_t = Rainfall for return period t

$\overline{X_n}$ = Mean of a series on n annual maxima

K_m = Frequency factor

S_n = Standard deviation of a series on n annual maxima

The initial assessment of an enveloping value for Km was conducted using 24-hour rainfall records from approximately 2,700 stations participating in the climatological observation

program. Conventional methods were employed to calculate the values of Xn and Sn, but the maximum recorded rainfall at each station was excluded from these calculations. The highest Km value derived from the data across all stations was 15 (WMO, 2009). Initially, it was believed that Km was unaffected by rainfall magnitude; however, it was later discovered that it actually varies inversely with rainfall. Consequently, a value of 15 may be too high for regions that typically experience heavy rainfall and too low for arid regions. Subsequent investigations (Hershfield, 1965) established Km values for other rainfall durations, revealing a maximum Km of 20 for durations of 5 minutes, 1 hour, 6 hours, and 24 hours. (WMO, 2009)

$$K = \frac{X_m - \overline{X}_{N-1}}{S_{N-1}}$$ (WMO, 2009)

X N-1 and SN-1 are the mean and standard deviation after removing the year with the maximum value

$$\overline{x} = \frac{\sum x}{n}$$

Where

$\overline{x}$ = ***is*** mean of rainfall data

x = is rainfall data

n = is number of rainfall data

$$S_n = \sqrt{\frac{\sum(x - \overline{x})^2}{n - 1}}$$

Were

Sn = is Standard deviation of rainfall data

$\overline{x}$ = is mean of rainfall data

x = is rainfall data

n = is number of rainfall data

Extreme rainfall events with a return period of 500 years or more are often recorded within much shorter timeframes, like 30 years. These rare occurrences, known as outliers, significantly impact the mean (Xn) and standard deviation (Sn) of annual rainfall data. The effect is more pronounced in shorter records and varies with the rarity of the event. Hershfield (1961b) studied this phenomenon using hypothetical data series of different lengths to determine necessary adjustments for Xn and Sn to account for outliers. (WMO, 2009)

$$\frac{\bar{x}_{n-1}}{\bar{x}_n}$$

$$\frac{S_{n-1}}{S_n}$$

Xn m- and Sn–m represents the mean and standard deviation of an annual series after removing the maximum item. These relationships focus solely on the impact of the maximum observed event.

We obtain the adjusted mean value and standard deviation value by using the graphs below, which employs the ratio of the mean rainfall data excluding the maximum to the mean of all rainfall data. The ratio of the standard deviation of rainfall data excluding the maximum to the standard deviation of all rainfall data. We use this ratio as the lower horizontal value of the graph, and from the vertical line on the left side of the graph, we obtain the corresponding adjusted value. (WMO, 2009)

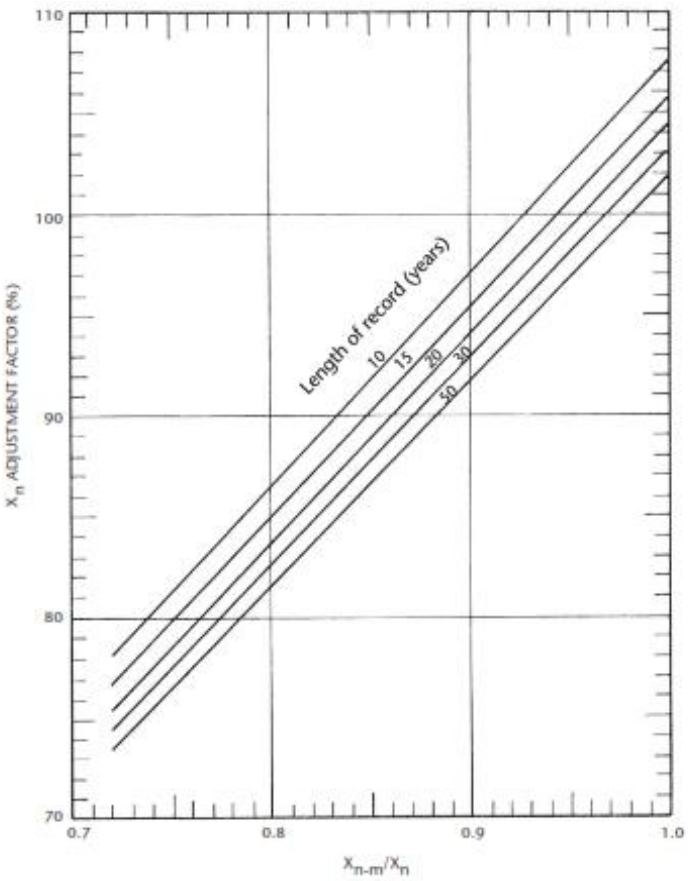

Figure 13 Mean Adjusment Factor Graph (Source WMO, 2009)

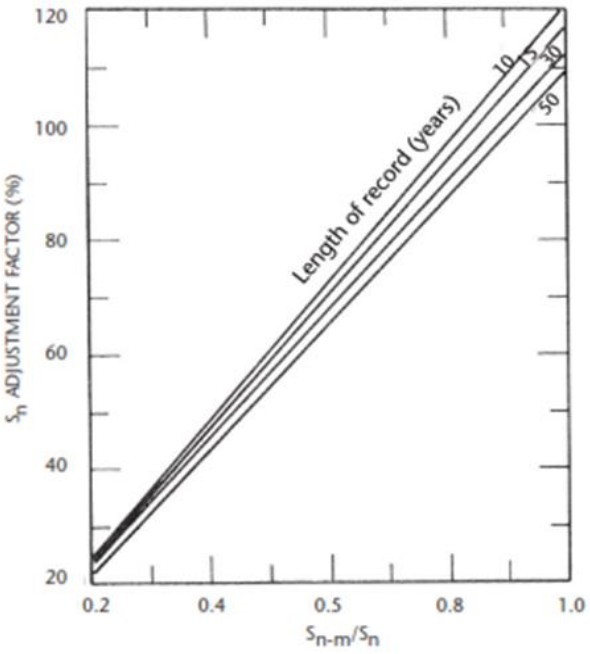

Figure 14 Standard Deviation Adjusment Factor graph (Source WMO, 2009)

Adjustments have been made to the mean and standard deviation to ensure accurate calculations of the Probable Maximum Precipitation (PMP) value, enabling a more reliable estimation of extreme rainfall events.

parameter	Station		
	Afriade	Gato	Konso
Pmax	112	217.5	96.9
Pave	2.288	2.29	2.15
δn	6.45	6.48	6.41
Pave (n-1)	0.99	0.99	0.99
δ(n-1)	0.98	0.95	0.99
Pave(adj)	2.36	2.38	2.22
δ(adj)	6.99	7.14	6.74
km	17	20	14.76
PMP 24 Hr.	142.28	145.15	137.02

Afriade(PMP) = 142.2801mm

Gato(PMP) = 145.1539mm

Konso(PMP) = 137.0159mm

		MAX	217.5						
mean	2.310473	INCMAX	2.290805	EXMAX			Xn-m/Xn		0.991487
stdev	6.798767	INCSTD	6.4803	EXMAX					
							Sn-m/Sn		0.953158
			215.2092						
			33.20976						
							AdjXn	1.03	2.379788
		Km	20				AdjSn	1.05	7.138705
						GATO	PMP	145.1539	
							AREA(%)	0.530894	
							AREAPMP	77.06133	mm

$$X_t = AdjX_n + K_m \times AdjS_n \quad \text{GATO}$$

4.4.2 Determination of Areal Precipitation

Raingaugcs represent only point sampling of the areal rainfall data. To convert the point rainfall values at various stations into an average value over a catchment Theison polygon methods was used.

Theison polygon methods estimate the rainfall amount of a location as a weighted average of the rainfall number of adjacent stations and the weights are considered as the percentage areal coverage of gauging station from the entire catchment.

Figure 15Percent Area Ratio for the Rainfall Station of the Watershed by Theison polygon

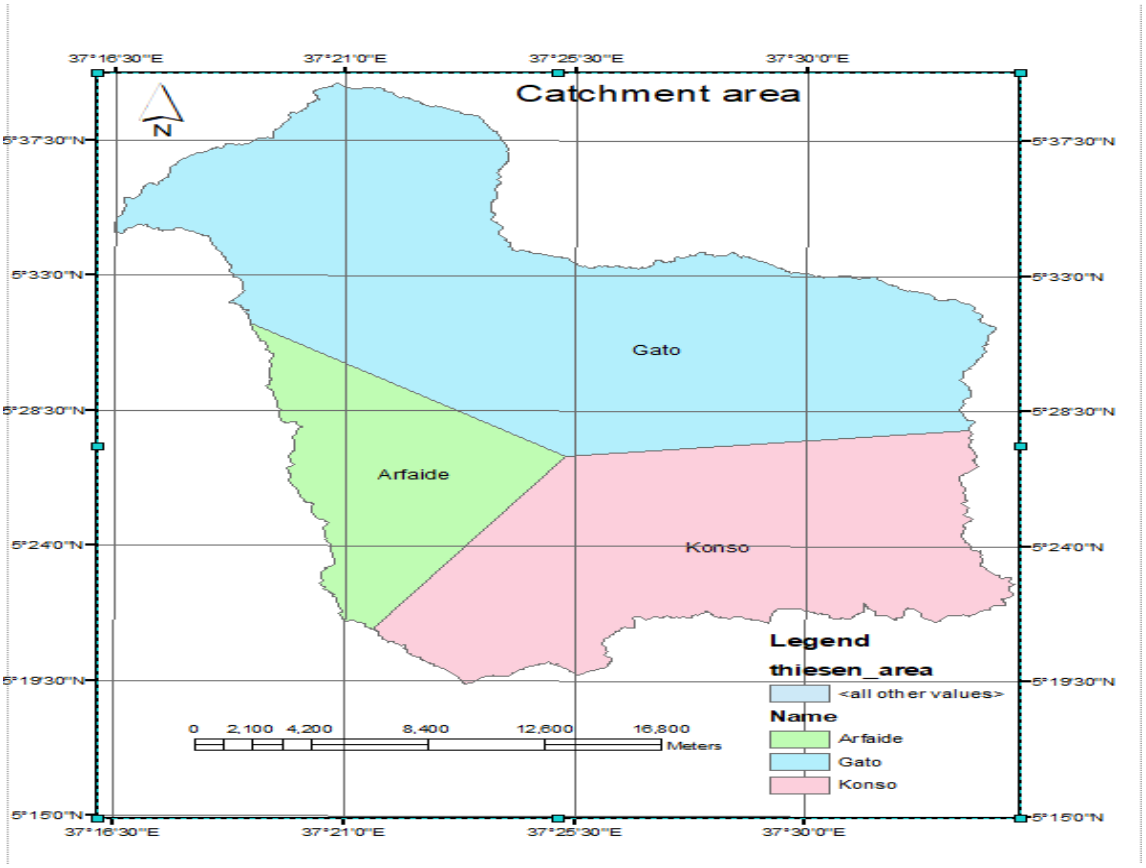

No	Name	Area(km2)	percent
1	Konso	215.342631	32.38523
2	Gato	353.012705	53.08934
3	Arfaide	96.585566	14.52544
Total area		664.940902	100%

Table 2Area of individual station by Theison polygon method

4.4.2.1 **Area reduction factor**

The Area Reduction Factor (ARF) is used to adjust point rainfall data for a larger area in hydrological studies, allowing for more accurate rainfall estimations over a broader region. Point precipitation data, typically gathered from a specific location, are often limited in their representation of rainfall patterns over an entire area. In this study, point rainfall data, arbitrarily accepted as representative for an area of 25.9 km², were used in the derivation of the Convergence Probable Maximum Precipitation (PMP), as outlined in the WMO (2009) guidelines. By applying the ARF, this process allows for the conversion of point-based data into values that can better represent the rainfall over a larger area, providing more reliable

inputs for hydrological modeling, flood prediction, and water resource management. (WMO, 2009)

$\boldsymbol{ARF = 1 - bD^{-a}}$ (Elizabeth M.Shaw et.al, 2011)

Flood Estimation Handbook (IoH, 1999) area reduction factor coefficients (Elizabeth M.Shaw et.al, 2011)

Area A (km^2)	A	B
$A \leq 20$	$0.40 - 0.0208\ln(4.6 - \ln A)$	$0.0394A^{0.354}$
$20 < A \leq 100$	$0.40 - 0.00382\ln(4.6 - \ln A)^2$	$0.0394A^{0.354}$
$100 < A \leq 500$	$0.40 - 0.00382\ln(4.6 - \ln A)^2$	$0.0627A^{0.254}$
$500 < A \leq 1000$	$0.40 - 0.0208\ln(\ln A - 4.6)$	$0.0627A^{0.254}$
$1000 < A$	$0.40 - 0.0208\ln(\ln A - 4.6)$	$0.1050A^{0.180}$

a = 0.386652, b = 0.326787

4.4.2.2 HYETOGRAPH by SCS TYPE II, 24-HR DESIGN STORM

In older hydrologic design methods, such as the rational method, only the peak discharge was considered in the analysis. These methods did not take into account how discharge varied over time (the discharge hydrograph) or how precipitation was distributed over time (the precipitation hyetograph). However, more modern design methods, which incorporate unsteady flow analysis, now require a more detailed approach. These methods rely on accurate predictions of the design hyetograph to generate the corresponding design hydrographs, providing a more comprehensive understanding of how both rainfall and runoff change over time. This shift reflects advancements in hydrological modeling that allow for more accurate flood predictions, particularly in areas where flow conditions are highly dynamic. (Ven Te Chow. 1988)

Triangular Storm Hyetograph method

$$h = \frac{2P}{T_d}$$ (Ven Te Chow, 1988)

The base length is Td and the height h, so the total depth of precipitation in the hyetograph is

given by

$$P = \tfrac{1}{2} T_d h,$$

$$h = \frac{2P}{T_d}$$

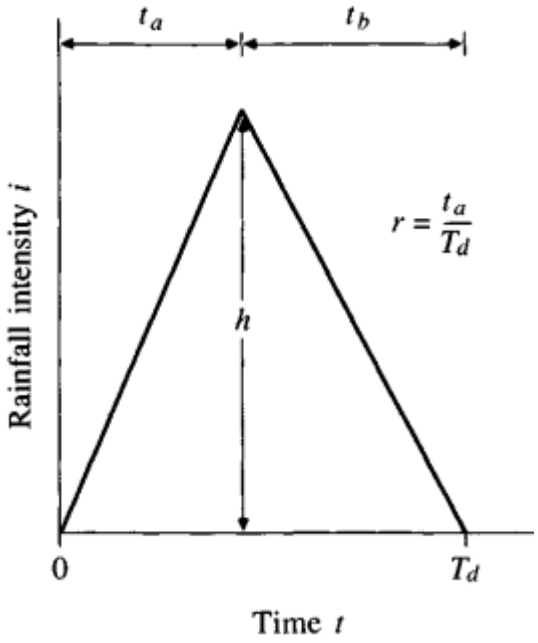

4.4.3 Conversion of gauged Stream flow to ungauged stream flow

Because there is no recorded stream flow data for the Yanda River where a dam is to be built, an estimation method is implemented to get stream flow data for the Yanda River.

One of the most popular and straightforward methods for obtaining regional estimates of runoff at ungauged locations is the area ratio approach.

Using the drainage area ratio (DAR) method, daily flows gauged at a nearby Wieto River station are transferred to the Yanda River (an ungauged) section.

The main watershed characteristics that affect hydrologic response include the size, shape, slope, soil type, and storage within a watershed area (P.B.Bendient, 2013).

The streamflow at an ungauged site is estimated by

$$Q_{ug} = (\frac{A_{ug}}{A_g}) \times Q_g$$

Where Qg is the streamflow observed at a gauged Catchment

Qug is the estimated discharge at an ungauged Catchment.

Aug and Ag is the drainage area of the gauged and ungauged catchment.

A = 665km2 for yanda catchment and 4344km2 for weito catchment (both area contained from Catchment area shape file)

When applying the area ratio method to transfer stream flow from a gauged to an unguaged stream, it is necessary to first check the similarity of their catchment characteristics. One of the characteristics that should be examined is the slope of the two catchments. The two catchments have almost similar slopes, with a value of 2.0% for Yanda and 2.6% for Weito.

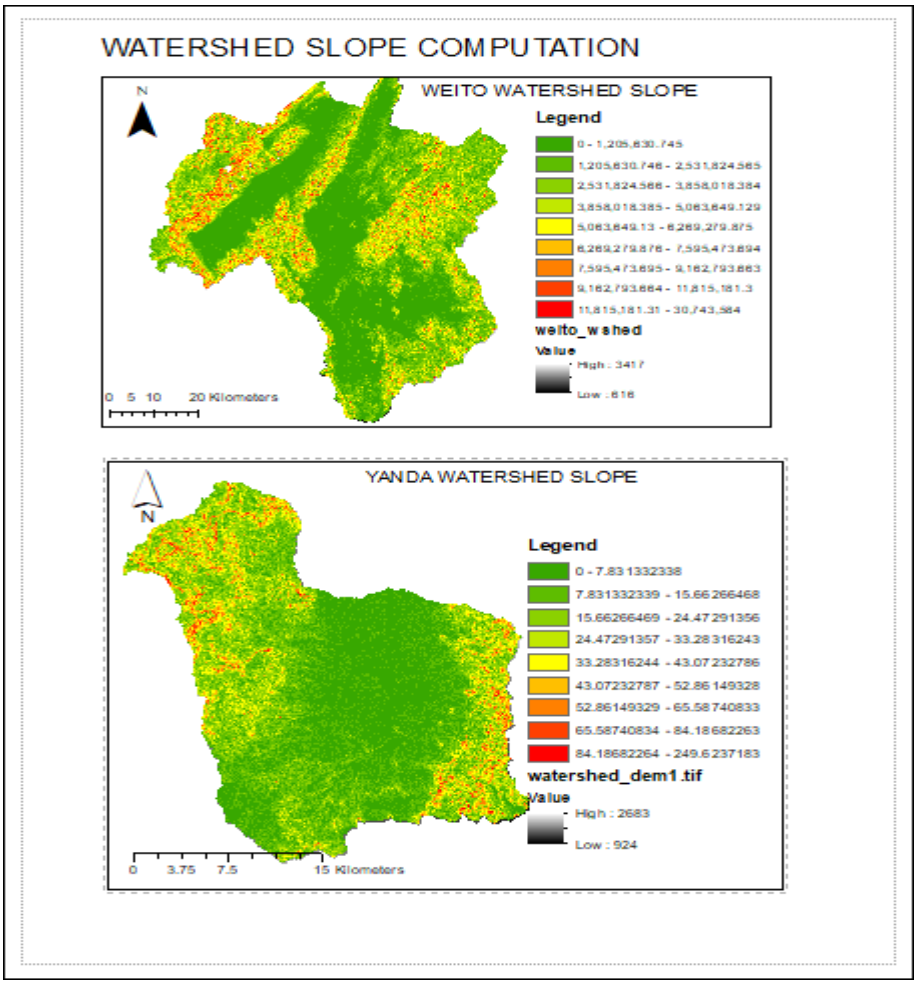

Figure 16 The slope of the watershed are

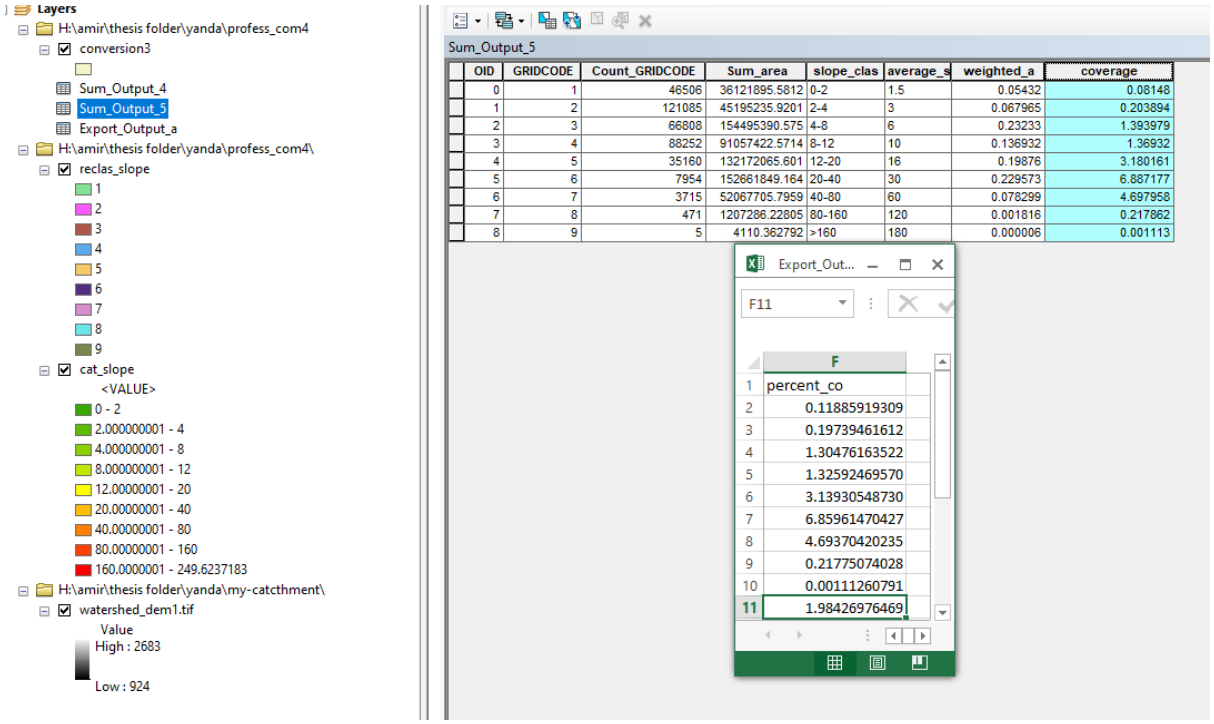

Slope from GIS for yanda Catchment is 2.0%

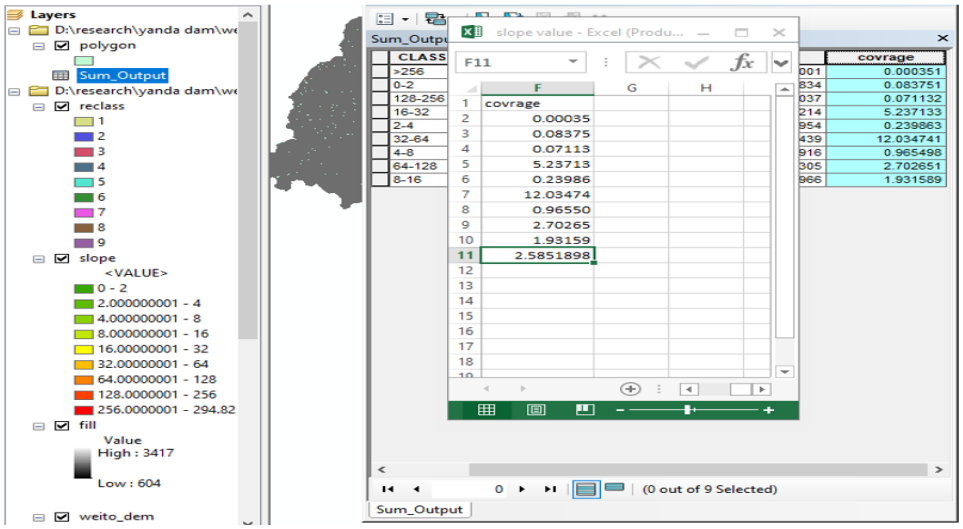

Slope from GIS for weito Catchment is 2.6%

The other characteristics that should be examined is catchment elevation

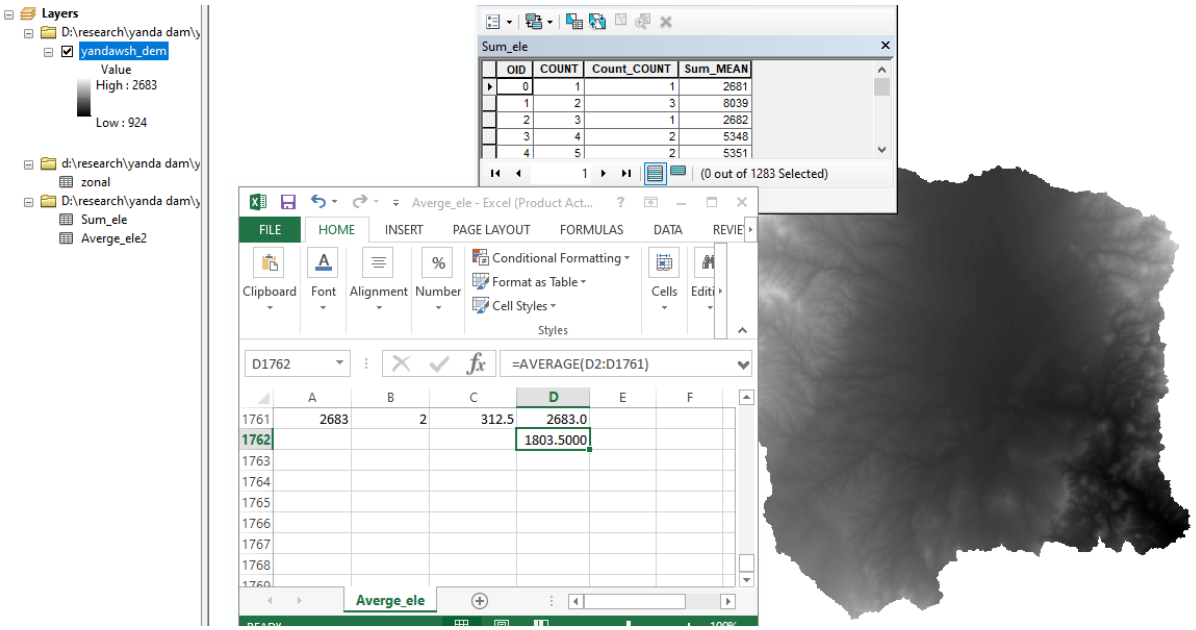

Average elevation from GIS for yanda 1803.5

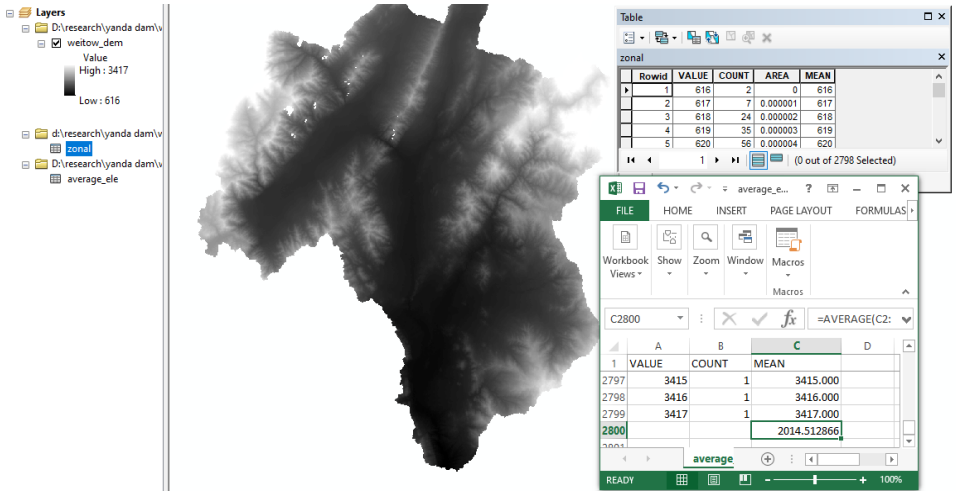

Average elevation from GIS = 2014.5m for weito catchment.

4.4.1 Analysis of Land use/ Land cover and soil data

By using ARCGIS 10.4 Software the study area was tabulated to quantify the area of each LULC class and soil type.

Analyzing land use, land cover (LULC), and soil data can assess the floodplain's hydrological characteristics, including its obstruction capacity and impervious surface percentages. In this

analysis, we utilized ArcGIS 10.4 to examine specific spatial characteristics of the study area The predominant soil types within the floodplain exhibited varying infiltration rates, from semi-permeable soil with low runoff potential to high runoff potential with very low infiltration rate. This stratification indicates differential hydrological behavior during flood events, influencing flood routing and the management of water runoff.

4.4.1.1 **LU / LC Type**

Land use/land cover of the project area varies with in the catchment the project area the main land use land cover of the project catchment in general can be categorized as shrub land, forest land, grass land and cultivated land. (ECDSWC) In terms of hydrological point of view brush land, grass land, forest land and cultivated land encourage infiltration and tend to decrease runoff.

CN estimation based on land cover and use. The potential for stormwater runoff in drainage areas is expressed by the curve number (CN), a hydrologic metric that depends on soil type, soil moisture content, and land use. To model the process of rainfall and runoff resulting from changes in land use. CN value is required for model as data input.

4.4.1.2 **Soil Type**

The dominant soil type along the project area are chromic vertisols, Eutric nitosols, chromic luvisols, Leptosols and Ortich solanchak. (ECDSWC). The eutric nitosols, chromic luvisols and Ortich solanchak soil type are categorized as semi-permeable soil of hydrological group B with moderate low runoff potential due to moderate infiltration rate.Chromic Vertisols and Leptosols . which is categorized under soil group D having a high runoff potential due to very low infiltration rate and impervious soil character.

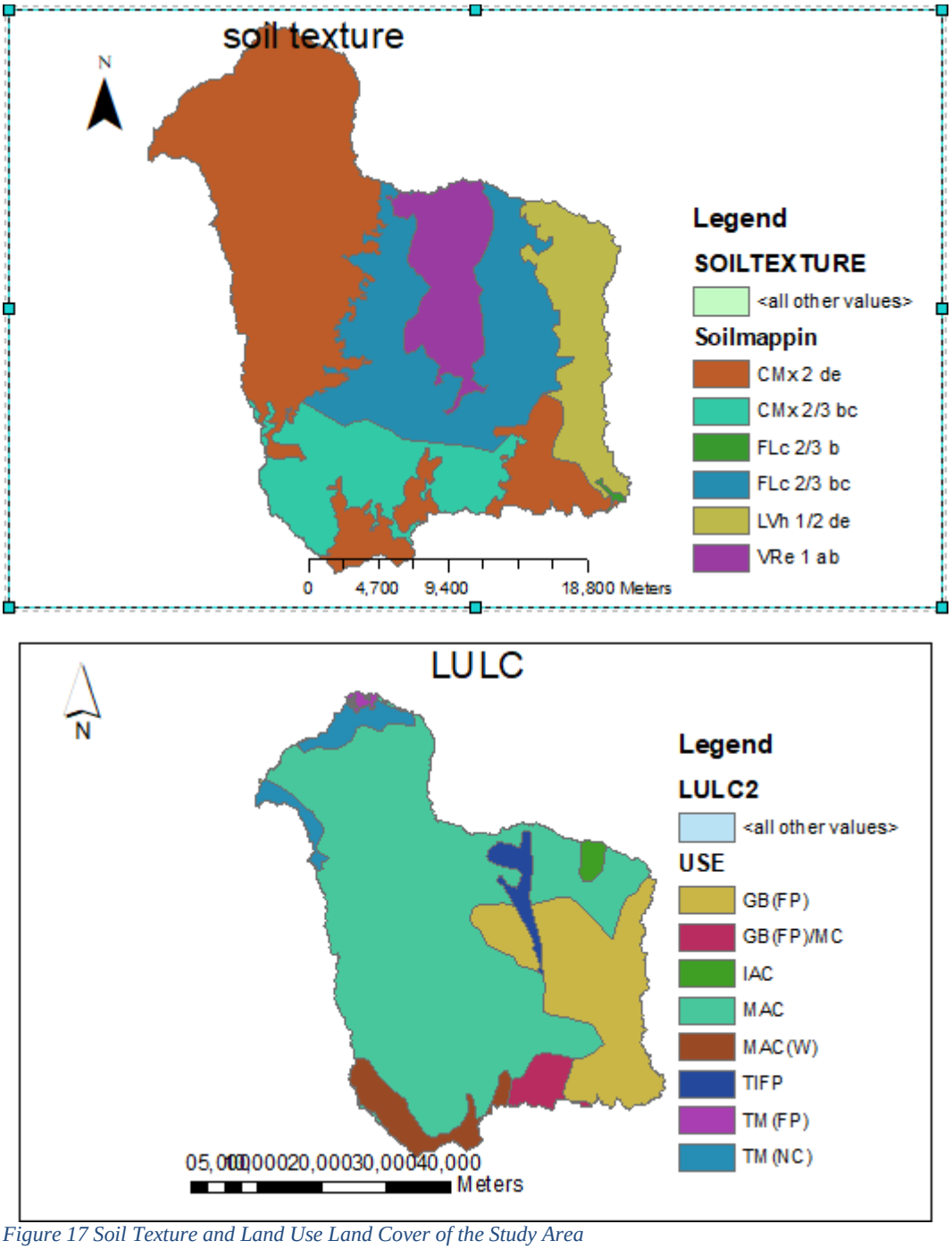

Figure 17 Soil Texture and Land Use Land Cover of the Study Area

4.4.2 Base flow Separation

Base flow refers to the subsurface-derived portion of streamflow, typically originating from groundwater discharge into streams. Understanding the contribution of base flow to streamflow is essential for comprehending watershed-scale hydrology. Accurate base flow

separation is crucial for understanding the natural flow conditions in a watershed and for calibrating hydrologic models. One of the tools used for this purpose is SEPHydro, a software developed by the U.S. Geological Survey (USGS) for separating baseflow from streamflow data. This knowledge provides valuable insights into groundwater-surface water interactions and highlights the influence of geology and landforms on base flow dynamics. (Serban Danielescu, 2018)

4.4.3 HEC-HMS Rainfall- Runoff Model

HEC-HMS is hydrologic modeling software developed by the U.S. Army Corps of Engineers' Hydrologic Engineering Center. It is designed to model rainfall-runoff processes across a broad spectrum of geographic areas, including flooding, water supply, and runoff from both large river basins and small urban or natural watersheds. (L.A. Jabbar et al , 2021)
The method used to model rainfall-runoff are: -

4.4.3.1 **Loss Methods: -** Loss methods in HEC-HMS are used to calculate the amount of rainfall that are lost before reaching the watershed outlet this is due to infiltration, evaporation, and other losses.

- **SCS Curve Number**: One of the components of this model is the Curve Number (CN) method, which estimates direct runoff from rainfall based on land use, hydrologic conditions, and the inherent characteristics of the soil. The Curve Number method is a simplified approach that translates rainfall into runoff by utilizing a dimensionless parameter known as the Curve Number, which varies between 30 and 100. A higher Curve Number indicates a higher potential for runoff, while a lower number signifies greater infiltration and lesser runoff. The curve number is derived from a combination of factors including:

Land use: Different types of land cover (urban, agricultural, forested, etc.) have distinct patterns of rainfall absorption and runoff.
Hydrologic Soil Groups (HSG): As a pivotal factor, soils are classified into four Hydrologic Soil Groups (A, B, C, and D) based on their infiltration rates and drainage characteristics
Soil moisture conditions: Preceding rainfall can influence the amount of moisture already present in the soil, thereby affecting subsequent runoff. Hydrologic Condition: This takes

vegetation cover and soil moisture into account

Initial Abstraction (Ia): Surface storage, evaporation, and infiltration are the first losses that occur prior to runoff starting. Usually, 20% of the possible maximum retention (S) is used to estimate it.

$$I_a = 0.2 \times S$$

Potential Maximum Retention (S): This represents the maximum amount of water that can be retained by the soil after runoff begins. It is related to the CN by the equation:

$$S = (\frac{1000}{CN} - 10)$$

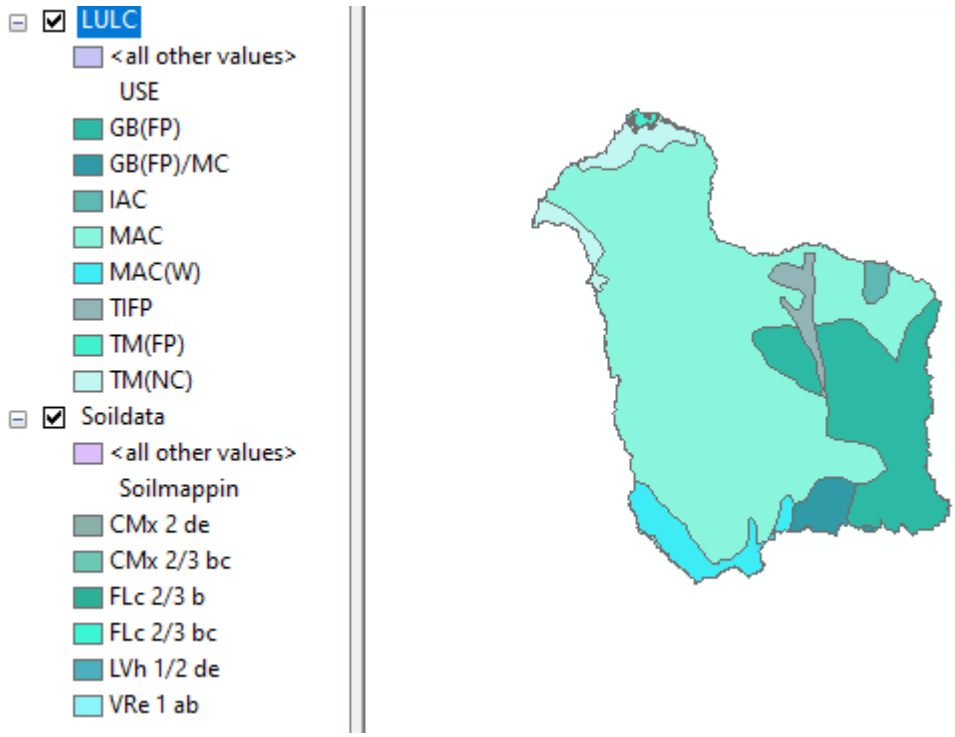

Summarize table for area (Polygon) which have the soil type and LULC to get percentage Their Coverage

Sum_Output_3

Cnt_Area	First_LULC	Last_LULC_	percent	hyd_cond	soil_class	CN	COVERAGE
2	MAC_CMx 2/3 bc	MAC_FLc 2/3 bc	0	good	C	81	0.000001
1	GB(FP)/MC_FLc 2/3 bc	GB(FP)/MC_FLc 2/3 bc	0.000018	poor	C	70	0.001256
1	TM(NC)_CMx 2 de	TM(NC)_CMx 2 de	0.00019	fair	C	73	0.01388
1	GB(FP)_VRe 1 ab	GB(FP)_VRe 1 ab	0.000454	poor	D	77	0.03493
1	TIFP_FLc 2/3 bc	TIFP_FLc 2/3 bc	0.000734	good	C	77	0.056514
1	GB(FP)_FLc 2/3 b	GB(FP)_FLc 2/3 b	0.001466	poor	C	72	0.10552
1	IAC_FLc 2/3 bc	IAC_FLc 2/3 bc	0.00144	good	C	81	0.116676
1	TM(FP)_CMx 2 de	TM(FP)_CMx 2 de	0.00334	fair	C	70	0.233779
1	GB(FP)_FLc 2/3 bc	GB(FP)_FLc 2/3 bc	0.004052	poor	C	72	0.291737
1	GB(FP)/MC_CMx 2 de	GB(FP)/MC_CMx 2 de	0.005994	poor	C	72	0.431595
1	IAC_LVh 1/2 de	IAC_LVh 1/2 de	0.006485	good	B	82	0.531775
1	TM(NC)_CMx 2 de	TM(NC)_CMx 2 de	0.013761	fair	C	70	0.963263
1	MAC(W)_CMx 2 de	MAC(W)_CMx 2 de	0.014974	fair	C	81	1.212853
1	GB(FP)/MC_CMx 2/3 bc	GB(FP)/MC_CMx 2/3 bc	0.017785	poor	C	70	1.244929
1	GB(FP)_VRe 1 ab	GB(FP)_VRe 1 ab	0.020406	poor	D	77	1.571262
1	TM(NC)_CMx 2 de	TM(NC)_CMx 2 de	0.022592	fair	C	70	1.581468
1	TIFP_VRe 1 ab	TIFP_VRe 1 ab	0.020574	good	D	77	1.584221
1	MAC_LVh 1/2 de	MAC_LVh 1/2 de	0.030943	good	B	72	2.227925
1	MAC(W)_CMx 2/3 bc	MAC(W)_CMx 2/3 bc	0.029517	fair	D	81	2.390869
1	GB(FP)_CMx 2 de	GB(FP)_CMx 2 de	0.032907	poor	C	77	2.533831
1	MAC_VRe 1 ab	MAC_VRe 1 ab	0.050644	good	D	85	4.304723
1	GB(FP)_LVh 1/2 de	GB(FP)_LVh 1/2 de	0.068747	poor	B	66	4.537275
1	GB(FP)_FLc 2/3 bc	GB(FP)_FLc 2/3 bc	0.062726	poor	C	77	4.829871
1	MAC_CMx 2/3 bc	MAC_CMx 2/3 bc	0.08552	Good	D	85	7.2692
1	MAC_FLc 2/3 bc	MAC_FLc 2/3 bc	0.157716	Good	C	81	12.774996
1	MAC_CMx 2 de	MAC_CMx 2 de	0.347016	Good	C	81	28.108297

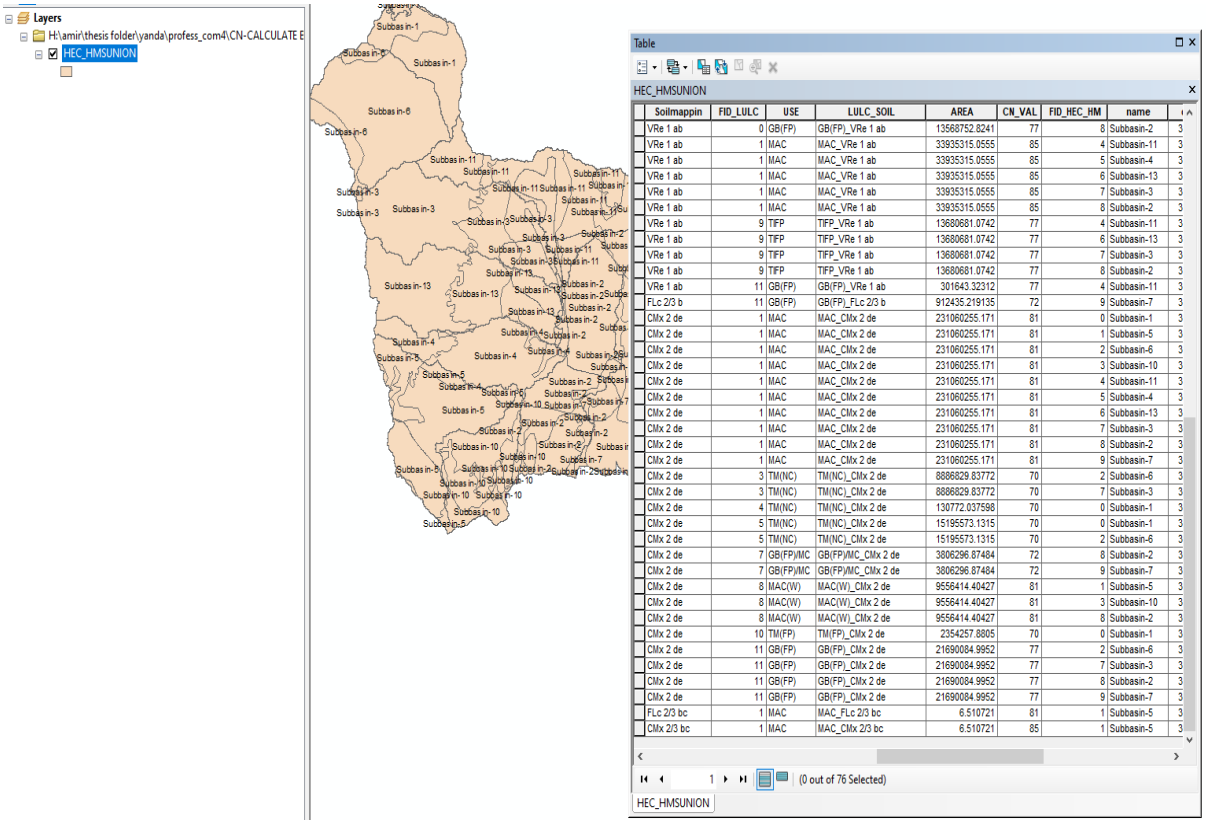

4.4.3.2 **Transform Methods:** After determining the amount of direct runoff, transform methods are used to convert rainfall into runoff by routing the excess rainfall through the watershed to the outlet point.

- **SCS Unit Hydrograph**: This method derives a synthetic unit hydrograph based on the SCS-CN method. The unit hydrograph is characterized by its peak flow, time to peak, and duration.

Kirpich Equation (1940)

$t_c = 0.01947L^{0.77}S^{-0.385}$ (K.Subramanya, 2008)

Where

Tc = time of concentration (minutes)

L = maximum length of travel of water (m)

S = slope of the catchment

4.4.3.3 **Routing Methods:** These methods simulate the movement of runoff through the watershed's river network.

- **Muskingum:** The Muskingum routing method is used to simulate the movement of flood waves through a river reach by accounting for storage and attenuation effects.

Parameters such as the peak rate factor (PRF) and lag time, estimated by calibration.

The following figure shows Model Structure such as basin model, including sub-basins and reaches

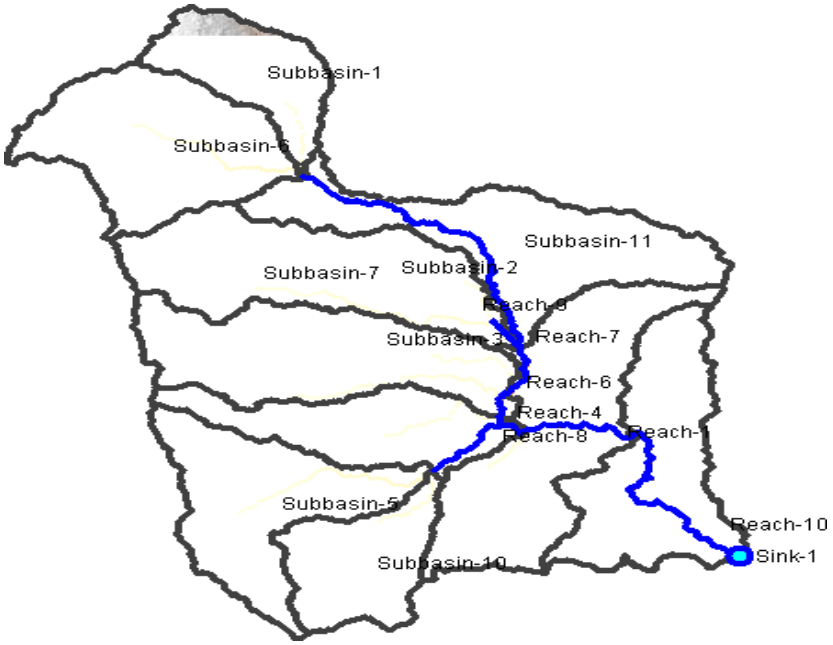

Figure 18 Sub-basin of HEC-HMS model result

In order to guarantee that the simulated outputs closely resemble the observed data, calibration is an essential in the HEC-HMS process.

4.4.3.3.1 **Sensitivity Analysis**

Sensitivity analysis determines which model parameters have the greatest impact on results. (J.M. Cunderlik et al, 2024). It can be local, where each parameter is tested individually, or global, where all parameters vary together using probabilistic methods (Haan, 2002). Sensitivity analysis was conducted for the PMP (Probable Maximum Precipitation) runoff model to evaluate the reliability and accuracy of model predictions, particularly with respect to how different input parameters influence runoff outcomes. The analysis aimed to identify which parameters have the most significant impact on the model's output. Key parameters such as rainfall intensity, basin characteristics, and soil properties were varied, focusing on changes in Tlag (lag time) and CN (Curve Number) values. By identifying the sensitive parameters, this analysis helps determine which parameters are most reliable for flood prediction, particularly when predicting extreme runoff events based on the given PMP values.

No	Subbasin	parameter 1			parameter 2			parameter 3		
		Lag Time			CN Number			Initial Abstraction		
		min	max	Value	min	max	Value	min	max	Value
1	Subbasin1	0.1	3000	60.30	35	99	67.15	0.001	500	24.847
2	Subbasin2	0.1	3000	34.7	35	99	70.5	0.001	500	21.262
3	Subbasin3	0.1	3000	33.71	35	99	71.3	0.001	500	20.44
4	Subbasin4	0.1	3000	55.94	35	99	74.2	0.001	500	17.649
5	Subbasin5	0.1	3000	55.88	35	99	75.78	0.001	500	16.232
6	Subbasin6	0.1	3000	64.26	35	99	68.77	0.001	500	23
7	Subbasin7	0.1	3000	58.78	35	99	68.86	0.001	500	22.97
8	Subbasin10	0.1	3000	45.13	35	99	16.47	0.001	500	16.47
9	Subbasin11	0.1	3000	41.4	35	99	72.46	0.001	500	19.3

4.4.3.4 **HEC-HMS Model Result Calibration and Validation**

Flood forecasting, streamflow forecasting, and rainfall-runoff processes are only a few of the hydrological processes of watersheds that are frequently simulated using HEC-HMS. Calibration is the methodical process of adjusting model parameters to align with observable data from similar conditions obtained through experimentation. (N.A.S. Nordin et al, 2024).The event hydrologic modeling calibration combined manual and automated methods. Manual calibration set initial parameters based on available data, while automated optimization fine-tuned them within these limits using a gradient search to minimize error.(J.M. Cunderlik et al, 2024)

Validation, involves testing the model's ability to predict hydrological behavior under different scenarios using separate data sets not involved in calibration. Validation is the process of evaluating the calibrated model's stability. The model parameter obtained will be used to validate it before it is proposed for use. (N.A.S. Nordin et al, 2024).

4.4.3.4.1 **Model Performance Evaluation**

The performance evaluation of the HEC-HMS model involves comparing simulated results with observed data using efficiency metrics. Model performance evaluation involves

sensitivity analysis, calibration, and validation (WALEGA, 2013). The sensitivity analysis was carried out to pinpoint the key parameters that have the greatest impact on runoff generation. (S.S Fanta, 2021).The performance of the models is evaluated based on the overall consistency between predicted and observed runoff discharges, as well as their ability to accurately predict the timing and magnitude of hydrograph peaks and runoff volume.(A.Asadi, et al 2013)

These metrics assess the model's accuracy in replicating real-world hydrological behavior, such as streamflow. The model's performance is considered acceptable if the evaluation metrics fall within a defined range. A forecast efficiency criterion is, therefore, necessary to judge the performance of the model. Assessing the performance of a hydrologic model requires to estimates the closeness of the simulated behavior of the model to observations. Three methods for goodness-of-fit to measure the model predictions during the calibration and validation periods were used, these three numerical model performance measures are coefficient of Correlation (R2), Nash-Sutcliffe simulation efficiency (NSE) and Percent bias (PBIAS)

4.4.3.4.1.1 **Coefficient of Correlation (R2)**

The coefficient of determination, R^2, indicates the proportion of variance in the observed data that is explained by the model. It serves as a measure of how closely the observed-predicted regression line matches the ideal fit. R^2 is a dimensionless value ranging from 0 to 1, where 0 means the model fails to explain any variance in the observed data, and 1 signifies a perfect fit. (Daniel Althoff, et. al. 2021)

The value of R^2 is calculated as follows

$$R^2 = \left[\frac{\sum_i^n (Q_O - \bar{Q}_O)(Q_S - \bar{Q}_S)}{\sqrt{\sum_i^n (Q_O - \bar{Q}_O)^2} \times \sqrt{\sum_i^n (Q_S - \bar{Q}_S)^2}}\right]^2$$ (HEC-HMS Technical Manual 2015)

Where, Qo= observed flow, Qs = Simulated flow, $\bar{Qo}$ = Average of observed flow and $\bar{Qs}$= Average of simulated flow.

4.4.3.4.1.2 **Nash-Sutcliffe Simulation Efficiency (NSE).**

The Nash-Sutcliffe Efficiency (NSE) is one of the most widely recognized and commonly

used goodness-of-fit measures in hydrological studies. It assesses how well the model's predictions align with the observed data, with higher values indicating better model performance. NSE is especially valued for its ability to evaluate the predictive accuracy of hydrological models. A value of 1 represents a perfect fit, where values close to 0 and negative values indicate poor model performance. (Daniel Althoff, et. al. 2021)
The user calibrates the model parameters by adjusting the values until a good fit is achieved with the observed discharge time series. In the early stages of using such models, this process was done through trial and error, with results assessed visually. More recently, automated optimization methods have been developed, and the goodness of fit is now evaluated using one or more numerical performance measures. One of the most widely used measures in hydrology is the Nash and Sutcliffe (1970) model efficiency, NSE (E.M.SHOW, 2011)

$NSE = 1 - \frac{\sum_{i=1}^{n}(Q_O - Q_S)^2}{\sum_{i=1}^{n}(Q_O - \bar{Q}_O)^2}$ (E.M.SHOW, 2011)

Where, Qo= observed flow, Qs = Simulated flow and $\bar{Qo}$ =Average of observed flow

4.4.3.4.1.3 **Percent bias (PBIAS)**

Percent Bias (PBIAS) is a metric that evaluates the overall tendency of simulated data to either overestimate or underestimate the observed data. PBIAS indicates whether the simulated values are generally larger or smaller than the corresponding observed values. It ranges from 0% to infinity, with 0 representing the optimal value. A positive PBIAS indicates the model underestimates the observed data, while a negative PBIAS means the model overestimates the observed data (HEC-HMS Technical Manual, 2015).

$PBIAS = \sum_{i=1}^{n} \frac{(Q_O - Q_S)100}{\sum_{i=1}^{n} Q_O}$ (HEC-HMS Technical Manual, 2015)

HEC-HMS Performance Ratings for Summary Statistics

Performance Rating	NSE	PBais(%)	R2
Very Good	0.75<NSE≤1.00	$\|PBIAS\|$ < ±10	R2 ≥ 0.85
Good	0.65<NSE≤0.75	±10≤ $\|PBIAS\|$ <±15	0.70≤R2
Satisfactory	0.50<NSE≤0.65	±15≤ $\|PBIAS\|$ <±25	0.5≤R2<0.70
Unsatisfactory	NSE≤0.50	$\|PBIAS\|$ ≥±25	R2≤0.5

4.4.4 Probable Maximum Flood (PMF)

The flood discharge resulting from the PMP is referred to as the PMF. When deriving the PMF from the PMP, special care must be taken to identify the type of storm mechanism that leads to the PMP, including factors such as storm volume and its spatial and temporal distribution, which together generate the PMF needed for a design project. One of the key steps is to determine the qualitative characteristics of the ideal or model storm. (WMO, 2009)

There are two methods for converting PMP into PMF:

1. **Traditional Unit Hydrograph Method**: Large watersheds are divided into sub-watersheds, and unit hydrographs are used to estimate outflow, which is routed using the Muskingum method, with base flow added to obtain the PMF.
2. **River-Basin or Hydrological Process Models**: These models, which differ in the factors considered for runoff and flow concentration, often use Sherman's or Nash's unit hydrographs for discharge estimation and Muskingum for routing. Complex models are usually unnecessary for PMP due to its extreme magnitude. (WMO, 2009).

Once the PMP value is calculated, it is used as input for the HEC-HMS runoff simulation. This model simulates the watershed's response to the extreme precipitation event defined by the PMP. The resulting runoff, generated from the PMP event, represents the Probable Maximum Flood (PMF) value. The PMF is the peak discharge or flow that would occur in the watershed under the most extreme precipitation event, and it is a critical value used in the design of flood control structures, such as dams and spillways, to ensure they can safely accommodate the worst-case flood conditions.

4.5 HEC-RAS Model

HEC-RAS software enables the execution of one-dimensional steady flow, as well as one- and two-dimensional unsteady flow hydraulics. It also supports sediment transport and mobile bed computations, water temperature modeling, and generalized water quality modeling. (CPD-69 2024).HEC-RAS is a comprehensive software system designed for interactive use in a multi-tasking, multi-user network environment. It includes a graphical user interface (GUI), distinct

hydraulic analysis components, data storage and management features, as well as graphics and reporting tools. (CPD- 69 2016).

Breach parameters for a PMF event will differ significantly from those for a failure at normal pool elevation. Therefore, for each combination of pool elevation and failure scenario, specific breach parameters must be defined.

Breach characteristics can be estimated using various methods, including comparative analysis with similar historical dam failures, regression equations based on past incidents, velocity or erosion rate analysis, and computer models simulating the breaching process through sediment transport, soil mechanics, and hydraulic principles. (TD-39, 2014).

The governing equations for unsteady flow derive from the St. Venant equations, using upstream hydrographs for boundary conditions. (TD-39, 2014)

4.5.1 Modelling with 2D Flow area

Using HEC-RAS for dam break analysis involves three main processes. These comprise specifying the parameters of a dam breach, modeling flood routing in the downstream section of the dam, and routing the inflow flood through the upstream reservoir.

Before beginning the unsteady flow analysis, mesh was generated using Terrain data. Then, BCs for the 2D flow were established. Two BCs, one upstream and one downstream, were added near the 2D flow area. Flow data added for the unsteady flow analysis, providing all necessary details. The model receives a time series file of discharge in the form of a hydrograph for the upstream boundaries and a normal depth for the downstream boundary.

4.6 Creating the 2D Computational Mesh

The study area, including the reservoir and flooding zone, was modeled as a single 2D flow region with a resolution of 30 meters per cell. Accurate hydraulic modeling with HEC-RAS requires a high-resolution digital elevation model (DEM) and boundary condition data. This study used 12.5-meter DEM data from USBR Web.

The 2D flow area is converted into a computational mesh, with each cell defined by three characteristics: water surface height at the cell center, and a hydraulic connector (SA/2D Area Conn) linking upstream and downstream areas. The upstream area is the headwater, while the downstream area is the tail-water, connected by a dam.

Boundary conditions are set in the Unsteady Flow Data Editor and include standard depth for flow exiting the area, while flow enters through a hydrograph represented as Q vs. time.

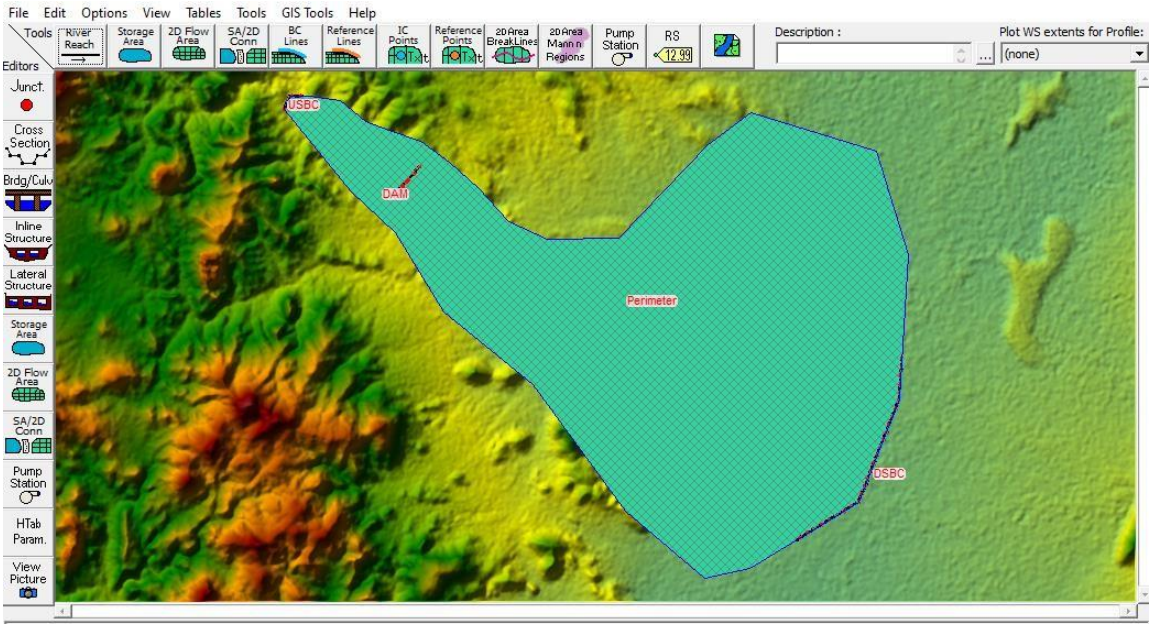

Figure 19Points are the ends of the Cell Faces.

When creating a dam line employing SA/2D connections as the entire flow region as a 2D flow area. For long, narrow reservoirs, the unstable Full Dynamic Wave Routing approach is the most accurate method to simulate reservoir storage, elevations, and outflows upstream.

Using the SA/2D Conn tool, the dam was defined in the model. A 42.3-meter-high dam was then defined using the "weir/embankment" tool.

4.6.1.1 **Estimating Breach Parameters**

The breach parameter calculator under Dam (inline structure) is available on HEC-RAS for determining breach parameters. This window tab is used to calculate all five regression equation methods. All that's needed is geometric data of the dam. 1, the dam's greatest height; 2, the water surface elevation; 3, the crest's width; 4, the dam's bottom elevation; 5, the reservoir's storage volume; and six, the upstream and downstream slope.

The parameters involved in estimating breach formation include breach width, breach depth, and breach formation time. In this study, the estimation of breach parameters is based on empirical formulas derived from historical data and analyses of past dam failures. These parameters are calculated using five different methods: Froehlich (1995a), Froehlich (2005), Von Thun & Gillette, Macdonald & Langridge, and Xu & Zhang. Each method calculates

breach parameters based on observed relationships between various characteristics, such as type (earthfill, rockfill), height, volume, and material properties. Additionally, the failure mechanism is considered, determining whether the breach occurred due to overtopping or internal erosion (piping). (TD-39, 2014)

Froehlich (1995a)

Height of the dams: 3.66 – 92.96 meters (12 – 305 feet)
(with 90% < 30 meters, and 76% < 15 meters)

Volume of water at breach time: 0.0130 – 660.0 m^3 x 10^6 (11 - 535,000 acre-feet)
(with 87% < 25.0 m^3 x 10^6, and 76% < 15.0 m^3 x 10^6)

of historical data values), and are presented in greater detail in this document:

Where:

Bave = average width of the breach (in meters)

Ko = constant (1.4 for overtopping failures, 1.0 for piping failures)

Vw = volume of the reservoir at the time of failure (in cubic meters)

hb = height of the finished breach (in meters)

tf = time taken for the breach to form (in hours) (TD-39,2014)

Froehlich(2008)

- **Height of the dams:** 3.05 – 92.96 meters (10 – 305 feet)
(with 93% < 30 meters, and 81% < 15 meters)
- **Volume of water at breach time:** 0.0139 – 660.0 m^3 x 10^6 (11.3 - 535,000 acre-feet)
(with 86% < 25.0 m^3 x 10^6, and 82% < 15.0 m^3 x 10^6)

Froehlich's regression equations for average breach width and failure time are:

$$B_{ave} = 0.27\ K_o\ V_w^{0.32}\ h_b^{0.04}$$

$$t_f = 63.2\sqrt{\frac{V_w}{g h_b^2}}$$

Where:

Bave = average width of the breach (in meters)

Ko = constant (1.3 for overtopping failures, 1.0 for piping failures)

Vw = volume of the reservoir at the moment of failure (in cubic meters)

hb = height of the completed breach (in meters)

g = acceleration due to gravity (9.80665 meters per second squared)

tf = time required for the breach to form (in seconds)

MacDonald & Langridge Monopolis (1984)

For earthfill dams:

$$V_{eroded} = 0.0261 \left(V_{out} * h_w\right)^{0.769}$$

$$t_f = 0.0179 \left(V_{eroded}\right)^{0.364}$$

For earthfill with clay core or rockfill dams:

$$V_{eroded} = 0.00348 \left(V_{out} * h_w\right)^{0.852}$$

Height of the dams: 4.27 – 92.96 meters (14 – 305 feet)
(with 76% < 30 meters, and 57% < 15 meters)

Breach Outflow Volume: 0.0037 – 660.0 m^3 x 10^6 (3 - 535,000 acre-feet)
(with 79% < 25.0 m^3 x 10^6, and 69% < 15.0 m^3 x $10^{6)}$

Where:

Veroded = volume of material eroded from the dam embankment (in cubic meters)

Vout = volume of water flowing through the breach (in cubic meters)

hw = depth of water above the bottom of the breach (in meters)

tf = time taken for the breach to form (in hours) (TD-39,2014)

Von Thun & Gillette

Height of the dams: 3.66 – 92.96 meters (12 – 305 feet)
(with 89% < 30 meters, and 75% < 15 meters)

Volume of water at breach time: 0.027 – 660.0 m^3 x 10^6 (22 - 535,000 acre-ft)
(with 89% < 25.0 m^3 x 10^6, and 84% < 15.0 m^3 x 10^6)

The Von Thun and Gillette equation for average breach width is:

$$B_{ave} = 2.5\, h_w + C_b$$

where:

Bave = average width of the breach (in meters)

hw = depth of water above the breach bottom (in meters)

Cb = coefficient that depends on the size of the reservoir

Xu & Zhang (2009)

Height of the dams: 3.2 – 92.96 meters (10 – 305 feet)
(with 78% < 30 meters, and 58% < 15 meters)

Volume of water at breach time: 0.105 – 660.0 m^3 x 10^6 (11.3 - 535,000 acre-feet)
(with 80% < 25.0 m^3 x 10^6, and 67% < 15.0 m^3 x 10^6)

Xu and Zhang's regression equation for average breach width is:

$$\frac{B_{ave}}{h_b} = 0.787 \left(\frac{h_d}{h_r} \right)^{0.133} \left(\frac{V_w^{1/3}}{h_w} \right)^{0.652} e^{B_3}$$

where:

Bave = average width of the breach (in meters)

Vw = volume of the reservoir at the time of failure (in cubic meters)

hb = height of the final breach (in meters)

hd = height of the dam (in meters)

hr = reference height of fifteen meters, used to differentiate between large and small dams

hw = height of the water above the breach bottom elevation at the time of the breach (in meters)

B3 = coefficient calculated as b3 + b4 + b5, which depends on dam characteristics

b3 = coefficients of -0.041, 0.026, and -0.226 for dams with core walls, concrete-faced dams, and homogeneous/zoned-fill dams, respectively

b4 = coefficients of 0.149 and -0.389 for overtopping and seepage/piping, respectively

b5 = coefficients of 0.291, -0.14, and -0.391 for high, medium, and low dam erodibility, respectively(TD-39,2014)

4.6.1.2 **Breach Characteristics**

Identifying the location, size, and timing of a dam breach is crucial for assessing potential risks, as these factors affect peak flow predictions and warning times for downstream areas. However, estimating these breach characteristics can be uncertain. Each failure scenario requires specific breach parameters, which vary significantly between events like a probable maximum flood (PMF) and a sunny day failure at normal pool levels.

To estimate dam breach characteristics Regression equations from past incidents to predict peak outflow and breach size was employed

These methods are useful for understanding and estimating breach characteristics.

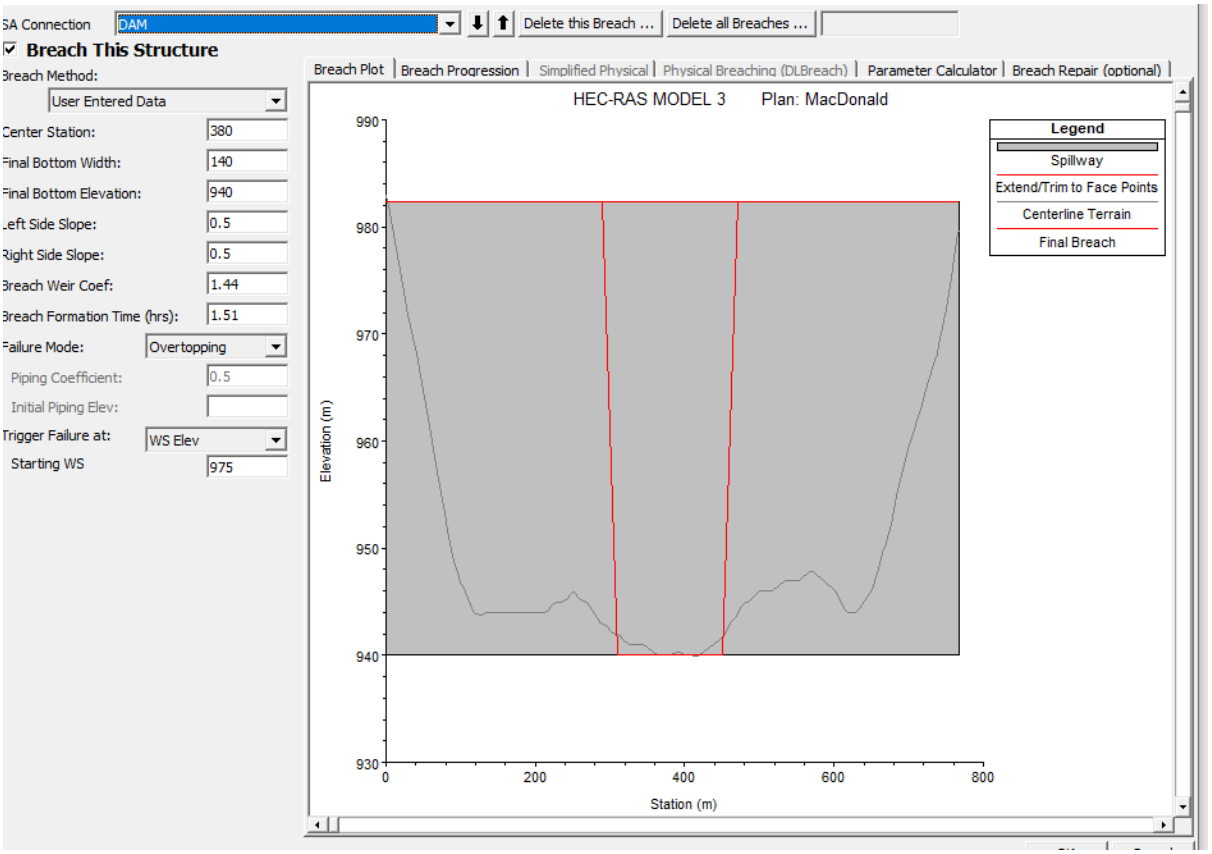

Figure 20Dam breach Location

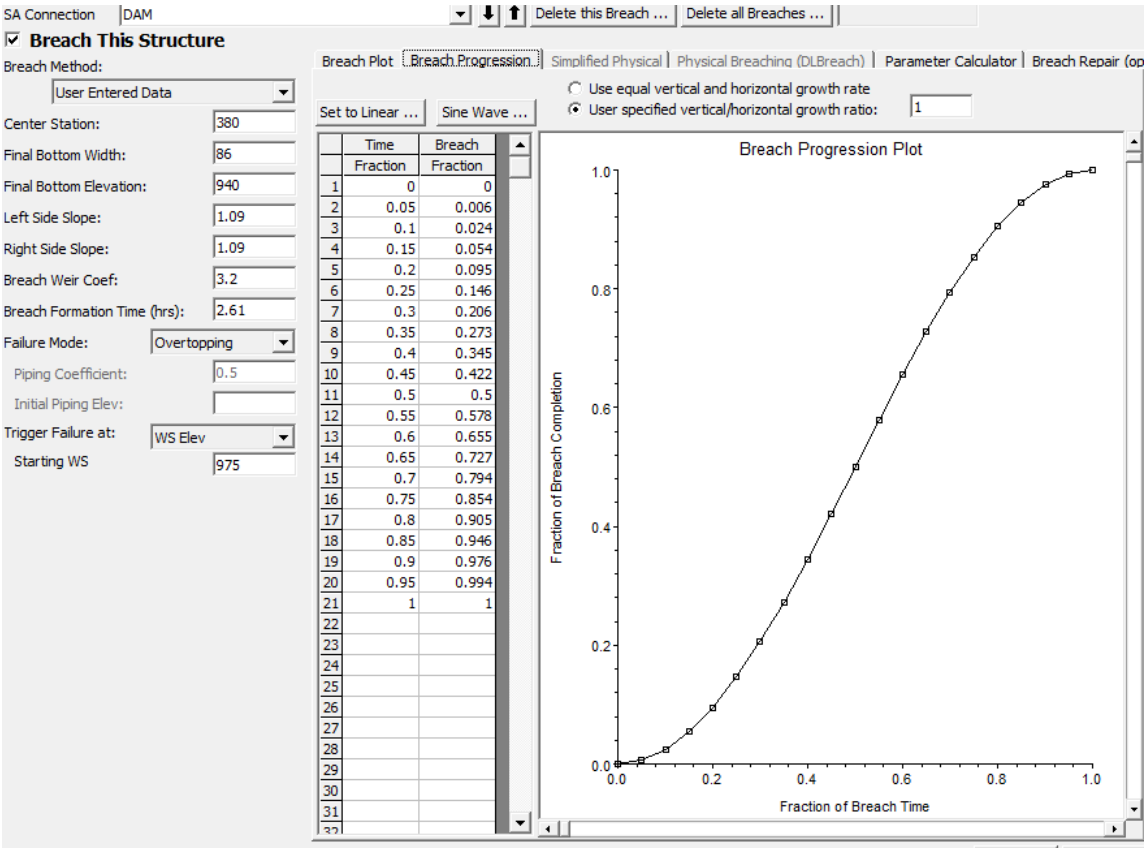

Figure 21 Graph of Breach Progression Method

4.7 Unsteady Flow Data

We assign the starting flow, storage area conditions, and boundary conditions to the 2D flow area at the start of the simulation in order to perform 2D unsteady flow analysis. This allows the model computations to be built up in a way that incorporates 2D flow areas (mesh networks). A well-known inflow hydrograph is frequently the upstream boundary condition (BC).

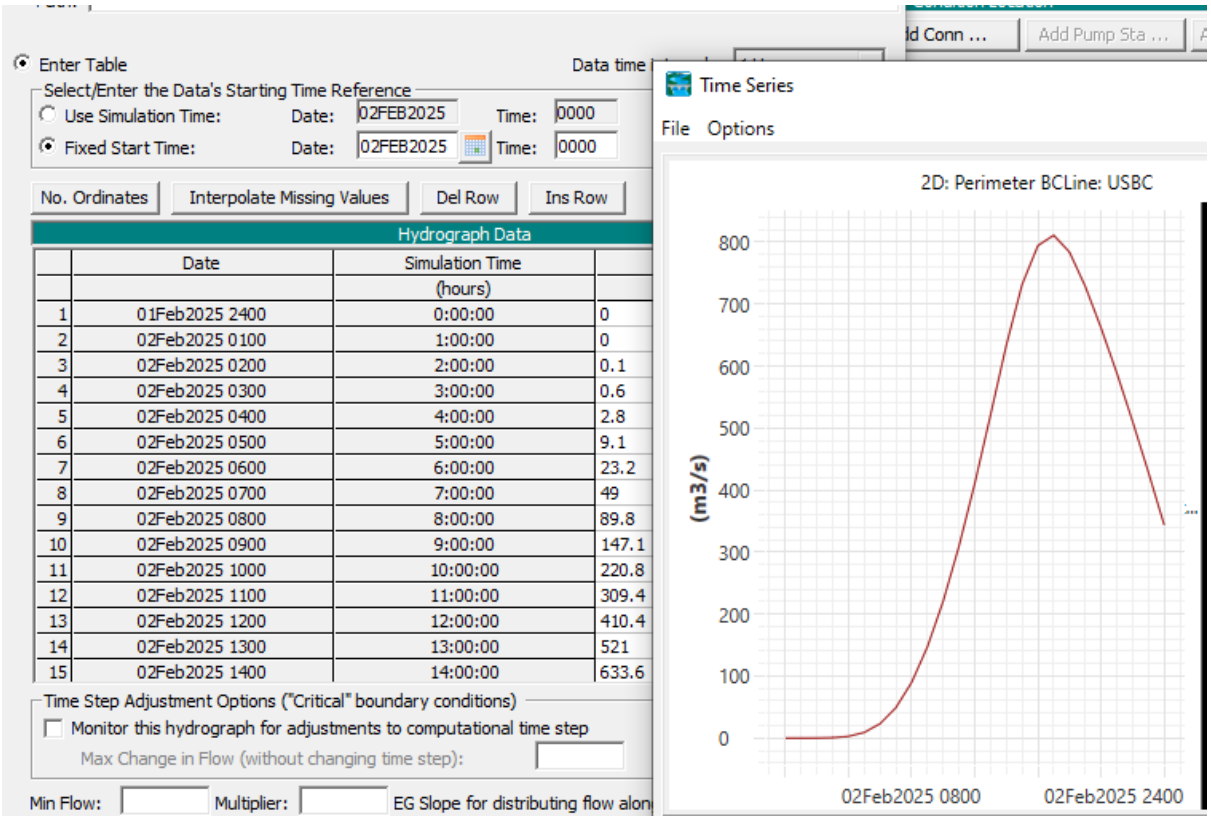

Figure 22Inflow Data for Unsteady Flow

4.7.1 Manning's Value

First, Manning’s n values must be determined for each of the land cover classifications within the land cover layer based on data from the Ministry of Water.

In order to produce a more accurate simulation of water flow, the Manning's value about the existence of agricultural areas was established. This value was then assigned based on the different types of land cover and used to determine surface roughness, Manning value for the flow area is set to its corresponding land cover type.

The HEC-RAS RAS Mapper model uses Manning’s n values for 2D flow areas s for the associated geometry land cover layer.

4.7.1.1 Manning’s Value For calibration

The land cover data set is created and then specified as Manning’s n values to be used for each land cover type and percent impervious for each of the land cover types.

The Land Cover layer (with Manning's n values set) is created and associated with a specific Geometry data set. Calibration is done by overriding all the Manning's n values associated with land cover within the polygon in which the model was simulated.

The geometry data set has n calibration regions. The user can create calibration region polygons to calibrate the result.

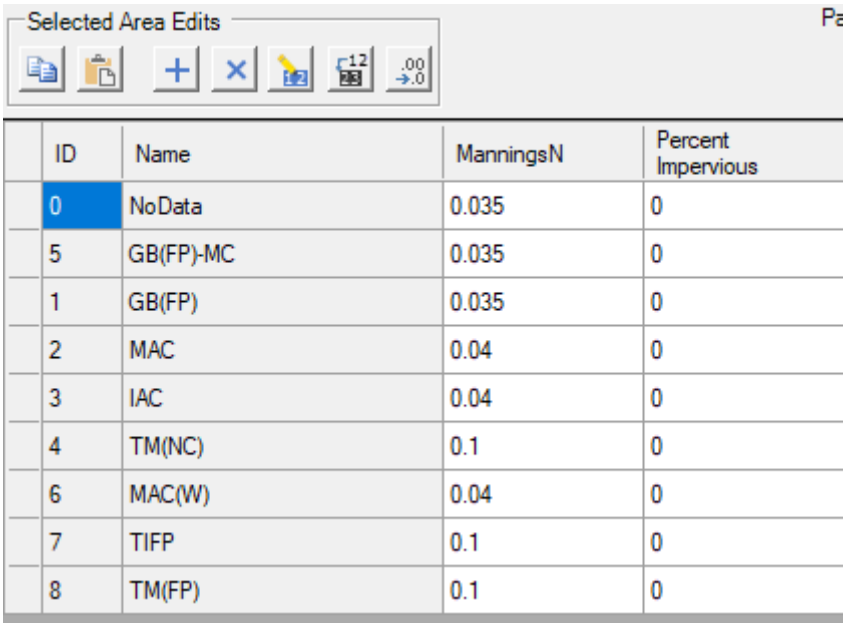
Selected Area Edits

ID	Name	ManningsN	Percent Impervious
0	NoData	0.035	0
5	GB(FP)-MC	0.035	0
1	GB(FP)	0.035	0
2	MAC	0.04	0
3	IAC	0.04	0
4	TM(NC)	0.1	0
6	MAC(W)	0.04	0
7	TIFP	0.1	0
8	TM(FP)	0.1	0

Figure 23Manning's n values based on Land Use Land Cover

There are two available methods for breaching: the first relies on input from the user's entered data, while the second takes a less physical approach. The UED methodology, which incorporates a regression equation derived from actual failure observation data, was used to estimate the geometrical and temporal parameters for this inquiry.

1.19.1.1 HEC-RAS Model Result

Earth dams are one of the most common types of dams because of their versatility and ability to accommodate different foundation conditions.

The dam break causes previously impounded water to leak upstream, creating a flood wave that travels downstream from the dam.

4.7.1.1 Unsteady Flow Hydrodynamics

In HEC-RAS dam breach analysis using the 2D unsteady flow method, the hydraulic method

typically used to model flood flow is **the Shallow Water Equations (SWE)**, which are based on the **continuity equation** and **momentum equation**. These equations govern the flow of water over a surface, considering both the flow depth and velocity in two dimensions. The 2D unsteady flow method simulates how water moves across the floodplain and other areas, providing detailed results for flood wave propagation, flow depth, and velocity over time.(CPD-69, 2016).

The full **2D shallow water equations** (St. Venant equations) for the simulation of free-surface flows, consisting of:

- A **continuity equation** (mass conservation)
- Two **momentum equations** (momentum conservation) in the x- and y-directions.

4.7.1.1.1 Hydraulic equation

1. A continuity equation (mass conservation)

The unsteady differential form of the mass conservation (continuity) equation

$$\frac{\partial H}{\partial t} + \frac{\partial (hu)}{\partial x} + \frac{\partial (hv)}{\partial y} + q = 0$$

Where t is time and v are the velocity components in the x-and y-direction respectively and q is a source/sink flux term.

2. Two **momentum equations** (momentum conservation)

When the horizontal length scale are much larger than the vertical length scale, volume construction implies that vertical velocity is small. The Navier-Stokes vertical momentum equation can be used to justify that pressure is nearly hydrostatic.

$$\frac{\partial u}{\partial t} + u\frac{\partial u}{\partial x} + v\frac{\partial u}{\partial y} = -g\frac{\partial H}{\partial x} + v_t\left(\frac{\partial^2 u}{\partial x^2} + \frac{\partial^2 u}{\partial y^2}\right) - c_f u + fv$$

Where u and v are the velocities in the Cartesian direction, g is the gravitational acceleration, v_t is the horizontal eddy viscosity coefficient, c_f is the bottom friction coefficient, R is the hydraulic raduis and f is the Coriolis parameter.

4.8 Limitation

In this study, a significant limitation was encountered regarding the hydrological data utilized, as all data were obtained through estimation methods due to the lack of recorded data. This reliance on estimations introduces uncertainties that may affect the accuracy of the model

outputs, particularly in scenarios involving extreme weather events. Without direct measurements, it is difficult to validate the estimations and their impact on the overall findings

4.9 Summery

This study aims to assess the impact of a dam breach on downstream areas using HEC-RAS 2D modeling, which utilizes a dynamic flow routing method. It incorporates hydrological data in the form of inflow hydrographs for extreme weather events, along with detailed geometric data, to determine key breach parameters. These parameters are essential in dam breach modeling and include estimates of breach geometry, such as width, depth, shape, and time of failure.

5 RESULT AND DISCUSSION

To analyze dam breach modeling, it is essential to begin by assessing the hydrology of the study area. This involves examining streamflow patterns, rainfall trends, and the characteristics of the downstream area. Understanding the hydrological dynamics of the region is critical, as variations in rainfall and streamflow can significantly influence the behavior of a dam during a breach.

5.1 Rainfall Data Analysis result

Determining the hydrological characteristics of a study area is crucial when analyzing dam breaches, especially in the context of extreme weather conditions.

Analyzing historical precipitation data and understanding the area's hydrological characteristics enables the development of accurate models of surface water flow.

Extreme weather conditions, such as intense storms, can dramatically alter surface water flow behavior. Determining the study area's hydrological characteristics helps predict potential changes in flow patterns.

Understanding the hydrological characteristics aids in assessing the vulnerability of a dam to breach under specific conditions. A detailed analysis of watershed characteristics such as slope, land use, infiltration rates, and prior flood events can reveal how a dam's catchment might respond to extreme rainfall, informing design and operational guidelines.

5.1.1 Areal PMP Result

Afriade Areal (14.52%PMP) = 20.66689mm

Gato Areal (53.08%PMP) = 77.06133mm

Konso Areal (32.38%PMP) = 44.373mm

Total Areal (PMP) = 142.1012mm

5.1.1.1 **PMP Result after Area Reduction Factor**

ARF = 0.904368

PMP = 128.5107mm

5.1.1.1.1 **HYETOGRAPH by SCS TYPE II, 24-HR DESIGN STORM**

Through the analysis of historical storm data, the typical time patterns of precipitation in various storms can be identified. Huff (1967) developed time distribution relationships for intense storms across areas as large as 400 mi² in Illinois. These patterns were categorized into four probability groups, ranging from the most extreme (first quartile) to the least severe (fourth quartile). The curves representing the probability distribution of first-quartile storms are smooth, reflecting an average rainfall distribution over time, and do not capture the sudden bursts of rainfall that are often seen in actual storm events. (Ven Te Chow, 1988)

A triangle is a straightforward shape for designing a hyetograph because, once the total precipitation depth PPP and the duration TdT_dTdare given, the base length and height of the triangle can be easily calculated. . (Ven Te Chow, 1988)

Table 3PMF HYDROGRAPH

HOUR	HYETOGRAPH
1	0.82
2	1.7
3	2.678
4	3.57
5	4.464
6	5.357
7	6.25
8	7.143
9	8.036
10	8.929
11	9.821
12	11
13	9.821
14	8.929
15	8.036

16	7.143
17	6.25
18	5.357
19	4.464
20	3.57
21	2.678
22	1.7
23	0.82
24	0

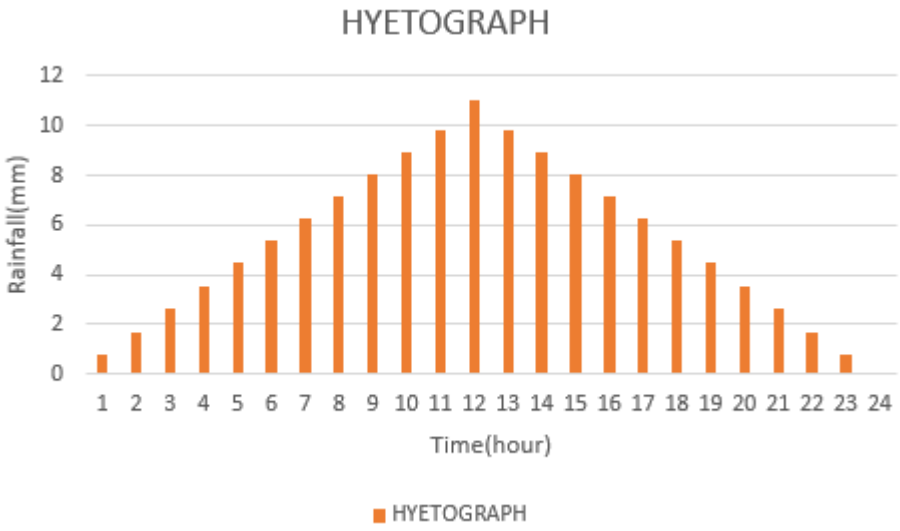

Figure 24 Hyetograph of PMP

5.1.2 Base flow Separation by SepHydro

Base flow separation is performed using the SepHydro online tool, which includes one-parameter filters, multipara meter filters, and graphical separation methods.
Baseflow separation helps to isolate the groundwater contribution to streamflow from the quick runoff generated by rainfall events. The Two-Parameter Digital Filter method (Eckhardt, 2005) was selected for base flow separation. Digital filters are commonly used for this purpose, as they effectively distinguish between "high" frequency signals, such as surface runoff, and "low" frequency signals, like base flow. This separation is achieved through a

mathematical technique applied to the stream discharge time series, allowing for a clearer understanding of base flow's contribution to overall streamflow. The method isolates the slower variations in streamflow, which are attributed to base flow, from the faster fluctuations caused by surface runoff.

5.1.3 Rainfall-Runoff Model Result

The HEC-HMS (Hydrologic Engineering Center's Hydrologic Modeling System) model was used to simulate the hydrologic conditions, which were then input into HEC-RAS for the dam breach analysis. It also demonstrates the hydrological behavior of the catchment area

5.1.3.1 Calibration and Validation of Model Result

The accuracy of the HEC-HMS model's predictions relies on the spatial and temporal variability of the watershed's morphological and hydrological characteristics. (S.S Fanta, 2021). However, poor quality streamflow data in the Weito watershed, as highlighted by M.T. Ayna (2019), presents challenges. The study observed sudden spikes in river discharge despite the absence of corresponding high precipitation events. These abrupt fluctuations in flow values do not match the recorded precipitation data. For example, the 7-day, 15-day, and 30-day average minimum flow plots suggest that the river had considerable water flow in most years. However, the recorded data showed average minimum flows of around 22, 23, and 32 cumecs during the 7-day, 15-day, and 30-day periods in 2010, respectively. Similarly, in 2011, minimum average flows of 5, 10, and 32 cumecs were recorded for the same periods. These figures imply that the river had an average flow of at least 5 cumecs per week in 2010 and 22 cumecs per week in 2011. Despite these numbers, local communities reported significant water shortages starting in 2009. Additionally, historical accounts from the community indicated that the river dried up for over a week in both 2010 and 2011. (M.T. Ayna 2019).

Observed streamflow data from the study area was available for the period from 1990 to 2007. The data was divided into two distinct periods: the calibration period (1990 to 2001) and the validation period (2002 to 2007).

5.1.3.1.1 **Calibration of HEC-HMS Model Result**

The HEC-HMS model was calibrated using observed streamflow data for the watershed of interest. The calibration process involved adjusting model parameters to match the observed streamflow at specific gauging stations. The model's performance was evaluated using model efficiency metrics, with the resulting values falling within an acceptable range for hydrological modeling.

The calibration process aimed to minimize the difference between the simulated and observed streamflow values. Several performance metrics were used to evaluate the calibration results, including Nash-Sutcliffe Efficiency (NSE), Coefficient of Determination (R2) and Percent Bias (PBIAS).The calibration was carried out iteratively, adjusting parameters and evaluating the performance until satisfactory agreement between the observed and simulated data was achieved. The model performance result shows for Nash-Sutcliffe Efficiency (NSE) = 0.608, for Coefficient of Determination (R2) = 0.74 and for Percent Bias (PBIAS) = 6.74 the result shows the model performance is fairly good.

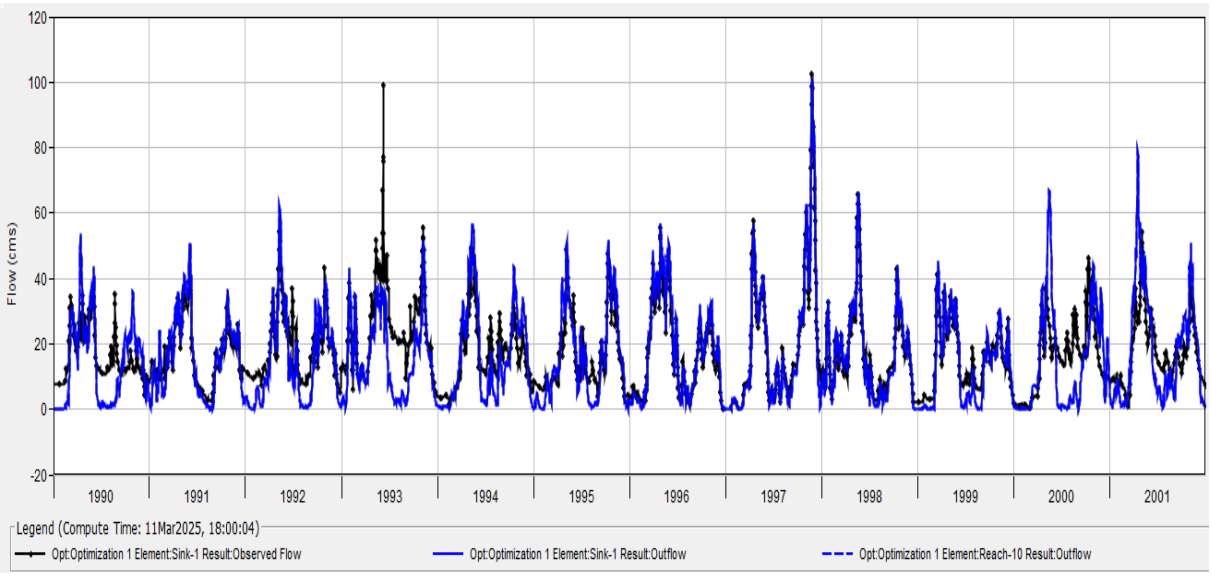

Figure 25 Graph Calibration Result

5.1.3.1.2 **Validation of HEC-HMS Model Result**

After the calibration was completed, the model was validated using the observed streamflow data from 2002 to 2007

The performance of the model was evaluated using several key metrics, including Nash-Sutcliffe Efficiency (NSE), Coefficient of Determination (R^2), and Percent Bias (PBIAS).

The coefficient of correlation (0.695) indicates that the model's simulated data is within an acceptable range compared to the observed data. The Nash-Sutcliffe Efficiency value (0.557) suggests that the model's performance is moderately satisfying. Additionally, the Percent Bias (2.33) indicates that the model's results show a good level of performance, with only a small bias between the simulated and observed data.

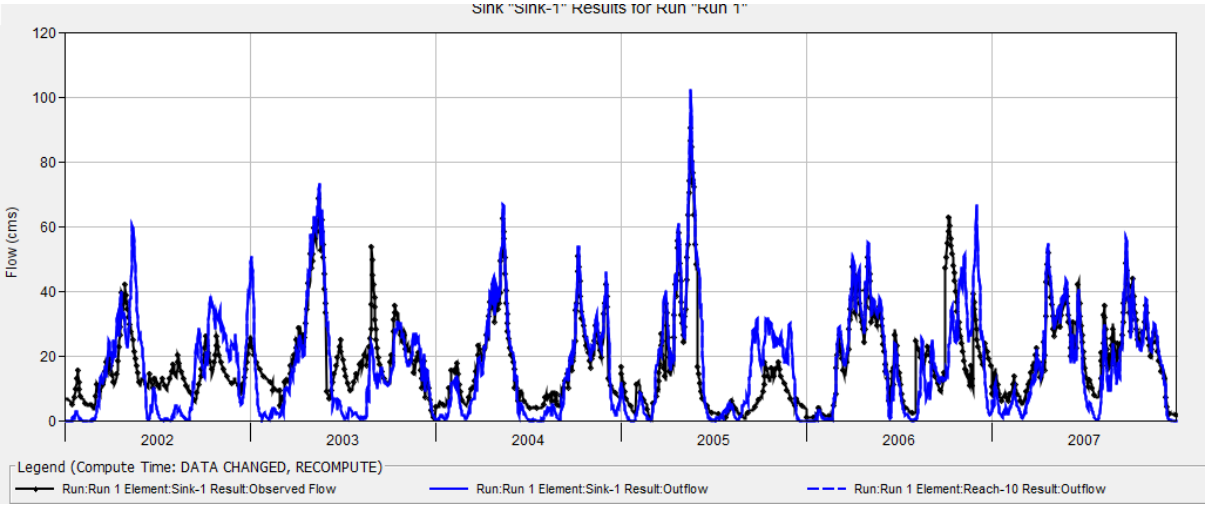

Figure 26 Graph of Validated result

5.1.4 PMF Hydrograph

The identification of PMP and the resultant peak discharge values are essential for understanding the hydrological behavior of the study area. The methodologies employed in this analysis provide a framework for predicting flood events, which can aid in enhancing preparedness and mitigating potential impacts from such natural hazards.

The HEC-HMS model generated inflow hydrographs based on the Probable Maximum Precipitation (PMP) values, which were derived from an hourly hyetograph. The generated hydrograph, representing the inflow due to extreme precipitation, was considered the Probable Maximum Flood (PMF) hydrograph, which is critical for simulating the worst-case flood scenario associated with a dam breach. The hydrographs showed a rapid rise and fall in flow, typical of storm runoff following extreme rainfall.

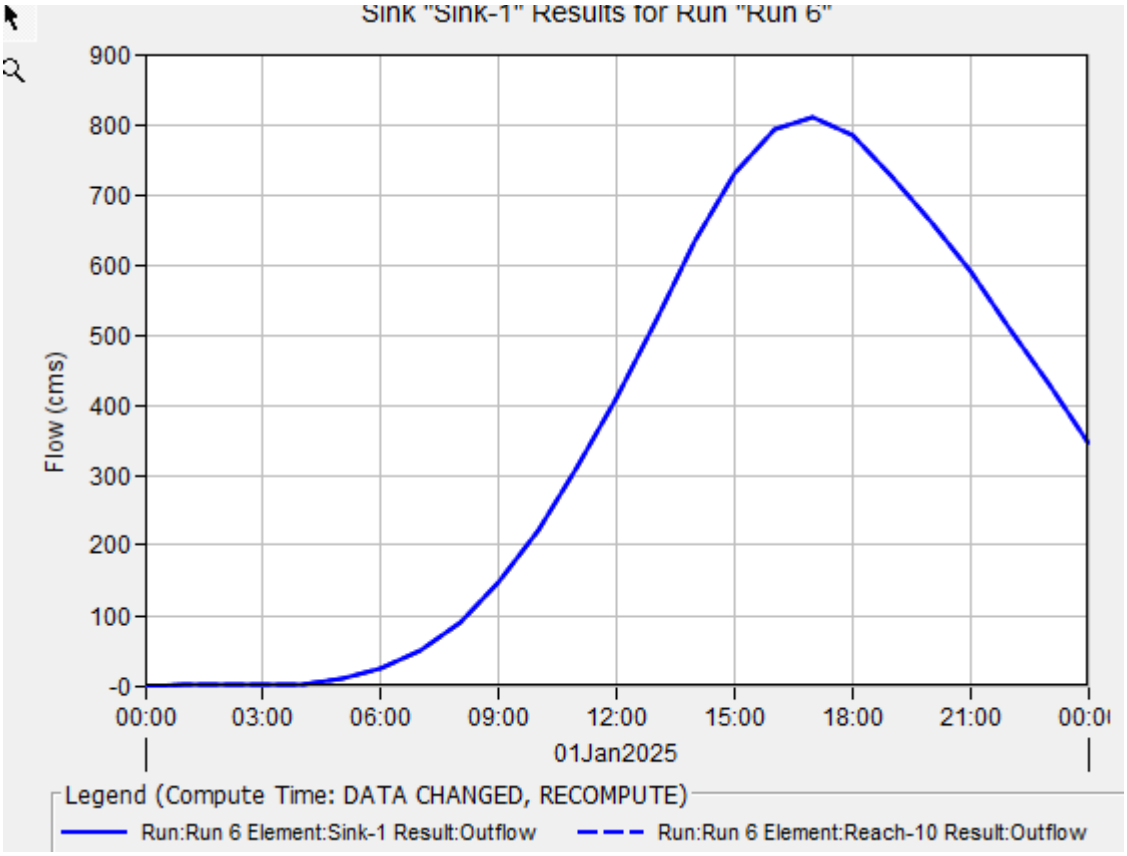

Figure 27Graph of Inflow Hydrograph from Peak Discharge

5.2 Breach Parameter Calculation Result

This study utilizes currently available regression equations from five methods: Froehlich (1995a, 2005), Van Thun, MacDonald, and Xu Zhang, to assess various breach parameters. Each of these parameters contributes to our understanding of the dynamics and impacts of breaches of dams.

Breach parameter result Froehlich (1995a) presents a breach width of 75 and a breach development time of 0.88(hr), Froehlich (2005) shows a breach width of 64 and a breach development time of 0.79, Van Thun breach width of 121 and a breach development time of 0.95, MacDonald indicates a breach width of 140 and a breach development time of 1.51, while Xu Zhang provides a breach width of 86 and a breach development time of 2.61;

The discrepancies in results among the different studies highlight the complexity of breach behavior. Each method incorporates varying assumptions and parameters, which leads to

diverse estimates.

Method	Breach Bottom Width (m)	Side Slopes (H:V)	Breach Development Time (hrs)	
MacDonald et al	140	0.5	1.51	Select
Froehlich (1995)	75	1.4	0.88	Select
Froehlich (2008)	64	1	0.79	Select
Von Thun & Gillete	121	0.5	0.95	Select
Xu & Zhang	111	1.14	2.27 *	Select

Figure 28Result of Breach parameter by HEC-RAS

5.3 HEC-RAS Model Result

Using HEC-RAS Software Tools for dam break analysis, there are three fundamental parts to the process: identifying the features of the dam breach, simulating the downstream portion of the dam's flood path, and directing the input flood through the upstream reservoir.

HEC-RAS model result shows three dynamic results layers called **Depth, Velocity, and WSE** (Water Surface Elevation). The model findings can be seen in an inundation mapping form (such as a two-dimensional map of the geometry with layers of water.

After the dam breach occurred, multiple profile lines were set at different locations downstream. This helps to identify the characteristics of flow along the profiles and provides a clear understanding of the different floodplains

Depth: - water depths calculated using variations in the water's surface level. The depth of water flow downstream from a dam breach can vary significantly

Depth of water at 2km from Dam

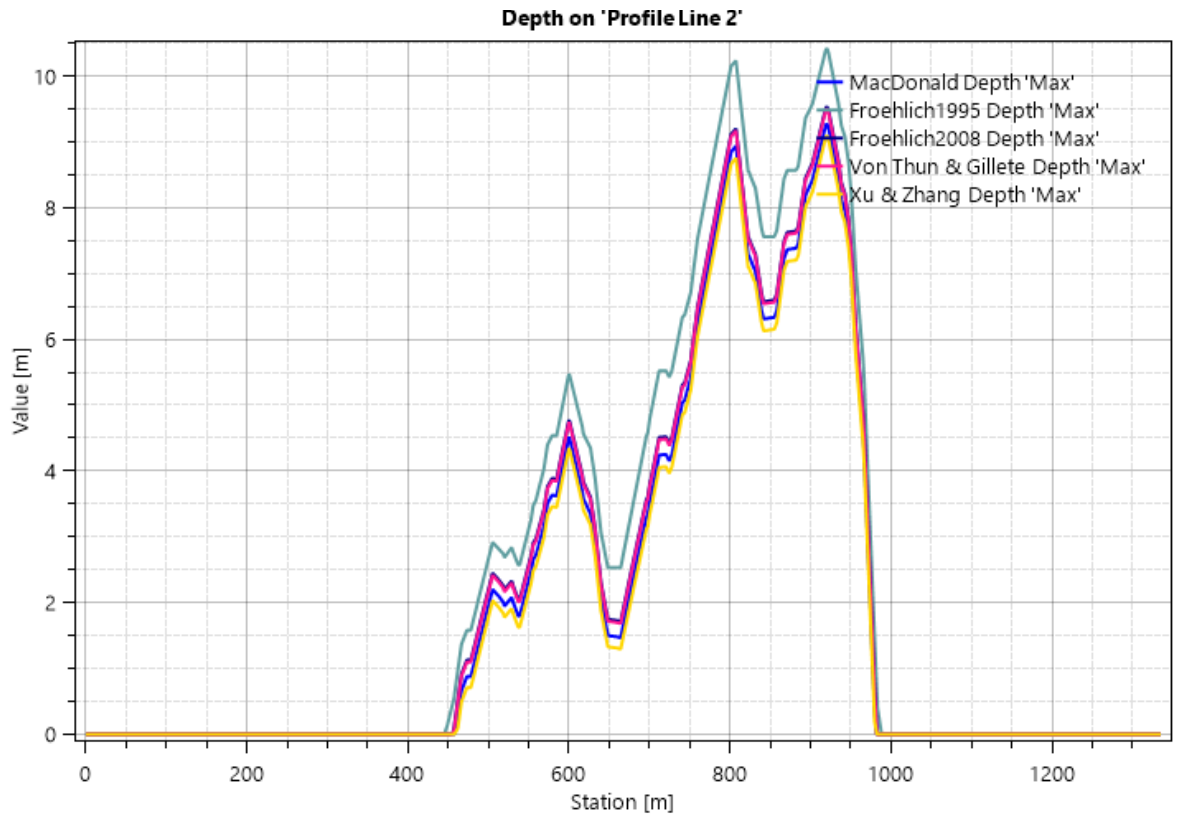

Figure 29Deph of flood at 2km from the dam

Velocity of flow at 2km downstream from the Dam

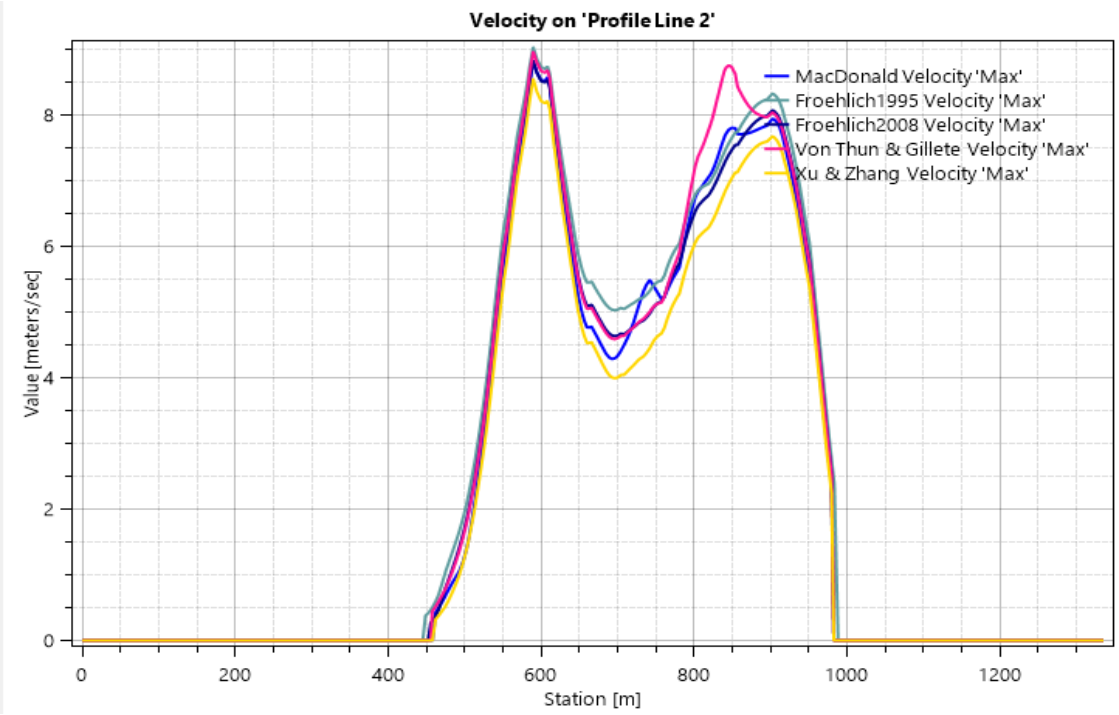

Figure 30velocity of flood at 2km from the dam

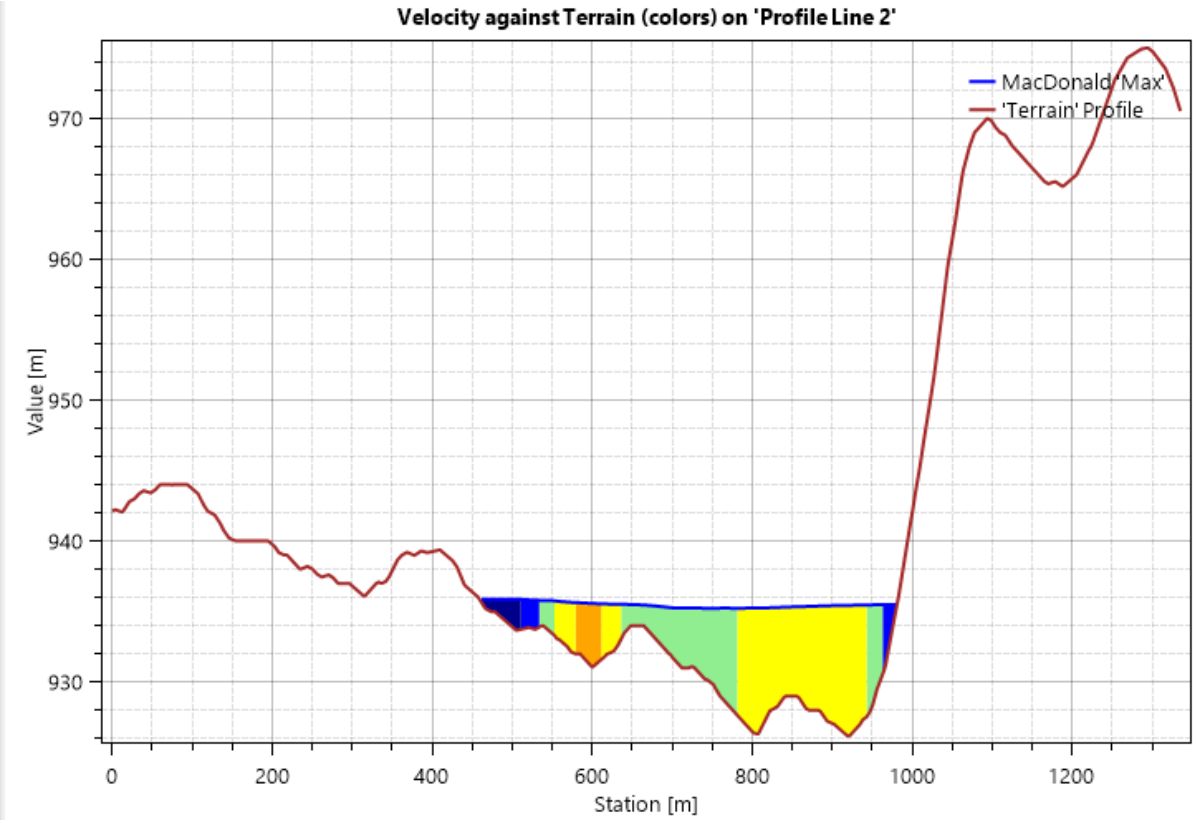

Figure 31 velocity against terrain due to friction at 2km from the dam

As the profile indicates, at a distance of 2km from the source, the floodwaters are contained within a narrow space but exhibit a high-water depth. The landscape upstream features steep gorges, which funnel the water and increase its velocity. In contrast, the downstream area is relatively flat, leading to significant changes in the dynamics of flooding.

When floodwaters flow down from the gorge, they gain speed and volume due to the steep gradients of the terrain. As these fast-moving waters reach the flat downstream area, their velocity decreases, allowing the water to spread out over a larger expanse. This transition can lead to widespread inundation of the flat areas, as the floodwaters fill depressions and low-lying regions.

The flat terrain enables the flood to cover a greater area, which increases the risk of prolonged flooding. This prolonged inundation can have severe consequences, potentially affecting agricultural land, damaging infrastructure, and disrupting local habitats. Understanding these dynamics is crucial for effective flood management and mitigation strategies

Depth of water at 5km from Dam

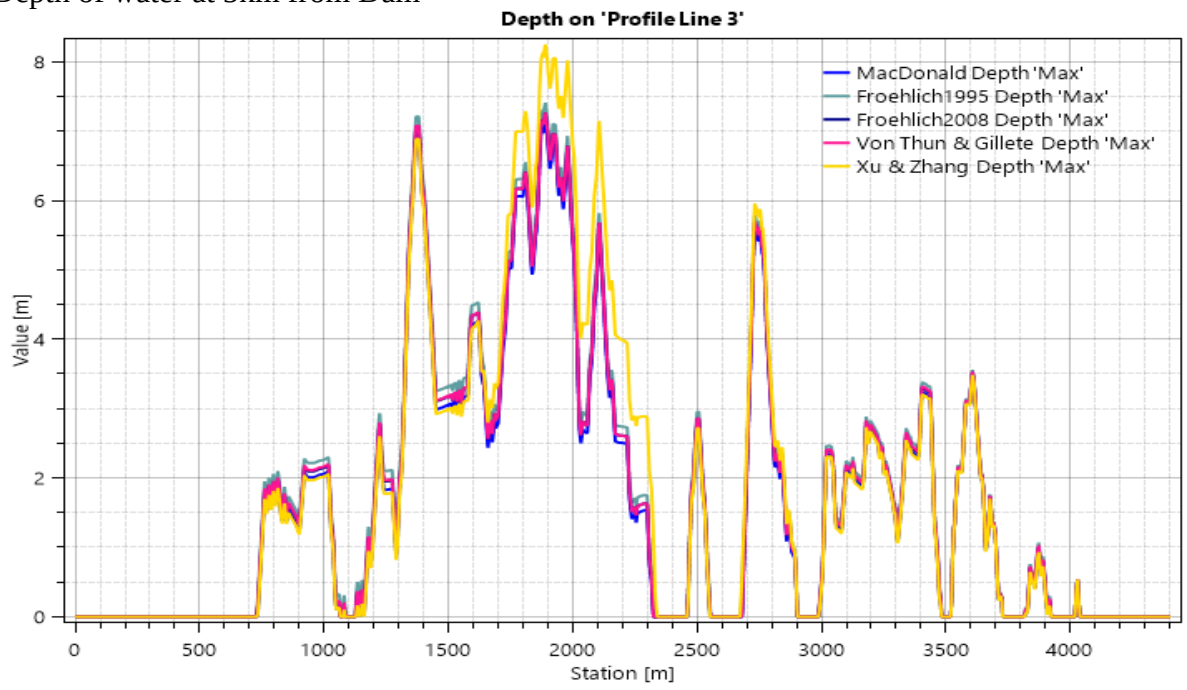

Figure 32Depth of flood at 5km from the dam

Velocity of flow at 5km downstream from the Dam

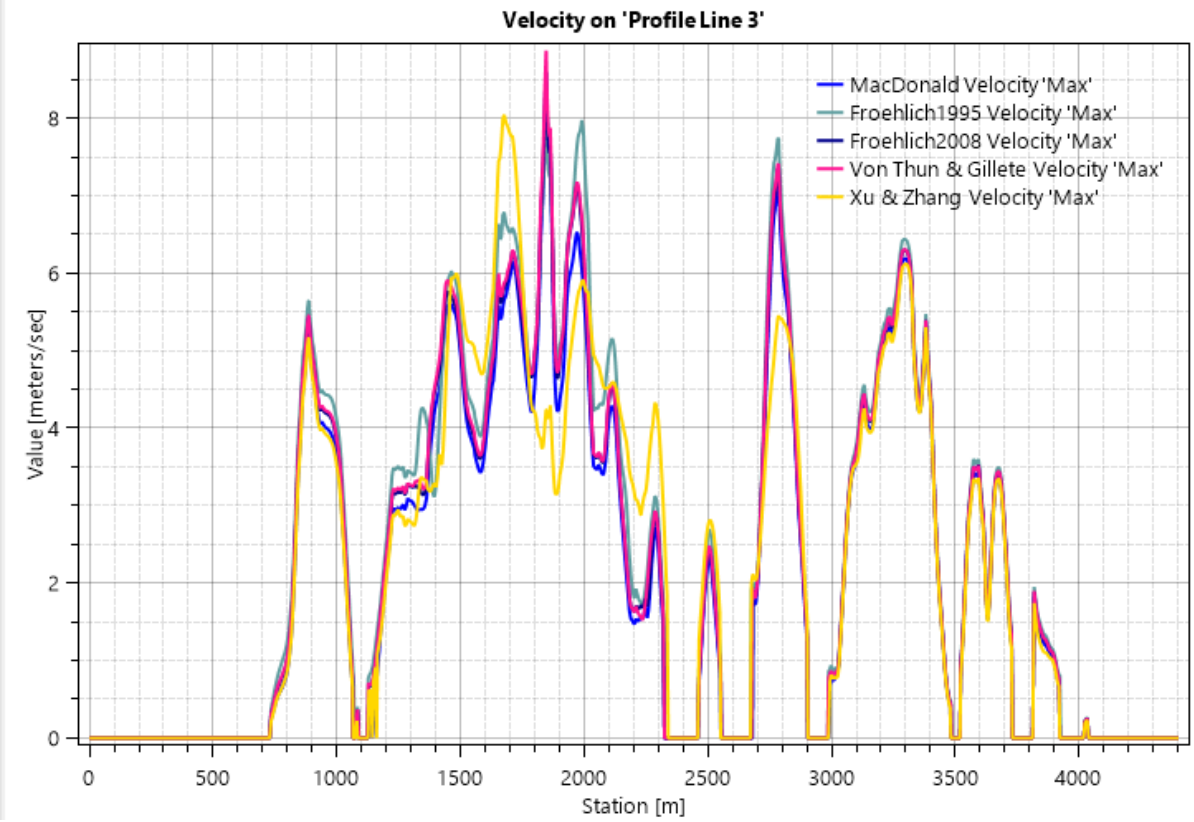

Figure 33 Velocity of the flood at 5km from the dam

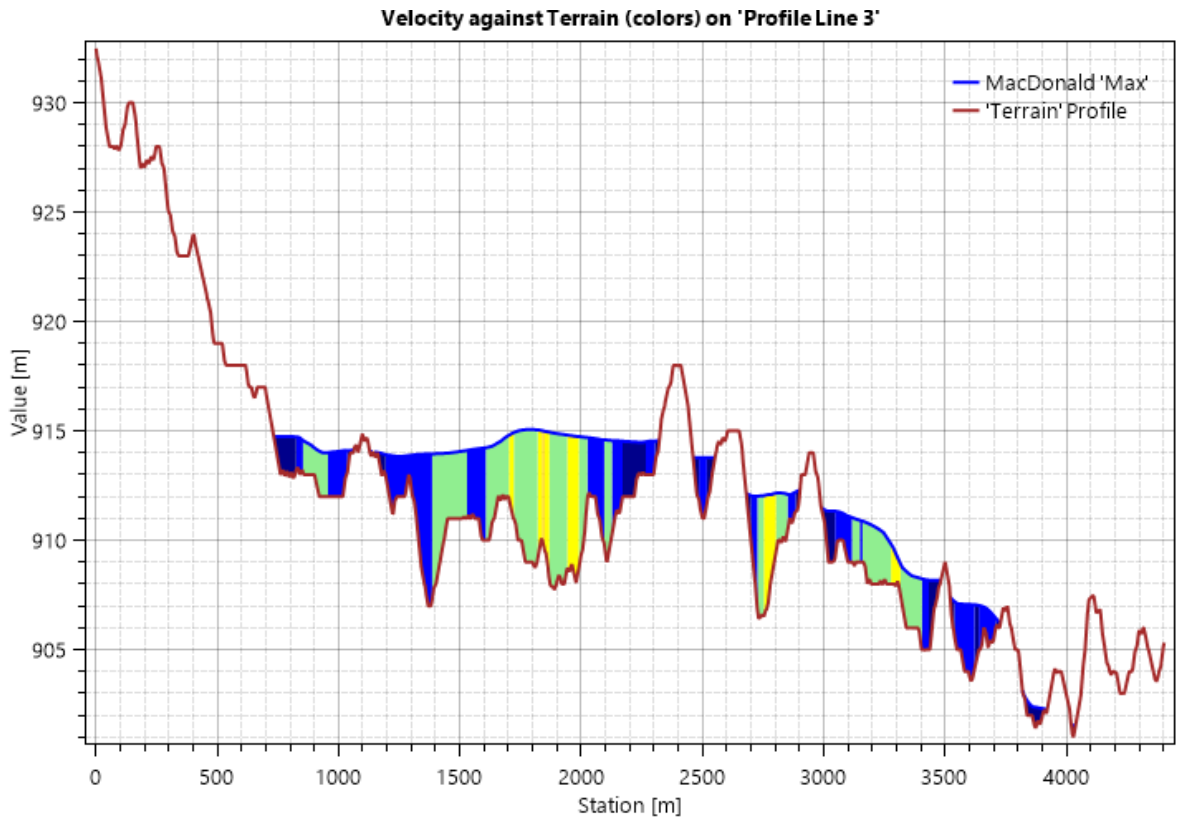

Figure 34 Velocity agiast terrain due to friction at 5km from the dam

The flat terrain allows the flood to cover a greater area, increasing the risk of prolonged flooding and potentially affecting agricultural land, infrastructure, and habitats.

The transition from the narrow, confined gorge to the open flatlands creates a distinct change in flood behavior, transforming fast-moving water into a more distributed and shallow flow. This phenomenon highlights the importance of understanding topography in flood management and planning efforts, as the impact on downstream communities can be extensive and damaging

Depth of water at 7km from Dam

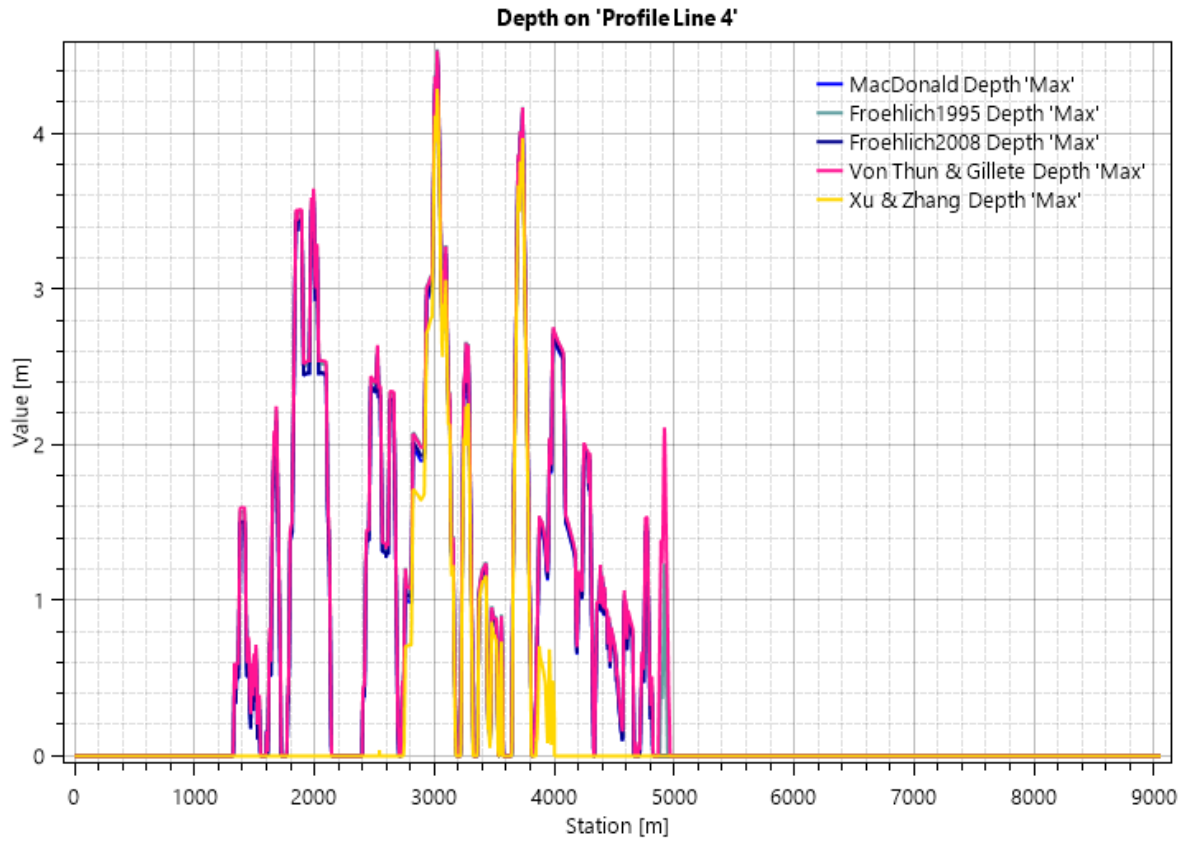

Figure 35 Depth of flood at 7km from the dam

Velocity: - The total velocity, as well as the spatially interpolated velocity between each calculated point.

As the water flows to downstream end the slope of the topography become flat and the velocity is decreased.

Velocity of flow at 7km downstream from the Dam

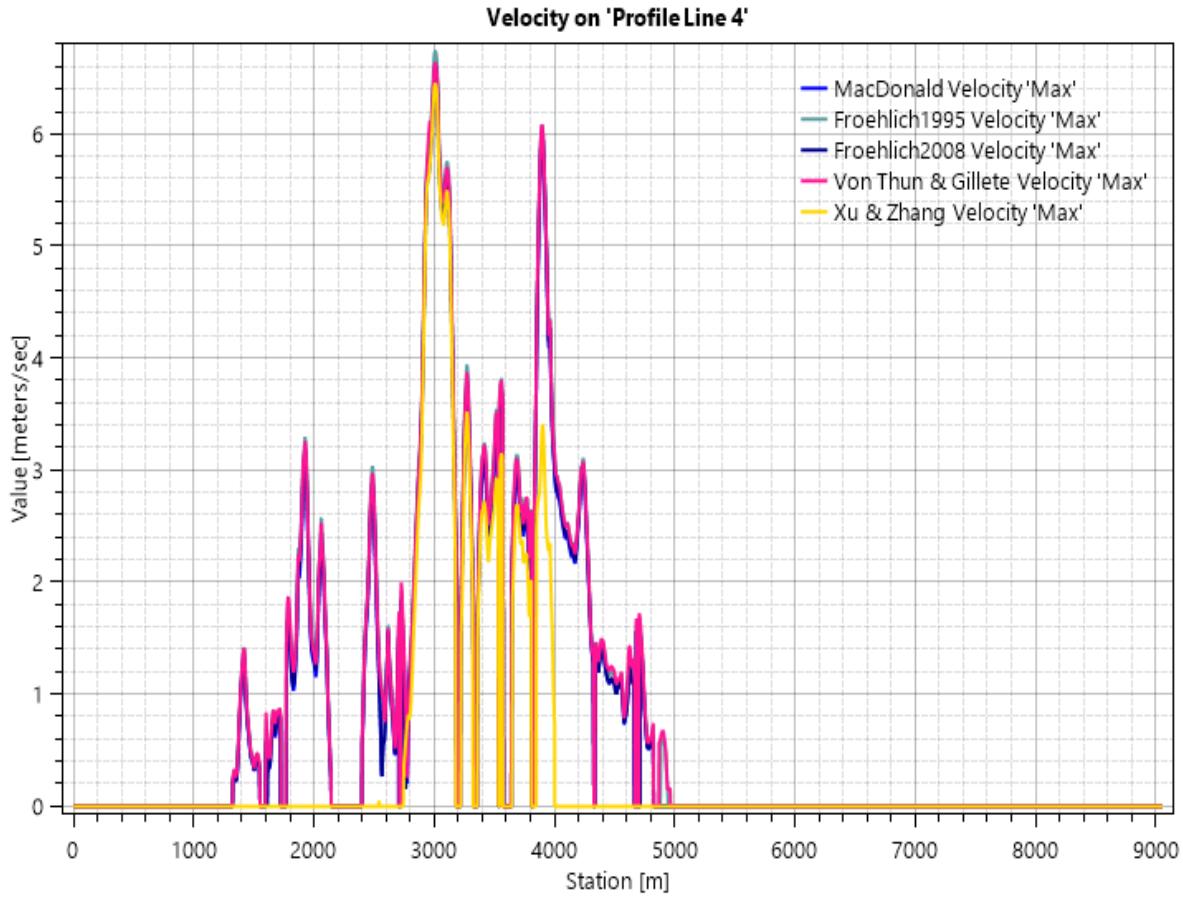

Figure 36 Velocity of the flood at 7km from the dam

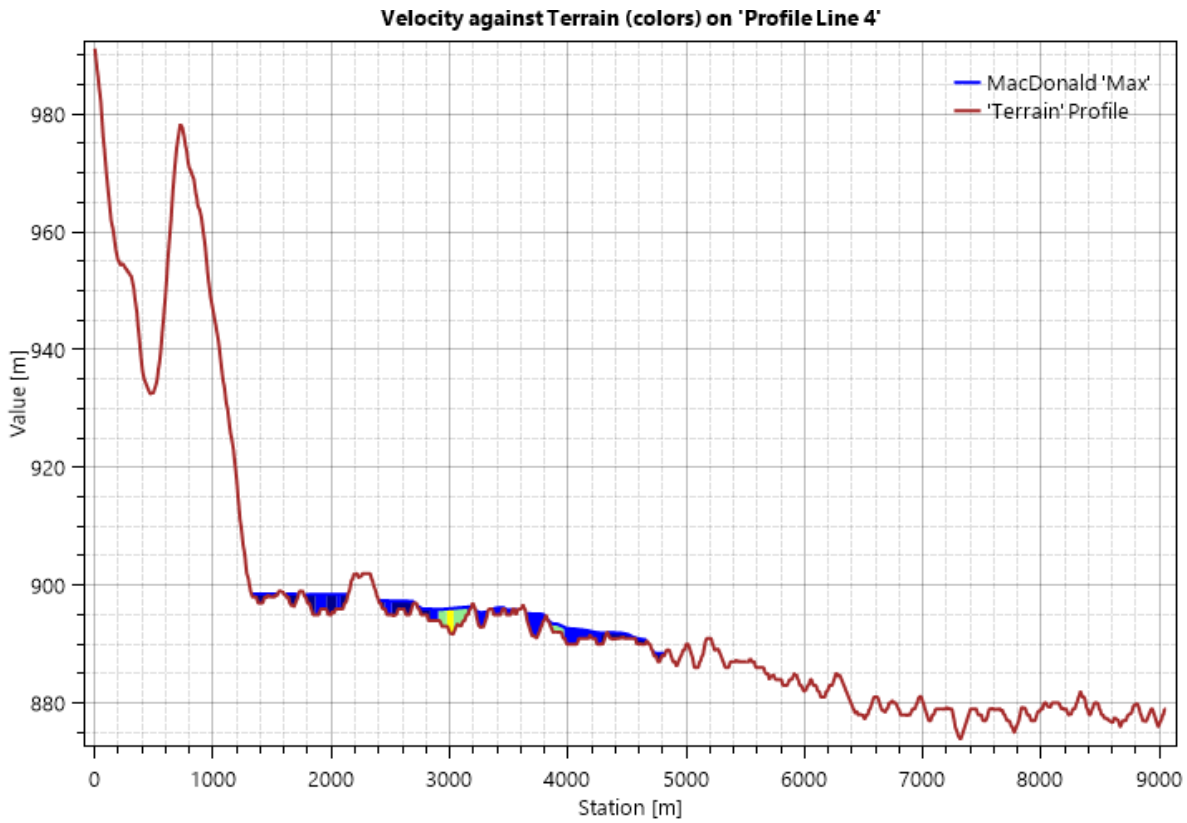

Figure 37 Velocity against terrain due to friction at 7km from the dam

When flood routing is applied to the downstream end of the inundated area, this process tracks how a flood wave progresses along a river or channel. Key aspects of flood routing include: the decrease in peak flow as it moves downstream (known as attenuation); the time it takes for the flood peak to travel between significant locations; the highest water levels at these points; and the alterations in the shape of the flood hydrograph as it progresses downstream.

These characteristics are influenced by several factors, including: the slope of the channel bed; the dimensions and shape of the main channel and surrounding areas; the roughness of both the channel and floodplain; the presence of areas that can temporarily hold floodwater away from the main flow paths; and the initial shape of the flood hydrograph entering the channel. These factors influence the expected levels of attenuation.

5.3.1 Peak Outflow

To check the dam failure by over topping PMF is used as the reservoir inflow hydrograph.

Dam failure during a flood mostly produces a larger dam break flood than a failure at normal pool because of the larger quantity of stored water.

The model result displays the peak outflow as time series plots and tables data from unsteady flow analysis.

After the dam breach the immediate segments of downstream area experienced peak flows.

Table 4 DAM Breach Out Flow Result

No	Name	Q(CMS)	H(m)
1	MacDonaldet al	14441.92	35.19
2	Froehlich (1995a)	17990.85	35.2
3	Froehlich (2008)	15528.94	35.22
4	Von Thun & Gillette	15526.33	35.12
5	Xu & Zhang	13525.53	35.34

The result of the peak discharge from the model is compared to the envelope curve of historical dam failures.

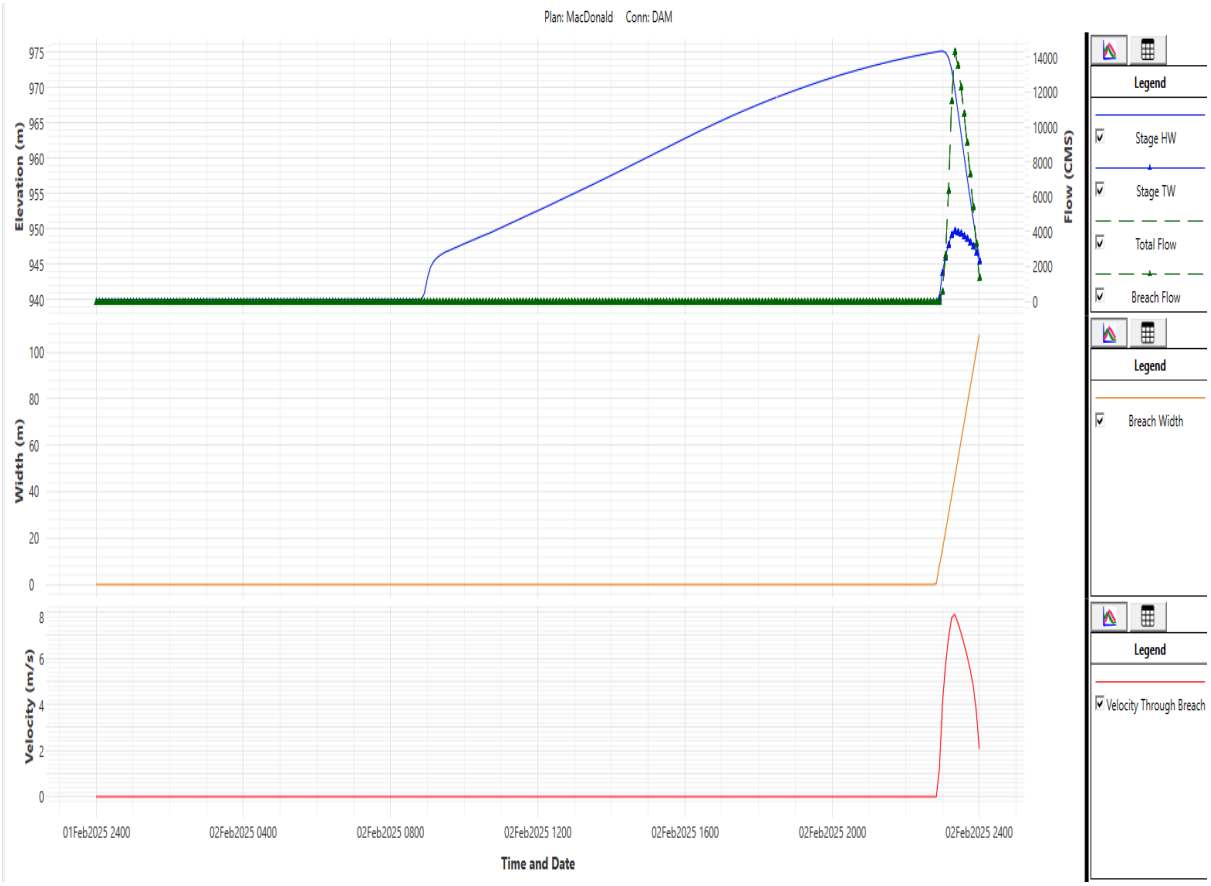

Figure 38 Dam Breach result

The peak outflow discharge from the dam breach is compared to the peak flow equation derived from data for earthen dams, zoned earthen dams with an impervious core, and rock-fill dams.

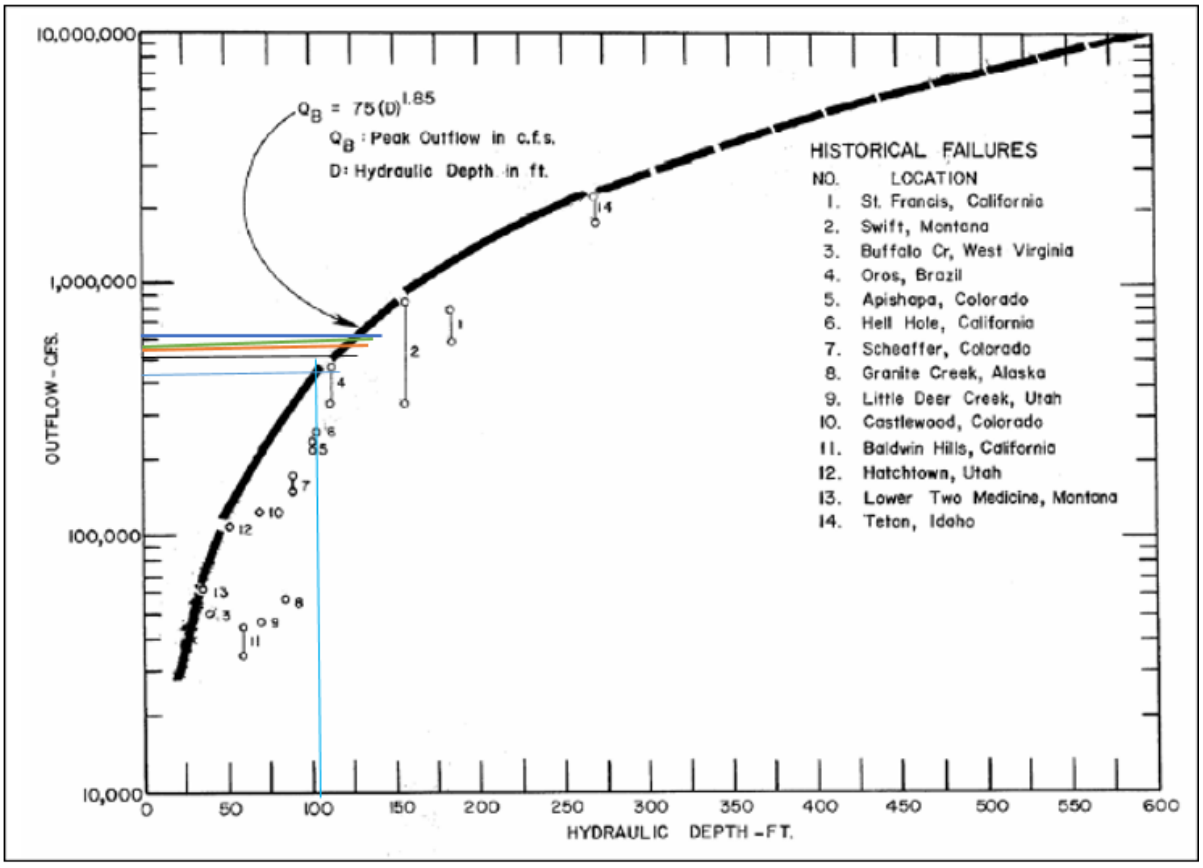

Figure 39Historical dam failure envelop curve

The HEC-RAS model predicted breach discharge values for the simulated flood scenarios were compared with the historical Dam Failure envelope curve peak discharge Equation.

When comparing the simulated results to the historical dam failure peak discharge envelope curve, Xu Zhang's method shows a ratio of 5.0%, Froehlich (1995a) is at 28.4%, Froehlich (2008) is at 10.78%, Von Thun & Gillette is at 11.6%, and MacDonald & Langridge-Monopolis is at 3.7%. MacDonald's method has a closer ratio for peak discharge of envelop curve of peak discharge equation.so for downstream flood routing the MacDonald and Langridge method result was used.

The maximum breach outflow and its arrival time of MacDolnald & Langridge-Monopolis method at different location on the downstream flood area.

Table 5 Peak Discharge Arival Time

Distance	Time(hr)	Q(m3/s)	Depth(m)	Velocity(m/s)
At Dam	10:55	14441.92	35.19	7.9
At 2km	11:15	14212.5	9.28	8.8
At 5 km	11:25	13348.5	7.15	8.4
At 7km	11:40	7878.69	4.4	6.5

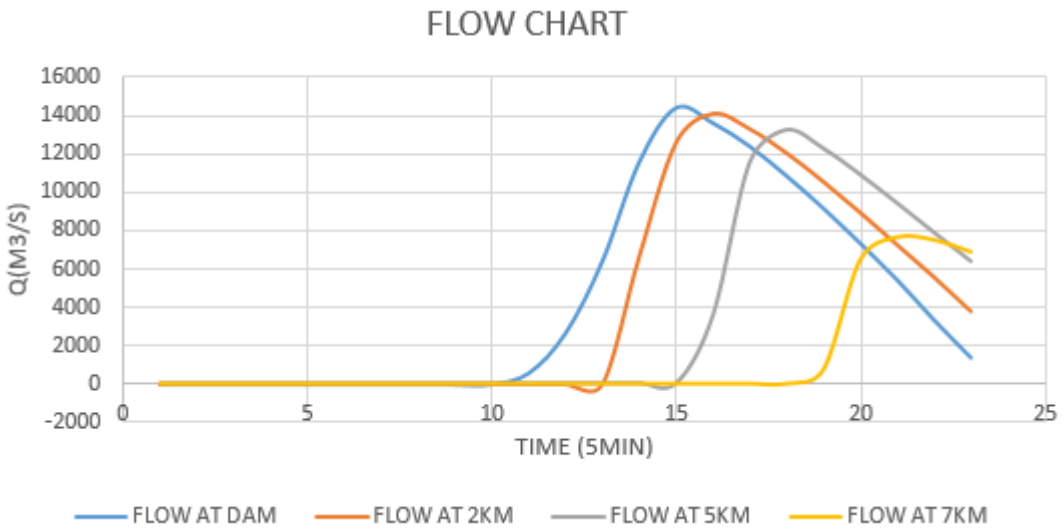

Figure 40Breach Discharge Graph at Different Station

5.3.2 Inundation Maps

An inundation map illustrates a flood or indicates a possible danger area that extends downstream from the dam's site to a point where there is no longer a chance of property damage or human casualties due to a breach flood.

The map shows visualized model results of inundated area. Map of water depth computed from the difference in water surface elevation.

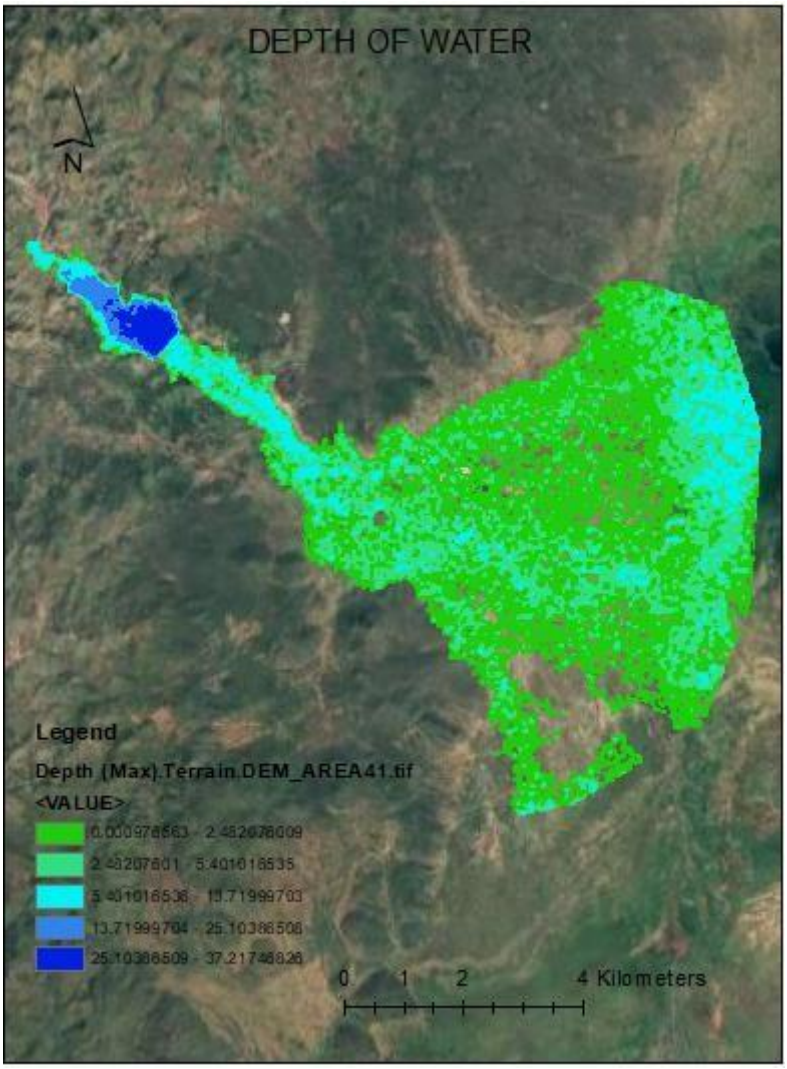

Figure 41Map of depth of water

An inundation map is a critical tool used in flood risk assessment and management, illustrating the areas that would be submerged under water in the event of a flood or dam breach. Its primary purposes include assessing flood risk, guiding emergency response planning, and informing land use planning. Key components of inundation maps include flood extent, which delineates the expected flooded areas, and water depth, often shown through contours or color gradients to assess potential impacts on structures and ecosystems. Velocity zones may also be indicated to understand erosion and structural damage risks.

These maps are created using hydrological modeling, which simulates water behavior during floods, considering inflow hydrograph, and dam breaches.

Inundation maps are applied in public awareness about flood risks and are used to enforce regulatory compliance, preventing development in high-risk areas.

However, there are limitations; inundation maps are often based on specific scenarios and may not account for future changes in land use, climate change, or extreme weather patterns. The effectiveness of these maps also depends on the accuracy and quality of the underlying data and modeling techniques. Overall, inundation maps are essential for understanding flood risks and planning for potential flood events, ultimately helping to mitigate the impacts of flooding on human life and infrastructure

Map of the velocity from the model Velocity at all computed locations and spatially interpolated velocity between those locations.

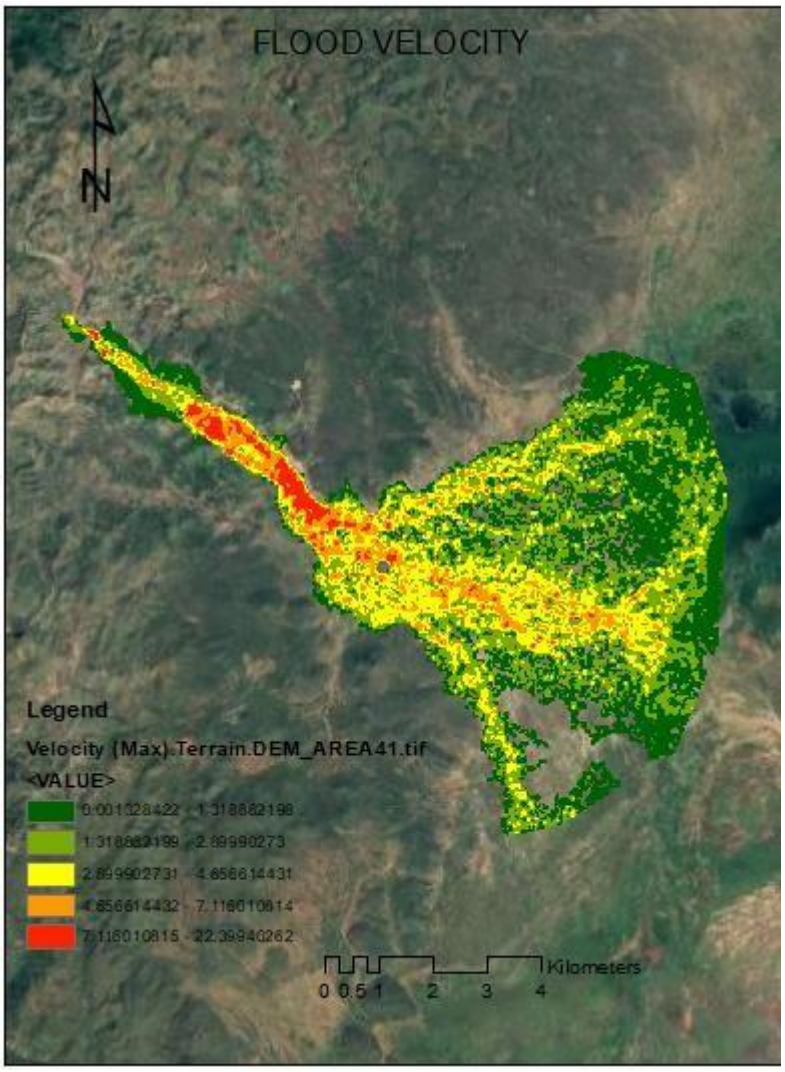

Figure 42Map of velocity of water

Map water surface elevation

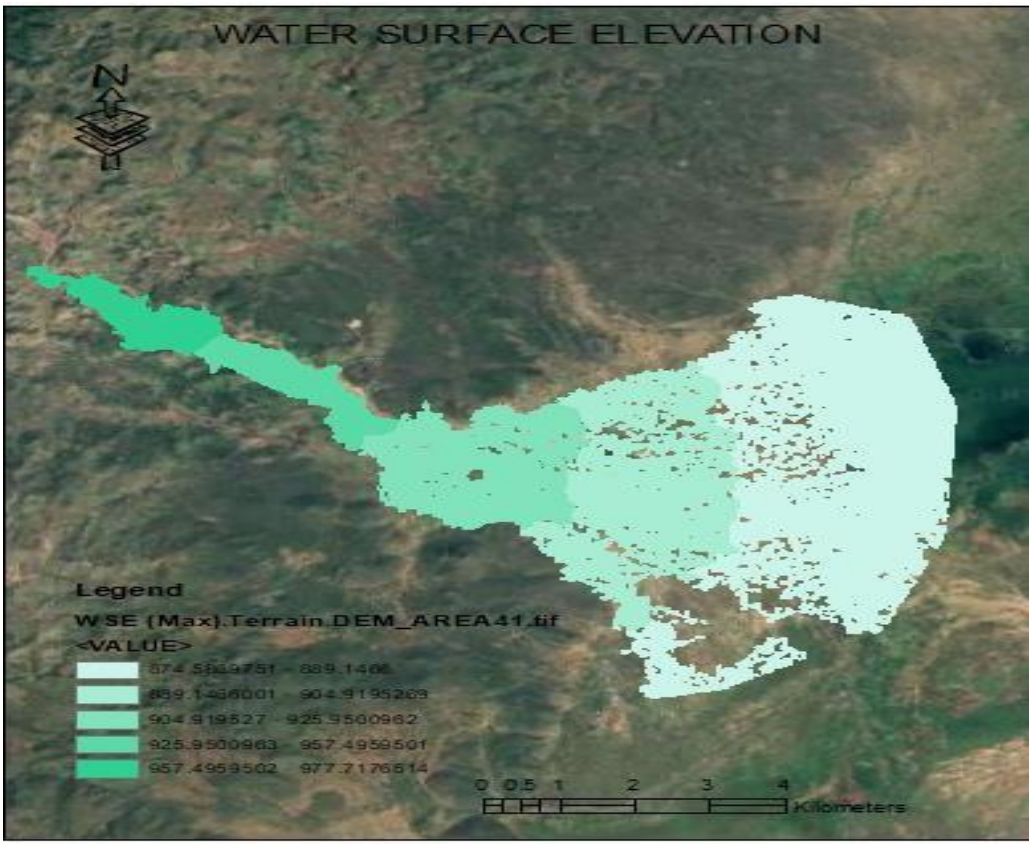

Figure 43 Map of water surface elevation

Inundation Map Inundation boundary computed from the zero-depth

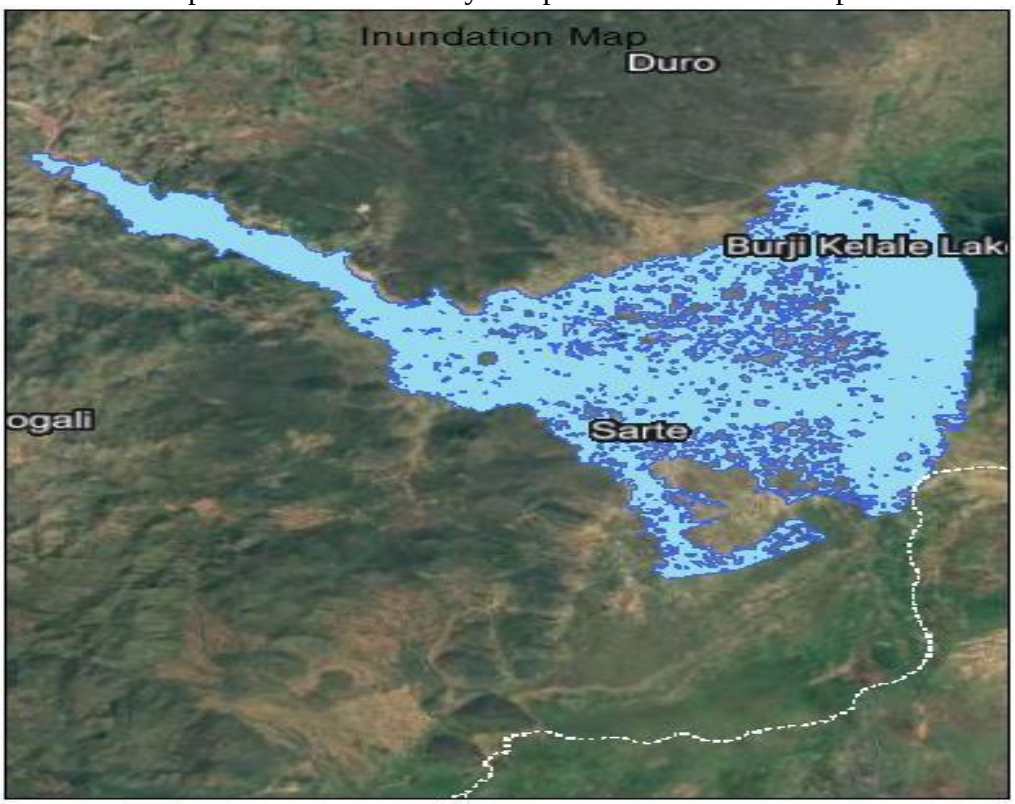

Figure 44Inundated Area Map

Inundation maps: - serve multiple purposes, such as developing Emergency Action Plans (EAPs), planning for mitigation strategies, coordinating emergency responses, and assessing potential consequences.

A breach of the dam will significantly affect approximately 450 house hold living downstream, who will be at risk of flooding, displacement, and potential loss of property or life.

Emergency Action Plans (EAPs): An EAP is an official document outlining possible emergency situations at a dam and detailing predetermined actions to mitigate property damage and protect lives. It outlines the steps the dam owner should take, in collaboration with emergency management agencies, to address incidents or emergencies concerning the dam. The plan includes procedures and information to aid the dam owner in issuing timely warnings and notifications to relevant downstream emergency management authorities.

Emergency Response: -Emergency response involves the steps taken during and shortly after an incident to safeguard lives, address fundamental human needs, and lessen property damage along with the effects on essential infrastructure and the environment.

Mitigation Measure: -Mitigation involves proactive measures aimed at minimizing loss of life and property by diminishing the impact of disasters. This is done by identifying potential hazards and their associated risks in a specific area, exploring mitigation options to lower those risks, and analyzing the effectiveness of these alternatives.

- **Determine Other Potential Consequences**

Assessing the potential consequences of the dam failure scenario includes identifying expected effects aside from fatalities and injuries

- **Economic Impacts**

The economic effects of dam failure reach beyond the immediate inundation zone, affecting infrastructure and resources that support a wider area. Besides the direct damage caused, these impacts include the time needed to repair or replace damaged businesses, government entities, and industrial facilities. This guide offers a method for estimating the economic consequences of the identified dam failure scenario. (FEMA, 2013)

5.4 Similar Study

Similar study on Dam Breach (M.Beza, 2023) Dam breach modeling was conducted using HEC-RAS 6.3.1 on proposed Gumara Dam Ethiopia applying a 1-day inflow magnitude equivalent to the base flow discharge. The simulation utilized five methods: USBR, MacDonald et al., Von Thun and Gillette, and Froehlich. The resulting outflow discharges were 19,753.68 cms and 14,674.12 cms from the overtopping breach methods using Von Thun and Gillette and MacDonald, respectively. The peak flow from the piping failure was 25,128.1 cms. The maximum flood depth and velocity downstream were 15 meters and 15 meters per second, respectively. According to the study, the results indicate that the design discharge is less than what was obtained, meaning the dam breach will completely affect the downstream area and its villagers. Additionally, the irrigation fields located 28 km away will also be impacted. The study concluded that the results of piping failure should be considered to reduce downstream hazards and improve preparedness.

5.5 Limitation of the Result

The HEC-RAS model may inadequately capture complex flow conditions during a breach, such as

turbulence and three-dimensional effects, relies on the assumption of uniform material properties, necessitates high-quality input data for reliable simulations, faces calibration difficulties due to limited historical data, primarily considers basic breach mechanisms, and may oversimplify the temporal dynamics of breaches, which can impact flood prediction accuracy.

6 CONCLUSION AND RECCOMENDATION

6.1 Conclusion

The analysis of dam breach modeling revealed critical insights into the hydrological dynamics of the study area and highlighted the potential flood risks associated with dam failures. Through a thorough examination of the rainfall-runoff relationships and the corresponding hydrological characteristics, this study enables accurate predictions of discharge during extreme weather events.

Using the HEC-HMS rainfall-runoff model generates the PMF hydrograph from the PMP hyetograph. The resulting PMF value is essential for conducting dam breach analysis in the study area, considering extreme weather conditions because of the region's vulnerability to flash floods.

The HEC-HMS model was calibrated using observed streamflow data from the watershed of interest. The calibration process involved adjusting parameters to minimize the difference between simulated and observed streamflow values. The model performed fairly well, with performance metrics of Nash-Sutcliffe Efficiency (NSE) = 0.608, Coefficient of Determination (R^2) = 0.74, and Percent Bias (PBIAS) = 6.74.

After calibration, the model was validated using data from 2002 to 2007. The validation results showed a coefficient of correlation of 0.695, indicating a good match with the observed data. The NSE value of 0.557 suggests moderately satisfactory performance, while the PBIAS of 2.33 demonstrates minimal bias, further indicating the model's reliability for hydrological analysis. Overall, the model exhibited a moderate level of performance during both the calibration and validation phases

The key parameters for dam breach modeling were estimated based on the provided data, which included the reservoir's storage volume and the geometry of the dam.

The breach parameter was estimated using validated regression equations from five different methods: Froehlich (1995a, 2005), Van Thun, MacDonald, and Xu Zhang.

The breach parameters derived from these empirical formulas provide a means to assess and analyze the characteristics of dam failures or flood-related events.

The analysis of dam breach discharges utilizing various methodologies has yielded a

range of discharge rates and heights, indicating the variability inherent in such assessments. The result for Froehlich (2008) estimated a discharge of 15528.94cubic meters per second (cms) at a height of 35.22meters, while Froehlich (1995a) provided a slightly higher estimate of 17990.85cms at 35.2meters. Von Thun and Gillette reported a discharge of 15526.33cms at a height of 35.12meters, and Xu Zhang identified a significantly lower discharge rate of 13525.53cms at a height of 35.34meters. Lastly, Macdonald's estimation suggested a discharge of 14441.92cms at 35.19meters.

The flood routing simulation conducted using the 2D flow method shows significant results. The profile line created 5 km from the dam indicates a water depth of7.15 meters and a discharge of 13348.5 m3/s. These results suggest that villagers in the downstream area will be devastated affected.

The inundation map has been created to help communities prepare for potential floods by clearly showing areas at risk, thus allowing for timely evacuation and emergency response planning, and illustrating the areas affected by flooding, extending from a specific location to a downstream boundary where the flood no longer has an impact.

6.2 Recommendation

An emergency action plan's component is to model a flood from a potential dam breach and map the downstream flood inundation area. The resulting flood inundation map can give local residents and emergency managers, important information for preparing for emergency responses in the event of a dam breach.

In future development the villager recommended to avoid construction in high-risk areas

Officials could identify and prioritize evacuation zones, ensuring timely and efficient rescue o perations.

Based on the result mentioned above indication population at downstream must be resettle to other places. To improve area safety or lessen any problems, the individual living downstream should evacuate. Future research should be done on the hazard classification on the downstream area.

Construct and improve levees, floodwalls, and retention basins in vulnerable areas to manage floodwaters effectively.

The current study uses regression equations to predict the breach parameters, but physically based dam breach models give more detailed results even though they are more difficult. Future dam breach studies should consider to use physically based model to predict dam breach parameters.

REFERENCES

FEMA, (2013) Federal guideline for Inundation mapping of flood risk Associated with Dam incident and failure.

FEMA, (2021) 2D Watershed Modeling in HEC-RAS Recommended Practices.

K.W.Hipel et.al, (1994) Stochastic and Statistical Methods in Hydrology and Environmental Engineering.

FEMA, (2004) SELECTING AND ACCOMMODATING INFLOW DESIGN FLOODS FOR DAMS

H.M.Raghunath et.al, (2006) Hydrology principle, analysis, design

P.B.Bendint et al, (2013) Hydrology and Floodplain Analysis

MESFIN KERE (2023), GEOTECHNICAL EVALUATION AND REMEDIATION STRATEGIES FOR SEEPAGE, PIPPING AND LIQUEFACTION HAZARDS AT YANDA DAM

Abdulawel Umer, (2018) Dam Breach Modeling and Inundation Mapping In A Case Study of Dabus Dam

Adisalem Eyob (2020). Dam Breach Analysis and Flood Inundation Mapping For Lower Awash Multipurpose Dam.

Kibire Tesema (2016), Dam Breach Modeling and Flood Inundation Mapping For Middle Awash Dam

Fasika Worku (2021), Dam Breach Modelling and Flood mapping, a Case Study of Ribb Dam.

Manamno Beza (2023), Dam Breach Modeling and Downstream Flood Inundation Mapping Using HEC-RAS Model on the Proposed Gumara Dam, Ethiopia

Yonatan Sisay (2016), Dam Breach Analysis & Inundation Map for Melka Wakena Dam.

Serban Danielescu, (2018) Sephydro: A Customizable Online Tool for Hydrograph Separation

Michael B. Abbott, (1996), Distributed Hydrological Modelling

Philip B. Bedient et al. (2013), Hydrology and Floodplain Analysis

Elizabeth M. Shaw et al (2011), Hydrology in Practice

Mohit Uniyal, (2024), Root Mean Square Error (RMSE) in Machine Learning

Daniel Althoff, et al. (2021), Goodness-of-fit criteria for hydrological models: Model

calibration and performance assessment
Ven Te Chow. (1988), Applied Hydrology

K. Eckhardt, (2004) How to construct recursive digital filters for base flow separation
ICOLD (2019), Statistical analysis of dam failures,
Ben R. Hudges. (2019), Conservative finite-volume forms of the Saint-Venant equations for Hydrology and urban drainage
TD-39. (2014), Using HEC-RAS for Dam Break Studies, U.S. Army Corps of Engineers Institute for Water Resources Hydrologic Engineering Center
ICOLD (2009), Dam-break Problems, Solutions and Case Studies
M.T.Ayana et al (2019), Quality of Hydro-Meteorological Data in Remote Stations: The Case of Weito River Watershed, Ethiopia.
HEC-HMS Technical Reference Manual (2015)
S.S.Fanta et al (2021), Performance evaluation of HEC-HMS model for continuous runoff simulation of Gilgel Gibe watershed, Southwest Ethiopia.
N.A.S. Nordin et al, (2024) Assessing Hydrological Response in the Timah-Tasoh Reservoir Sub-Catchments: Calibration and Validation using the HEC-HMS Model
.A.Asadi, et al, (2013), Performance Evaluation of the HEC-HMS Hydrologic Model for Lumped and Semi-distributed Stormflow Simulation (Study Area: Delibajak Basin)
D.D.More et al, (2024). Hydrologic Engineering Centers-River Analysis System (HEC-RAS)
N .N. Zainal et al, (2024), applications of the HEC-RAS model for flooding, agriculture, and water quality simulation
CPD-69, (2016), Hydraulic Reference Manual, US Corps of Engineers Hydrologic Engineering Center
CPD-69, (2024), Hydraulic Reference Manual, US Corps of Engineers Hydrologic Engineering Center
(H.P.G.M. Caldera et al. 2016).A Comparison of Methods of Estimating Missing Daily Rainfall Data
WMO, (2009), Manual on Estimation of Probable Maximum Precipitation (PMP)

APPENDIX A

Average monthly rainfall data

YEAR	MONTH											
	JAN	FEB	MAR	APR	MAY	JUN	JUL	AUG	SEP	OCT	NOV	DEC
1990	9.11	159.58	128.34	124.62	96.48	8.48	8.57	25.20	51.45	62.22	33.71	18.38
1991	97.71	44.91	106.71	113.80	129.81	54.33	17.26	28.59	35.86	74.15	52.47	24.78
1992	3.35	21.83	45.18	164.17	74.02	63.37	40.44	7.13	93.19	91.26	34.23	13.98
1993	130.24	95.03	18.53	70.39	98.28	102.52	14.57	16.29	33.20	105.06	27.40	14.98
1994	4.59	17.37	82.75	150.93	123.45	14.26	52.87	58.33	45.21	103.92	74.58	12.37
1995	10.30	29.71	33.21	169.49	37.81	86.78	42.79	12.51	85.61	147.21	38.42	9.07
1996	21.56	22.71	179.08	215.40	130.83	98.67	46.84	37.58	67.19	86.36	19.86	1.13
1997	13.25	0.00	35.04	180.29	73.20	21.78	77.88	22.98	40.79	192.58	330.59	39.58
1998	94.41	102.54	55.84	108.07	149.37	63.41	7.04	27.57	22.17	105.32	27.57	0.00
1999	2.73	2.03	153.36	127.06	39.68	14.50	30.79	23.67	34.11	50.72	20.27	55.90
2000	1.37	0.19	17.62	161.77	118.06	3.97	11.34	19.97	32.09	139.91	62.81	47.49
2001	34.22	7.33	130.64	258.31	95.15	44.22	25.42	52.51	74.07	127.38	49.64	8.08
2002	40.79	11.95	128.20	134.37	119.01	23.90	11.88	7.54	56.44	133.41	56.98	192.40
2003	6.04	13.70	76.39	194.07	169.65	24.93	14.93	72.71	14.65	70.76	57.32	32.92
2004	37.53	22.85	54.88	154.59	95.86	12.46	12.21	9.93	126.04	43.87	119.37	30.63
2005	20.74	6.06	126.94	162.19	289.64	8.91	21.07	15.51	81.76	78.43	50.03	0.00
2006	8.15	77.89	140.14	187.31	66.24	63.59	6.21	103.83	23.18	165.47	153.54	67.20
2007	14.08	22.93	47.48	160.91	93.51	116.80	44.61	100.06	172.86	70.17	48.96	0.80
2008	2.19	4.67	38.14	113.71	39.92	21.04	31.81	56.85	257.82	177.53	63.11	0.38
2009	38.07	6.52	63.81	86.30	77.64	20.67	8.69	3.01	55.80	113.77	59.73	54.02
2010	52.47	68.50	198.12	185.34	222.99	19.81	40.62	31.92	70.83	96.67	18.29	10.83
2011	6.75	20.22	57.74	75.38	154.45	20.67	72.63	58.76	73.48	126.36	270.56	43.47
2012	1.29	15.25	27.50	232.49	69.74	45.16	36.09	61.47	148.01	146.82	71.89	40.60
2013	28.29	20.02	78.82	216.87	44.35	19.73	25.36	63.79	92.80	73.50	139.73	12.65
2014	1.08	85.68	150.88	66.82	118.45	43.80	37.16	54.63	52.25	148.97	76.51	3.81
2015	0.00	9.48	84.37	193.07	91.46	83.19	50.23	18.50	51.08	184.81	141.00	113.79
2016	6.91	31.63	138.31	233.05	86.37	74.84	4.29	22.93	44.40	97.29	79.28	5.93
2017	1.26	5.73	50.16	110.41	152.50	28.60	53.71	32.88	114.04	146.13	67.94	0.00
2018	1.93	70.41	134.73	305.74	106.96	44.78	3.74	42.36	40.75	74.74	48.76	24.47
2019	0.00	1.82	44.91	149.70	62.00	105.92	42.57	47.99	29.79	162.79	257.04	48.32

Inflow Hydrograph

HOUR	DISCHARGE
1	0
2	0
3	0.1
4	0.6
5	2.8
6	9.1
7	23.2
8	49
9	89.8
10	147.1
11	220.8
12	309.4
13	410.4
14	521
15	633.6
16	731.3
17	794.1
18	810.8
19	783.8
20	728.5
21	661.6
22	588.8
23	510.8
24	428.9
25	344

BREACH FORMATION AND DOWNSTREAN STATION FLOOD ARRIVAL TIME

TIME	AT DAM	AT 2KM	AT 5KM	AT 7KM
02Feb2025 2220	0	0	0	0
02Feb2025 2225	0	0	0	0
02Feb2025 2230	0	0	0	0
02Feb2025 2235	0	0	0	0
02Feb2025 2240	0	0	0	0
02Feb2025 2245	0	0	0	0
02Feb2025 2250	0	0	0	0
02Feb2025 2255	10.44	0	0	0
02Feb2025 2300	592.48	0	0	0
02Feb2025 2305	2664.09	0	0	0
02Feb2025 2310	6401.96	0	0	0
02Feb2025 2315	11542.53	6654.648	0	0
02Feb2025 2320	14352.83	12592.24	0	0
02Feb2025 2325	13565.4	14101.39	3550.758	0
02Feb2025 2330	12353.41	13299.32	11537.44	0
02Feb2025 2335	10820.2	12048.53	13224.03	0
02Feb2025 2340	9134.57	10553.49	12245.26	742.326
02Feb2025 2345	7318.83	8945.999	10882.5	6474.39
02Feb2025 2350	5427.47	7263.743	9393.294	7642.125
02Feb2025 2355	3351.95	5584.784	7858.92	7498.414
02Feb2025 2400	1399.29	3803.42	6362.455	6873.749

HEC-HMS Rainfall-Runoff Simulated Result (Monthly)

YEAR	MONTH											
	jan	feb	mar	apr	may	jun	jul	aug	sep	oct	nov	dec
1990	0	33.2	727.7	927.8	862.3	422.4	36.7	66.2	364.4	732.5	630.3	277.2
1991	204.8	295.3	524.2	829.4	1078.3	712.9	128.8	30.5	390.2	732.3	687.1	347.8
1992	46.9	95.5	215.4	706.1	1264.9	528.1	284.6	23.9	444.5	831.9	767.1	233.3
1993	287.5	692.7	339.1	473.2	925.8	802.1	155	98.8	236.3	650.4	930.9	243
1994	22.2	44.4	280.6	846.6	1453.7	362.2	232	244.6	353.1	920.6	820.6	306.1
1995	51.6	115.4	270.2	708.1	1086	469	397	45.4	361.6	1118.1	869.8	192.3
1996	91.6	61.1	664.3	1215.5	1335.8	864.1	255.9	146.9	563.1	669.4	687.9	230.7
1997	23.4	40.3	149.6	1066.5	1046.6	339.6	233.1	239.3	266	887.9	1856.4	980.2
1998	493.1	323.2	555.9	655	1374.5	473.3	140.4	127.2	239.6	885.2	674.9	170.7
1999	8.6	8.1	722.3	761.7	963.1	259.5	141.5	66.8	419.6	508.1	684.2	452.6
2000	14	6.1	154.1	668.9	1458.3	302.1	27.6	129.3	284.6	803.8	947.6	491.3
2001	121.2	87.6	351.7	1523.1	1220.2	504.3	127.4	255.7	467.9	797.1	1029.5	218.4
2002	29.4	7.5	368.1	842.8	1144.1	262.4	32	73.9	438.7	871.9	765.7	585.7
2003	532.3	62.9	305.5	876.8	1782.3	356.1	70.8	228.4	402.7	727.3	663.2	356.2
2004	54.8	225.7	268.6	914.6	1257.9	224.9	11.1	93	372.9	1039.1	794.4	431.1
2005	85	102.3	616.2	1050	1823.1	461.6	53.7	91	555.3	789.5	708.6	184
2006	29.7	67.7	780.9	1179.7	1182.8	405	117.9	306.9	458.3	846.7	1177.5	733.5
2007	149.6	141.6	277.8	936.2	1099.3	772.3	124.8	493.5	893.5	909	781	146.9

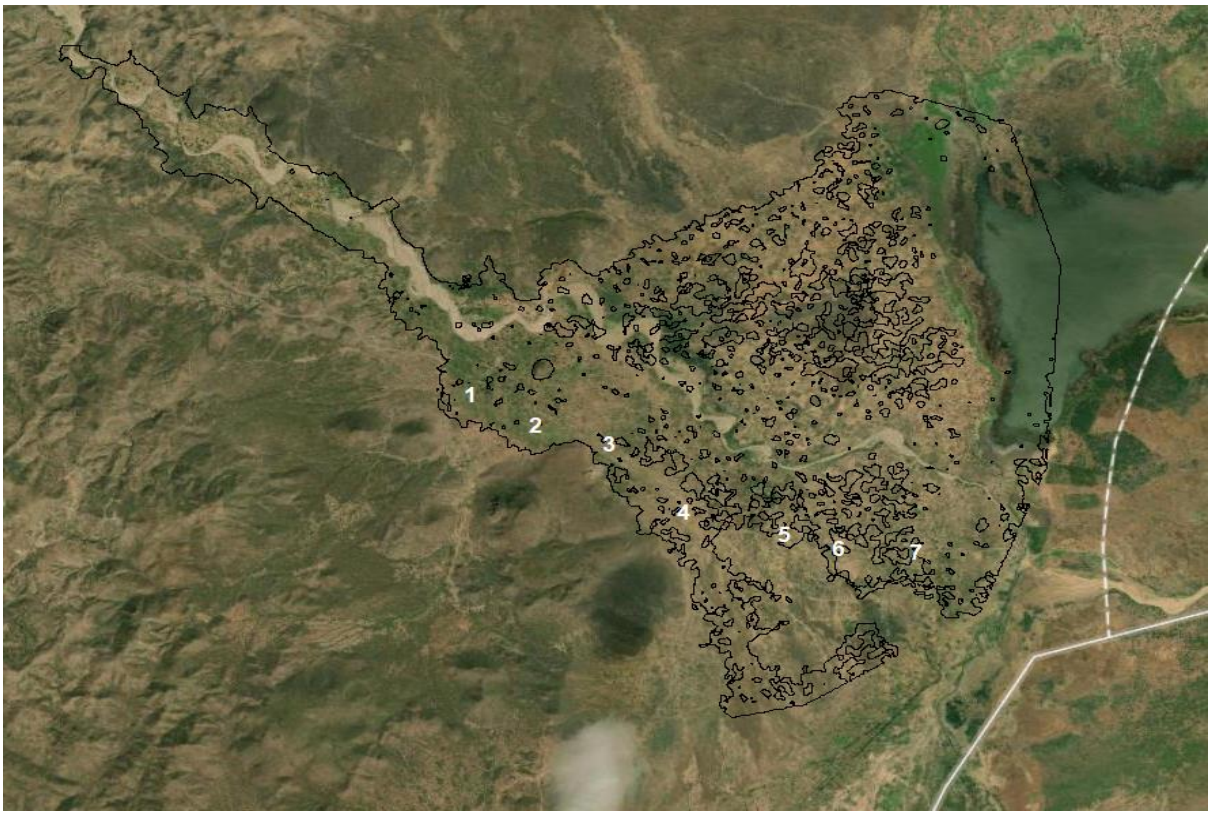

The area enclosed by the polyline represents the residential living area.

The area enclosed by the polyline represents the residential living area.

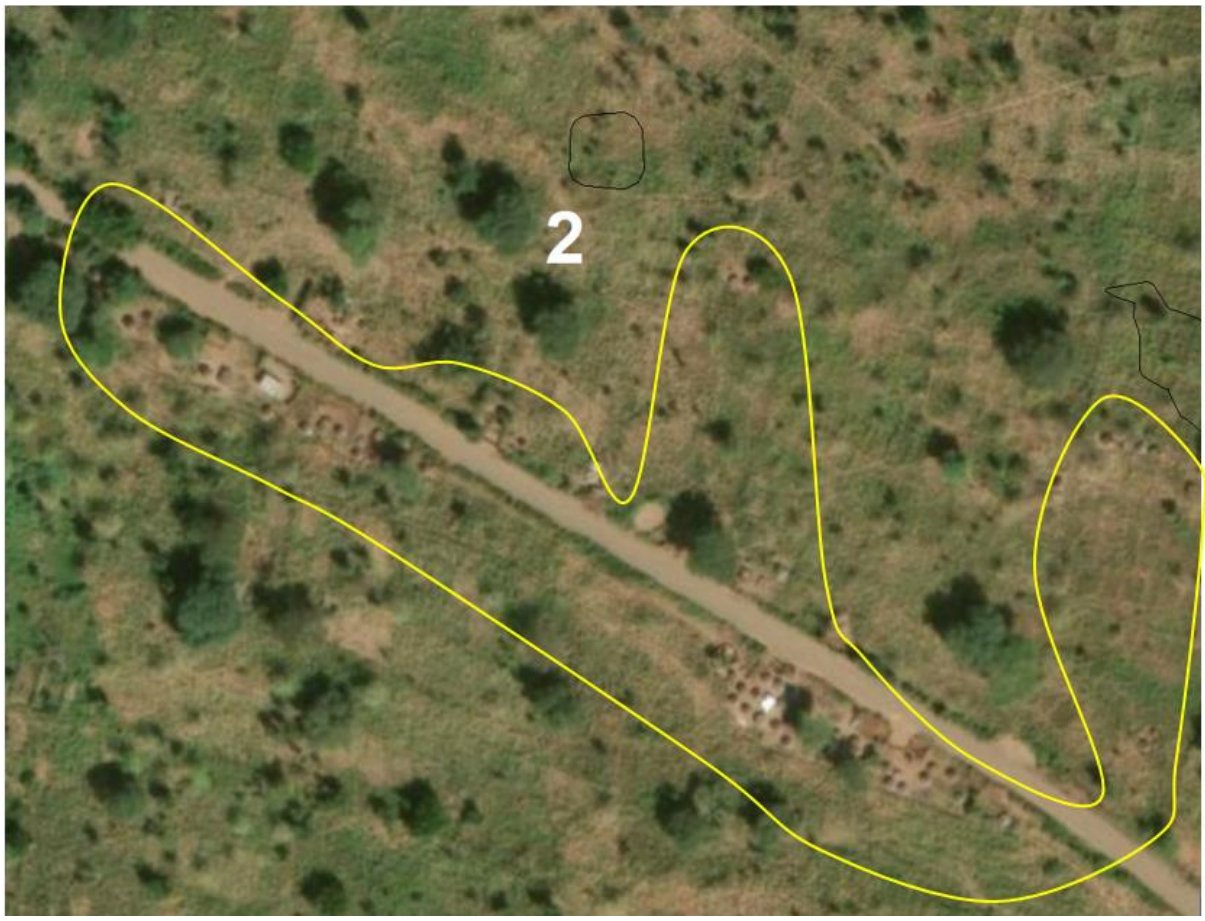
2

The area enclosed by the polyline represents the residential living area.

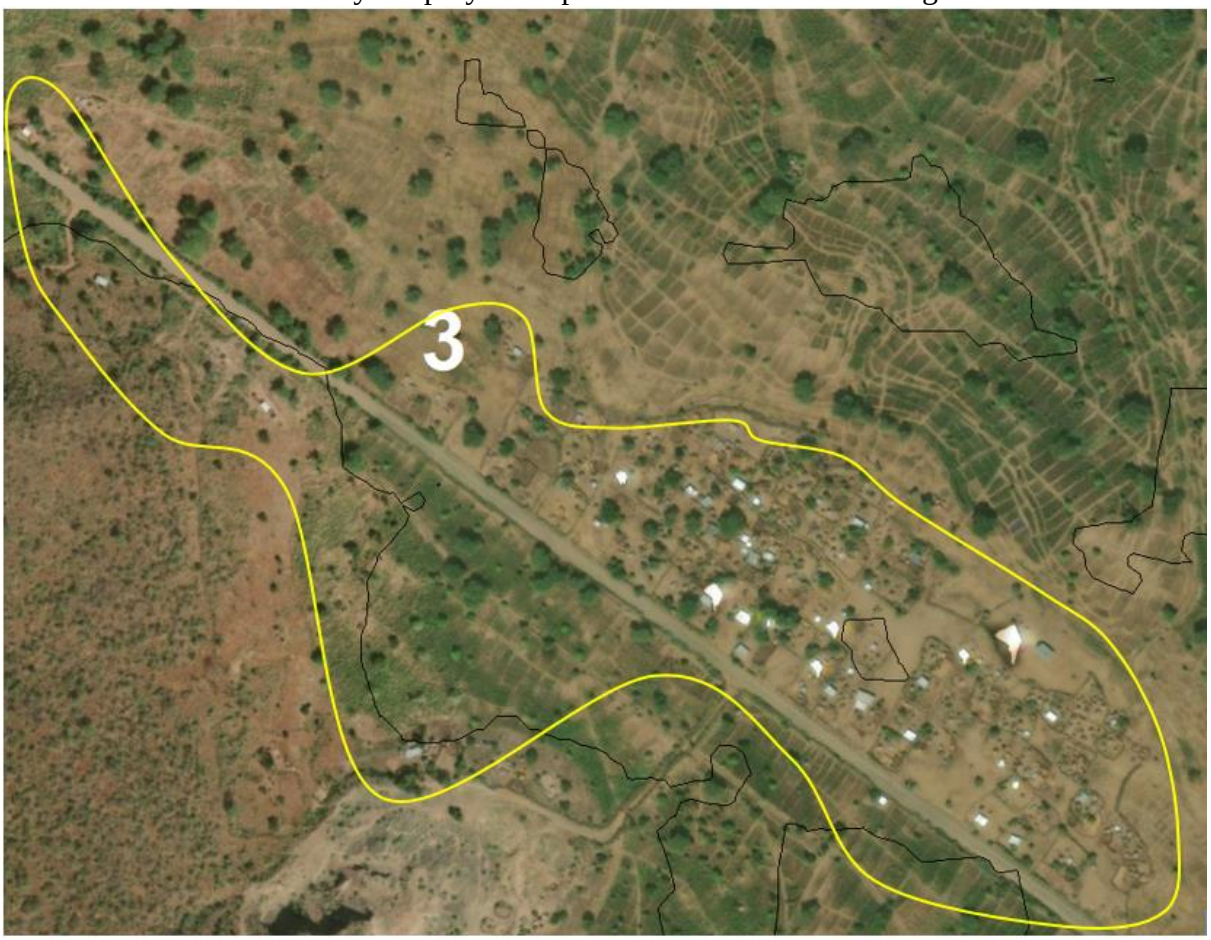

The area enclosed by the polyline represents the residential living area.

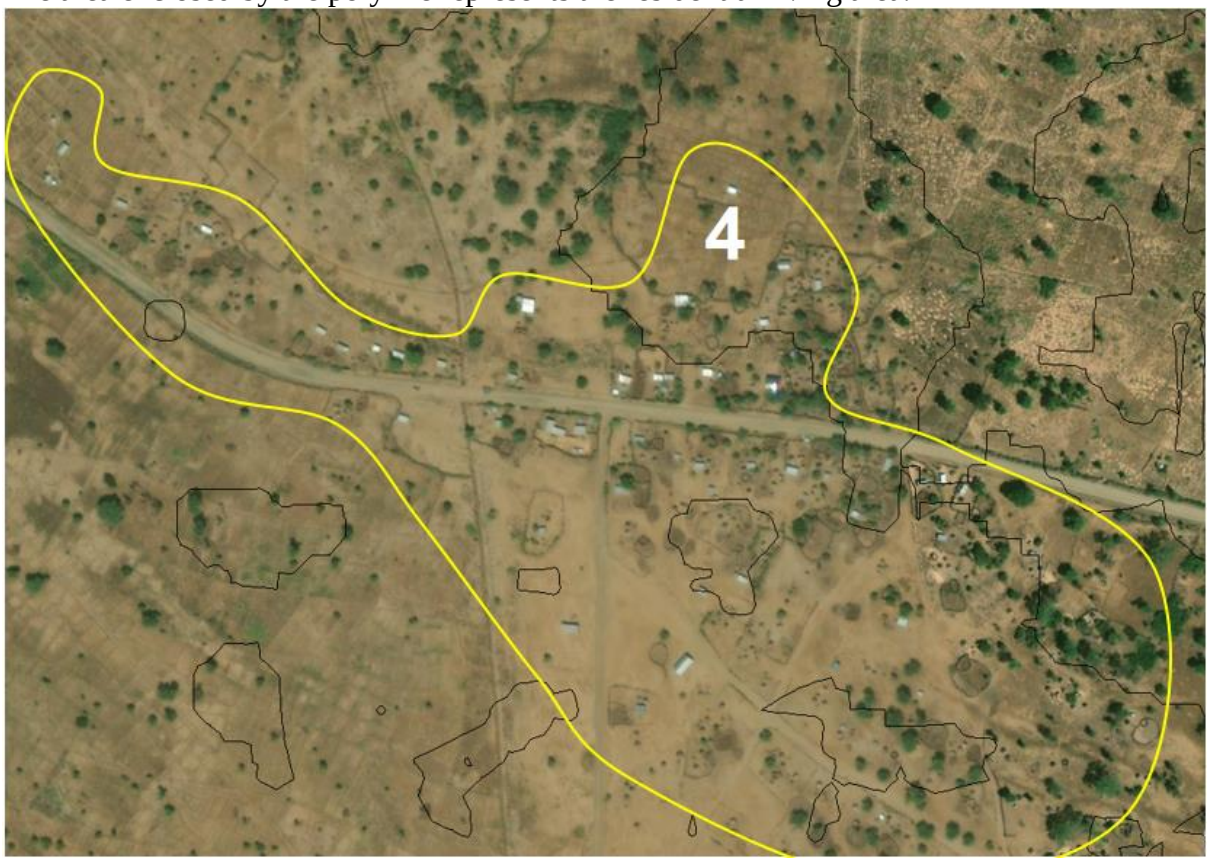

The area enclosed by the polyline represents the residential living area.

The area enclosed by the polyline represents the residential living area.

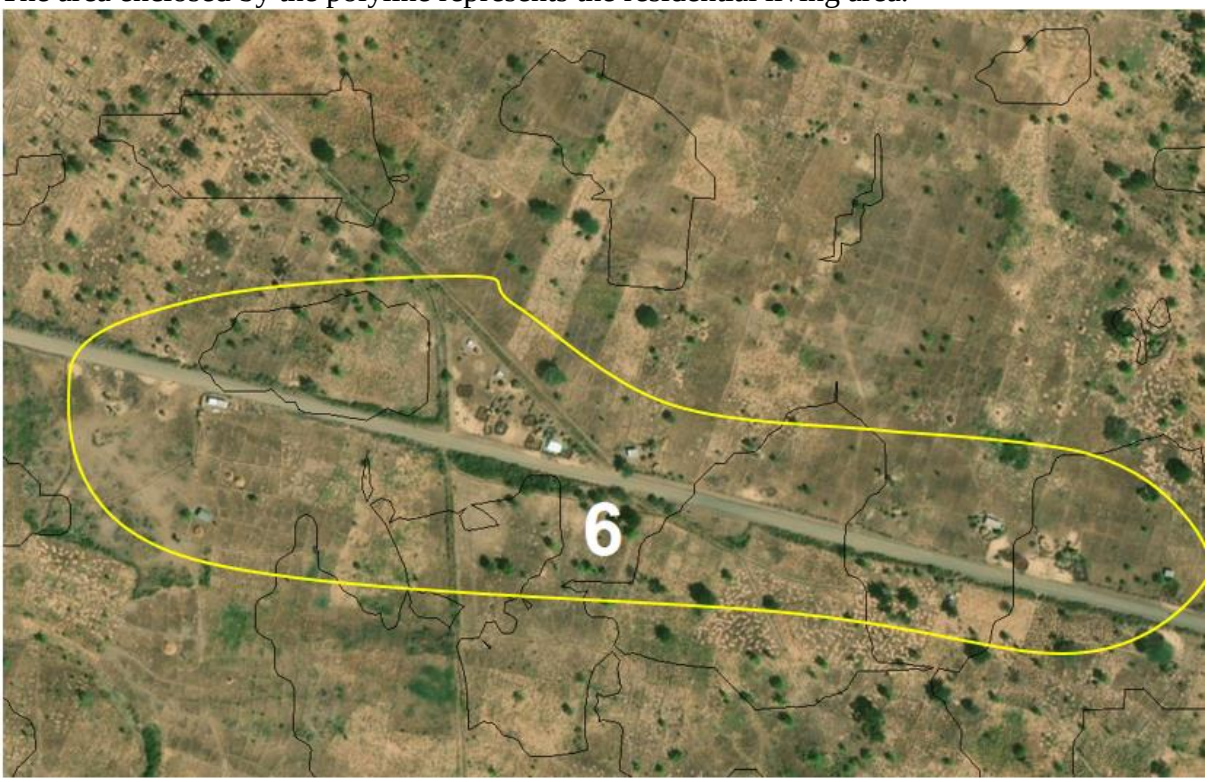

The area enclosed by the polyline represents the residential living area.